1-1-2013

Characterizing Hypoxia and Its Behavioral Effects In 3-Dimensional Cell Aggregates

Matthew Lorincz Skiles
University of South Carolina

Characterizing Hypoxia and its Behavioral Effects in 3-Dimensional Cell Aggregates

by

Matthew L. Skiles

Bachelor of Science
University of South Carolina, 2006

Submitted in Partial Fulfillment of the Requirements

For the Degree of Doctor of Philosophy in

Biomedical Engineering

College of Engineering and Computing

University of South Carolina

2013

Accepted by:

Dr. James Blanchette, Major Professor

Dr. Ehsan Jabbarzadeh, Committee Member

Dr. Susan Lessner, Committee Member

Dr. John Baynes, Committee Member

Lacy Ford, Vice Provost and Dean of Graduate Studies

Dedication

A portion of my life has been invested into the work that culminates with this dissertation. It is therefore dedicated to those who prepared me for the effort, helped me through it, and will (hopefully) enjoy the fruits that its labor bears: my parents, Pamela and Samuel, my wife, Jean, and my son, Robert Gabriel.

Acknowledgments

I would like to acknowledge, and thank, my advisor, Dr. James Blanchette, for the wisdom, guidance, and insight freely offered and invaluable to my growth and accomplishment as a researcher. I also offer appreciation to those who contributed to and/or facilitated the work that is presented here: Suchit, Romone, Nathan, Lindsay, Pritesh, and Kevin; the labs of Dr. Melissa Moss, Dr. Tarek Shazly, Dr. Ehsan Jabbarzadeh, Dr. Esmaiel Jabbari, and Dr. Michael Matthews at the University of South Carolina; the lab of Dr Kristi Anseth at the University of Colorado; and the Instrument Resource Facility at the University of South Carolina School of Medicine.

Abstract

Cell transplantation can be considered a regenerative therapy, an intervention which attempts to replace or restore the function of compromised tissue by harnessing innate properties of cells that cannot be replicated artificially. For such therapies to succeed, it will be necessary to understand and closely match the physiological conditions that govern cell behaviors *in vivo*. One important factor is low oxygen tension, termed hypoxia, which is often overlooked *in vitro*. Because oxygen insufficiency can lead to cell death, hypoxia has traditionally been viewed as a negative condition. However, hypoxia can also serve as a potent regulator of crucial cell behaviors involved in normal development, adaptation, and regeneration through transcriptional activity of hypoxia-inducible factors (HIFs). Characterizing HIF activity, especially in three-dimensional tissues which can experience oxygen heterogeneities, will be useful in investigating how culture parameters impact local microenvironmental conditions to affect cell behavior.

In the present work, a novel fluorescent reporter system was used to detect cellular HIF activity in islet-like clusters of pancreatic β-cells and adipose-derived stem cell (ADSC) spheroids, two cell systems used in transplantation therapies. Fluorescent signaling was observed in cultures incubated in reduced oxygen conditions and in large cultures, indicating the development of tissue size-dependent oxygen gradients. HIF activity could be monitored in the same samples over time and could be correlated to

other cell behaviors. In β-cells, signal was observed in all clusters incubated in 1% or 2% oxygen and in the center of large clusters (>300μm) incubated in 20% oxygen. In clusters that exhibited HIF activity, insulin secretion and cluster morphology were severely impaired. In ADSC spheroids, both reduction of external oxygen concentration and an increase in spheroid size increased HIF activity. Moderate HIF activity corresponded with increased vascular endothelial growth factor (VEGF) secretion from spheroids, while intense HIF activity corresponded with regional reduction of cell viability; therefore, an optimal size for VEGF secretion could be demonstrated. Altogether, the HIF reporter system represents a useful tool in monitoring cellular hypoxia so that culture parameters such as external oxygenation and culture size can be properly considered in order to guide desired cell behaviors in cell transplantation.

Table of Contents

Dedication iii

Acknowledgements iv

Abstract v

List of Tables viii

List of Figures ix

List of Abbreviations xi

Introduction 1

Chapter 1: Literature Review 3

1.1 Oxygen's Role as a Nutrient 3

1.2 Oxygen's Role in Cell Signaling 13

1.3 Regulating Hypoxia to Affect Cell Behaviors in Transplantation Therapies 39

Chapter 2: Correlating Hypoxia with Insulin Secretion Using a Fluorescent Hypoxia Detection System 56

Chapter 3: Identifying HIF Activity in 3D Cultures of Islet-Like Clusters 79

Chapter 4: Influence of Culture Geometry on Hypoxia and Hypoxia-Induced Secretion of VEGF in Human Adipose-Derived Stem Cell Spheroid 101

Chapter 5: Conclusions 126

References 131

List of Tables

Table 1.1 Normal pO_2 values reported in different human tissues 10

Table 1.2 Direct transcriptional targets of HIF-1 29

Table 2.1 Analysis of MIN6 aggregate sizes..... 70

Table 4.1 Mean values and standard deviation of VEGF release from ADSC cultures 117

Table 4.2 Table indicating statistical significance of differences in mean VEGF release from the cultures under study 118

List of Figures

Figure 1.1 Production of energy-carrying molecules in aerobic cellular respiration 5

Figure 1.2 Schematic of the ETC and production of ATP by proton motive force..... 6

Figure 1.3 Oxygen-dependent mechanisms of HIF regulation 22

Figure 1.4 Schematic of development of hypoxia in 3D cultures 42

Figure 2.1 Schematic of a novel hypoxia detection system in living MIN6 cells 66

Figure 2.2 Dissolved oxygen concentrations measured in 2 mL of growth medium..... 68

Figure 2.3 Daily one hour insulin release over 2 weeks..... 71

Figure 2.4 Fluorescently imaged aggregates 73

Figure 3.1 400,000 MIN6 cells aggregated to form islet-like clusters 88

Figure 3.2 Brightfield microscopy images of islet-like clusters
for the analysis of morphology 90

Figure 3.3 Top) Schematic of HIF-induced cellular fluorescence..... 92

Bottom) Hypoxic signaling in islet-like clusters of MIN6 cells..... 92

Figure 3.4 GSIS in clusters of MIN6 cells 93

Figure 3.5 Analysis of viability in clusters of MIN6 cells..... 95

Figure 4.1 Flow cytometry analysis of cell surface markers CD44
and CD105 in P6 ADSCs 107

Figure 4.2 Diameter of spheroids formed by centrifugally pelleting
different numbers of ADSCs 112

Figure 4.3 Fluorescent DsRed signaling as an indicator of HIF activity in
5k, 10k, 20k, and 60k ADSC spheroids 113

Figure 4.4 Fluorescent HIF reporter signal displayed at 1/5 the exposure length as in Figure 4.2 115

Figure 4.5 Levels of daily and total per-cell VEGF release from ADSC monolayers and 5k, 10k, 20k, and 60k spheroids 116

Figure 4.6 H&E staining of ADSC spheroid sections 120

Inset) Live/Dead viability assessment of ADSCs 120

List of Abbreviations

°C ..... Degrees Celsius
I..... ETC complex I (NADH-ubiquinone oxidoreductase)
II..... ETC complex II (Succinate-ubiquinone oxidoreductase)
III..... ETC complex III (Ubiquinol-cytochrome c oxidoreductase)
IV.....ETC complex IV (Cytochrome c oxidase [COX])
3D .....Three-dimensional
5k 5,000
10k 10,000
20k 20,000
60k 60,000
Acetyl CoA..... Acetyl co-enzyme A
A.C.S.....American Chemical Society
ADP .....Adenosine diphosphate
ADSC .....Adipose-derived stem cell
ANG-1 ..... Angiopoietin 1
ARNT ..... Aryl hydrocarbon receptor nuclear translocator
ATP..... Adenosine triphosphate
Bcl-2 .....B-cell lymphoma 2
bFGF.....Basic fibroblast growth factor
bHLH-PAS ..... basic helix-loop-helix PER-ARNT-SIM
bNGF .....Basic nerve growth factor
BNIP3 ..... BCL2/adenovirus E1B 19 kDa protein-interacting protein 3
cAMP..... Cyclic adenosine monophosphate
CBP/p300 ..... CREB binding protein/p300 transcriptional coactivator
cm^2 ..... Square centimeters
CMV .....Cytomegalovirus
CO_2..... Carbon dioxide
COX ..... Cytochrome-c oxidase
CREB.....cAMP response element-binding protein
CSF .....Colony stimulating factors
CTAD ..... C-terminal transactivation domain
Cyt C.....Cytochrome C
Da ..... Dalton
DNA.....Deoxyribonucleic acid
DsRed-DR .....Destabilized variant of the DsRed protein
ELISA .....Enzyme-linked immunosorbent assay
EPAS1.....Endothelial PAS domain protein 1

EPO ..... Erythropoietin
ETC ..... Electron transport chain
$FADH_2$ ..... Flavin adenine dinucleotide (reduced form)
Fe^{2+} ..... Iron II; Ferrous iron
FIH ..... Factor inhibiting HIF
g ..... Force of gravity
GFP ..... Green fluorescent protein
GSIS ..... Glucose-stimulated insulin secretion
^1H NMR ..... Proton nuclear magnetic resonance
H_2O_2 ..... Hydrogen peroxide
HBSS ..... Hank's Balanced Salt Solution
HGF ..... Hepatocyte growth factor
HIF ..... Hypoxia-inducible factor
HO· ..... Hydroxide radical
HRE ..... Hypoxia responsive element
Hrs. ..... Hours
IGF-1 ..... Insulin-like growth factor 1
IL ..... Interleukin
IU ..... International units
kDa ..... KiloDalton
K_m ..... Michaelis-Menten constant (half maximal rate of reaction)
L ..... Liter
LDH ..... Lactate dehydrogenase
LOX ..... Lysyl oxidase
LOXL2 ..... Lysyl oxidase-like 2
MCP ..... Monocyte chemoattractant protein
mg ..... Milligram
Min ..... Minutes
MIN6 ..... Murine insulinoma 6
mL ..... Milliliter
miRNA ..... MicroRNA
mm ..... Millimeters
mM ..... Millimolar
mmHG ..... Millimeters of mercury
MMP ..... Matrix metalloproteinases
M_n ..... Number average molar mass
MOI ..... Multiplicity of infection
MRI ..... Magnetic resonance imaging
mRNA ..... Messenger ribonucleic acid
MSC ..... Mesenchymal stem cell
mTOR ..... Mammalian target of rapamycin
mW ..... Milliwatt
NADH ..... Nicotinamide adenine dinucleotide (reduced form)
nm ..... Nanometers

NTAD ..... N-terminal transactivation domain
O_2 ..... Oxygen (dioxygen gas, molecular oxygen)
$\cdot O_2^-$ ..... Superoxide anion
O_2Hb ..... Oxyhemoglobin
Oct4 ..... Octamer-binding transcription factor 4
ODD ..... Oxygen-dependent degradation domain
OS-9 ..... Osteosarcoma amplified 9 protein
P4H2 ..... Prolyl 4-hydroxylase 2
PDGF ..... Platelet-derived growth factor
PEG ..... Poly(ethylene glycol)
PEGDM ..... PEG dimethacrylate
PER ..... Period circadian protein
PEST ..... Proline, glutamic acid, serine, threonine sequence
PET ..... Positron emission tomography
PHDs Prolyl-4-hydroxylases
PKM2 ..... Pyruvate kinase isoform M2
pO_2 ..... Oxygen partial pressure
pVHL ..... von Hippel-Lindau tumor suppressor protein
Q ..... Ubiquinone (oxidized) / ubiquinol (reduced)
RACK-1 ..... Receptor for activated C kinase 1
rcf ..... Relative centrifugal force
ROS ..... Reactive oxygen species
rpm ..... Revolutions per minute
RPMI 1640 ..... Roswell Park Memorial Institute medium 1640
RT-PCR ..... Real-time polymerase chain reaction6
Sbstr. lvl. ..... Substrate-level
SDF-1 ..... Stromal cell-derived factor 1
SIM ..... Single-minded protein
SIP1 ..... Survival of motor neuron protein-interacting protein 1
SIRT-3 ..... NAD-dependent deacetylase sirtuin-3, mitochondrial
SSAT2 ..... Spermidine/Spermine N1-Acetyltransferase 2
$t_{1/2}$ ..... Half-time
T1DM ..... Type 1 diabetes mellitus
TGF-β ..... Transforming growth factor-β
TNF-α ..... Tumor necrosis factor α
UV ..... Ultraviolet
VEGF ..... Vascular endothelial growth factor
Vol. ..... Volume
W ..... Watts
Wt. ..... Weight
wt% ..... Weight percent
µg ..... Microgram
µm ..... Micrometer
µL ..... Microliter

Introduction

This dissertation is concerned with presenting and discussing experimental data which contributes novel findings to the field of cell transplantation. Specifically, results from the included studies provide a better understanding of how hypoxia develops within 3-dimensional (3D) cultures of pancreatic β-cells and adipose-derived stem cells (ADSCs) and how knowledge of this hypoxic status can be used to rationally direct desired cell behaviors (insulin secretion and VEGF secretion, respectively) to improve outcomes in transplantation therapies intended to restore lost tissue function. The structure of this dissertation, then, is intended to both communicate peer-reviewed results from several separate studies and to make clear the underlying impetus by which they are unified. The document is structured in the following manner:

- Chapter 1 consists of a literature review intended to develop a framework explaining why the research was undertaken. This includes relevant historical studies, recent findings and advancements in the field, and identification of areas in which the current knowledge appears to be incomplete. Specifically, the essential role of oxygen as a both a nutrient and as a cell signaling molecule is first discussed. Next, the mechanism of hypoxia-mediated regulation of cell behavior is explained, and it is suggested that rational control of culture parameters can be used to regulate hypoxic status, thus driving desired cell function. A novel approach to identifying cellular hypoxia is also advocated.

Finally, the importance of hypoxic status is considered in two specific cell systems which exhibit potential usefulness in transplantion therapies: islet-like β-cell clusters and ADSC spheroids. The advantages of tracking hypoxia by use of a novel reporter system as well as the potential benefits of characterizing hypoxia in these two systems are highlighted.

- Chapters 2-4 are research studies that have been published or submitted for publication in peer-reviewed research journals. These chapters each include a brief introduction, description of experimental methods and design, study results, and discussion of the findings. Section, figure, and reference numbering has been altered to conform to the formatting of this dissertation. Chapter 2 reports on the use of the hypoxia reporter in encapsulated islet-like clusters of β-cells of different sizes cultured in 20% or 1% oxygen. Chapter 3 compares hypoxic status, function, and viability of encapsulated clusters of the same size cultured in 20%, 2%, or 1%. Chapter 4 reports how overall hypoxic status of ADSC spheroids, as indicated by the reporter, can be intentionally affected by spheroid size and culture oxygenation in order to direct optimal secretion of proangiogenic growth factors from the cells.
- Chapter 5 discusses the overall findings of the previous three chapters, tying together the results and making an argument for the importance of considering oxygen tension in cell-based therapies. The novel results of these studies as well as their contribution to the advancement of β-cell and ADSC transplantation are presented.

Chapter 1

Literature Review

1.1 Oxygen's Role as a Nutrient

Oxygen is an abundant element in nature, existing commonly as colorless, odorless dioxygen gas (O_2), or forming oxides with most other elements. Estimates suggest that oxygen presently accounts for roughly 49% (wt.) of Earth's crust and 21% (vol.) of Earth's atmosphere [**1** Duursma and Boissan, 1994]. Furthermore, molecular oxygen has been present in the environment, at varying levels, for the majority of the time span over which life has been evolving [**2** Castresana 1995],[**3** Dismukes 2001],[**4** Kump 2008],[**5** Stamati 2011]. From its ubiquity, it is not surprising, then, that oxygen plays an integral role in the biochemical processes of most known species. While certain unicellular organisms with ancient evolutionary origins have retained the capability to survive without oxygen, most other unicellular organisms, and virtually all multicellular ones, are dependent upon oxygen for survival. Indeed, incorporation of oxygen into biotic biochemistry may have been a prerequisite for the development of metazoan life [**3** Dismukes 2001],[**5** Stamati 2011]. The importance of oxygen to human biology, for instance, is evidenced by the complex mechanisms that have evolved to facilitate its availability: respiratory organs (lungs) to take in oxygen, carrier molecules (hemoglobin) to bind it, and a circulatory system (heart and blood vessels) to distribute

it throughout the body. In this regard, oxygen can be considered a nutrient, a chemical used in an organism's metabolism that is required to sustain its life and which must be taken in from its external environment [**6** Whitney 2005].

1.1.1 Aerobic Respiration

In living organisms, the presence of oxygen allows for increased efficiency in energy production. Organisms that do not utilize oxygen for energy production depend solely upon the process of glycolysis for the direct formation of adenosine triphosphate (ATP) and are termed "anaerobes". Anaerobes are typically unicellular and prokaryotic. Alternatively, aerobes use oxygen as the final electron receptor in the process of oxidative phosphorylation, a series of reactions that generate 16-18 times more ATP than glycolysis. In aerobic cells, mitochondria, the organelles in which the oxidative phosporylation process occurs, can account for 85-90% of cellular oxygen consumption [**7** Solaini 2010].

In the process of oxidative phosphorylation, pyruvate, the product of glycolysis, is further broken down in the citric acid cycle to produce more ATP as well as the reduced form of the molecules nicotinamide adenine dinucleotide (NADH) and flavin adenine dinucleotide ($FADH_2$), which act as energy carries (Figure 1.1). NADH and $FADH_2$ donate electrons to the electron transport chain (ETC), a series of membrane-associated protein complexes that are sequentially reduced by the electrons, resulting in protons being pumped out of the inner mitochondrial compartment against their concentration gradient. The electrons are finally passed to the enzyme, cytochrome-c oxidase (COX), which uses four electrons to catalyze the reduction of one molecule of O_2

to two molecules of water [**8** Brunori 1987]. The proton gradient generated by the ETC is used by the transmembrane protein complex, ATP synthase, to generate ATP (Figure 1.2). It is estimated that nearly 40% of the energy represented in the oxidation of glucose is converted to energy in the form of ATP [**9** Bergamini 2004], making aerobic respiration a highly efficient biological reaction.

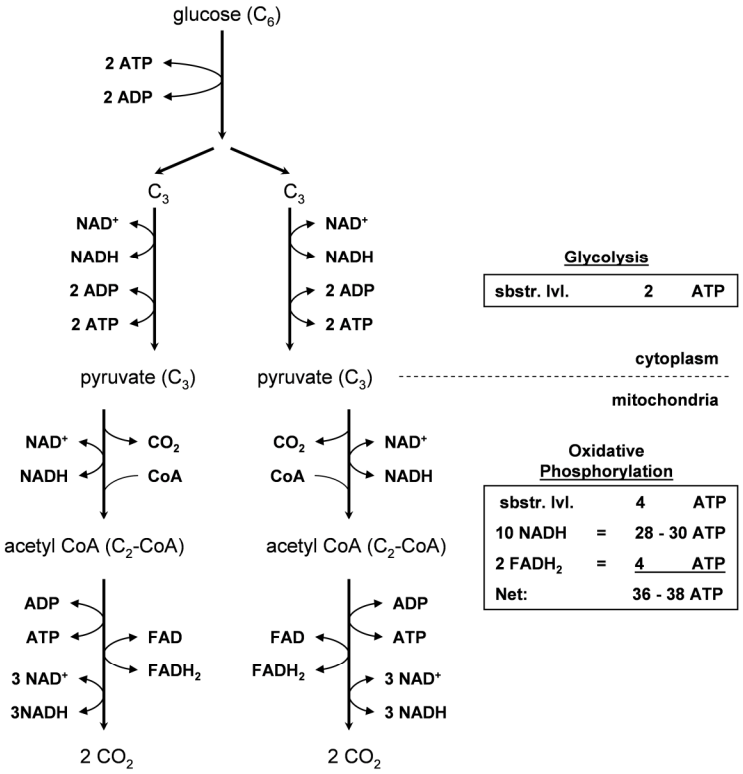

Figure 1.1 Production of energy-carrying molecules in aerobic cellular respiration. Comparison of ATP production in the aerobic and anaerobic processes is also shown. (ADP: adenosine diphosphate; CO_2: carbon dioxide; acetyl CoA: acetyl co-enzyme A)

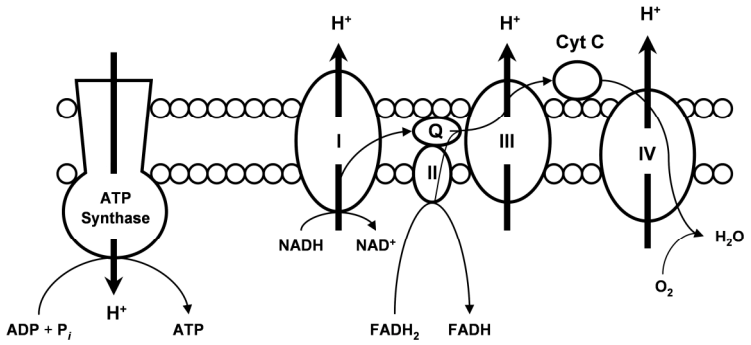

Figure 1.2 Schematic of the ETC and production of ATP by proton motive force. NADH and $FADH_2$ initially donate electrons to different complexes in the ETC, resulting in the transfer of a different number of protons for the two molecules.

1.1.1.1 Aerobic Respiration and Organismal Complexity

The energy yield from anaerobic respiration is relatively small in comparison to aerobic respiration. This energy limitation necessarily limits the diversity of molecules that can be produced in anaerobic species, and, in turn, restricts their potential size and complexity. Raymond and Serge predicted that at least 1000 metabolic reactions which occur in aerobic metabolism cannot occur under anaerobic processes [**10** Raymond 2006]. Specifically, these tend to be synthesis reactions of larger, more hydrophilic macromolecules. Additionally, certain molecules, such as sterols, that are essential to complex, compartmentalized cells, require oxygen for their biosynthesis and are thus typically lacking in anaerobic organisms [**11** Summons 2006]. Furthermore, elevated metabolic levels resulting from aerobic respiration have been suggested to have contributed to the development of nuclear signaling pathways in eukaryotes, as many nuclear factors are products of respiration [**12** Jiang 2010]. Thus, it is clear that the rise

of atmospheric oxygen and the emergence of aerobic metabolism were critical to the evolution of complex metazoans whose energy demands cannot be met by glycolysis alone [**5** Stamati 2011],[**12** Jiang 2010],[**13** Thannickal 2009]. In fact, oxygen is noted to be among the most commonly-used molecules in the metabolic and biosynthetic processes of multicellular animals [**10** Raymond 2006].

1.1.1.2 Aerobic Respiration and Reactive Oxygen Species

Evolution of the ability to use oxygen in the production of energy was a boon to organismal complexity. However, use of oxygen in metabolism presents a set of challenges for aerobic life forms. The large energy release from the reduction of O_2 to water is harnessed during oxidative phosphorylation in a series of less energetic reduction reactions in the ETC. Electron "leak" during these steps can result in premature and incomplete reduction of O_2 and formation of several different oxygen metabolites such as hydrogen peroxide (H_2O_2), superoxide anions ($\cdot O_2^-$), or hydroxide radicals (HO·). These products, known as reactive oxygen species (ROS), are significantly less stable than molecular oxygen and interact with other biomolecules much more readily than O_2.

At least nine mitochondrial enzymes in the ETC have been found to measurably contribute to ROS production in mammalian cells [**14** Andreyev 2005]. In fact, it has been estimated that 2-3% of the molecular oxygen utilized by mitochondria in oxidative phosphorylation is incompletely reduced [**15** Gibson 2008]. If not neutralized, excessive ROS levels can be extremely toxic to a cell. ROSs have the ability to damage lipids, proteins, and deoxyribonucleic acids (DNA), among other cell constituents [**9** Bergamini

2004],[**16** Chance 1955]. Furthermore, oxidative damage by ROSs to certain enzyme complexes involved in the ETC can cause an increased generation of more ROSs in a feed-forward manner. Cellular damage caused by ROSs is collectively referred to as "oxidative stress" and can result in cell death. The negative impact that ROSs can have on cellular function can be implied from the considerable number of protective mechanisms that aerobic cells have developed for detoxifying ROSs or mitigating their damage [**14** Andreyev 2005].

1.1.2 Hypoxia

In 1772, Joseph Priestley showed that depletion of an essential element in air by a mouse in a sealed glass jar resulted in the animal's death, and that a plant placed in the jar could restore the air's vitality [**17** Priestley 1772]. The element was subsequently isolated and identified as oxygen [**18** Lavosisier 1789]. The word "hypoxia" ("hypo" – low or less, and "oxia" – referring to oxygen), then, denotes a state of reduced oxygenation within a biotic environment, often used to mean "oxygen insufficiency". In humans, some common causes of hypoxia within bodily tissues include environmental limitation (thin air), respiratory disorder, blood disorder (anemia), vascular damage/occlusion, and elevated metabolic use (exercise). From Priestley's experiment, it is clear that the dire, organismal-level effects of hypoxia have long been known.

Different species can exhibit different tolerances to hypoxia. For instance, loggerhead turtles, marine reptiles, have been found to dive underwater for up to seven hours before resurfacing [**19** Hochscheid 2005], while sperm whales, marine mammals, can dive for thirty minutes to an hour [**20** Watkins 2002]. For many common terrestrial

mammals, including humans, the survival time without oxygen is generally found to be 4-6 minutes. (Indeed, Irving estimated that the maximal theoretical store of oxygen in an average adult male would be completely consumed by resting metabolism in no more than 11 minutes [**21** Irving 1939].) Resistance to hypoxia also varies among different types of tissue, depending largely upon their metabolic activity and energy requirement. For instance, the estimated survival times of different human tissues without oxygen vary widely: brain, < 3 min.; kidney and liver, 15-20 min.; skeletal muscle, 60-90 min.; vascular smooth muscle, 24-72 hrs.; hair and nails, several days [**22** Leach 1998]. However, no matter the cellular or organismal tolerance for hypoxia, all forms of life that are dependent upon aerobic respiration succumb to oxygen deprivation of sufficient severity or duration.

1.1.2.1 Hypoxia: Notes on Terminology

The term "hypoxia" is applied somewhat ambiguously in the biomedical literature, describing either an oxygen range, typically 0% – 5% O_2, or a comparative oxygen tension that is below the physiological norm for a given tissue. The difference is subtle yet relevant, as the native oxygen environment can vary significantly between different tissues in the body. For instance, from Table 2.1 it can be seen that some tissues constantly reside in an environment that is traditionally considered hypoxic, while others can experience a significant reduction in oxygen from normal levels while remaining above an oxygen partial pressure (pO_2) of 5% [**23** Carreau 2011],[**24** Fermor 2007].

Table 1.1 Normal pO_2 values reported in different human tissues.

Tissue	pO_2 mmHg	pO_2 %
Articular Cartilage		
superficial	53	7
deep zone	<7.6	<1
Bone Marrow	52-55	6.8-7.2
Brain	24-48	3.2-6.3 (>4.6 ensures normal function)
Intestine		
small bowel wall	61	8.0
solon wall	34	4.5
Kidney		
cortex	50	6.6
medulla	10-20	1.3-2.6
Liver	31-42	4.1-5.5
Lungs		
alveolar surface	100-120	13.2-15.8
Muscle		
biceps	25	3.3
deltoid	34	4.5
gastrocnemius	29	3.8
quadriceps femoris	32	4.2
tibial muscle	21	2.8
Skin		
superficial region	8	1.1
dermal papillae	24	3.2
sub-papillary plexus	35	4.6

Compiled from references in **24** Carreau 2011 and **24** Fermor 2007.

Due to such imprecise terminology, attempts to clarify the language have been sporadically, though increasingly, seen. The more accurate terms “atmospheric normoxia” and “hyperoxia” have been used to describe atmospheric oxygen pressure, while “physiological normoxia”, “physioxia”, and “in situ normoxia” have been used to express normal physiological oxygen pressure [**23** Carreau 2011],[**25** Ivanovic 2009]. For such discriminating authors, “hypoxia” is reserved to denote an abnormally reduced pO_2. Such descriptions are further complicated, however, by the somewhat variable reports

of the "physionormal" pO_2 range, e.g. 3-10% [**23** Carreau 2011], 2-9% [**26** Simon 2008], 3-5% [**27** Semenza 2012a], 1-14% [**5** Stamati 2011]. Additionally, normal tissue oxygen pressure can vary from individual to individual and can be affected by various activities. In any case, the traditional use of "normoxia" to represent atmospheric oxygen pressure (21%) and "hypoxia" to represent oxygen pressures below 5% persists in the vast majority of the published literature.

That conditions which are traditionally viewed as "hypoxic" can be both physionormal and pathological depending upon the local microenvironment is a central theme of the present work. In either case, oxygen tension acts as a stimulus, affecting cell behavior and function. Therefore, this work will attempt to characterize "hypoxia" in such terms.

1.1.2.2 Hypoxia: Effects of O_2 Limitations on Aerobic Respiration

Lack of oxygen is lethal to cells that rely on aerobic respiration, though the process of hypoxic cell death is not always straightforward. Some cellular effects of hypoxia can include dramatically reduced protein production and turnover, mitochondrial derangement, loss of osmotic balance, increased oxidative stress, and cell death by necrosis, apoptosis, or autophagy [**7** Solaini 2010],[**28** Hochachka 1996],[**29** Shimizu 1996], [**30** Zhang 2008],[**31** Azad 2008],[**32** Kumar 2010]. As O_2 is required to accept electrons at the end of the ETC, it would be reasonable to assume that a paucity of oxygen would result in the dysfunction of oxidative phosphorylation. Indeed, in a traditional view, hypoxic cell death proceeds as follows: inhibition of the ETC, cessation of ATP production, depletion of ATP pools through utilization in cellular processes,

failure of membrane ion pumps, loss of osmotic balance, and, finally, necrotic cell death. However, more thorough investigations over the past several decades have found that disruption of the ETC due to oxygen limitation is not normally the precipitating cause of death in hypoxic cells.

By examining the relationship between oxygen concentration and electron flux in isolated mitochondria, it was found that COX activity did not become oxygen limited until oxygen concentrations fell below <0.1% [**33** Wilson 1979],[**34** Erecinska 1982],[**35** Rumsey 1990]. In other words, the ETC could still function to produce ATP even at oxygen concentrations well below the levels of physiological hypoxia. Interestingly, global cellular responses to hypoxia are often seen at oxygen concentrations in the range of 1-3% O_2, higher than the concentration at which oxygen becomes limiting for ETC function [**36** Schumacker 1993] [**37** Budinger 1996],[**38** Chandel 1997],[**39** Budinger 1998]. Such changes include reduction of energy-intensive processes, activation of glycolytic pathways, and changes in mitochondrial respiratory rate. This implies, somewhat counter intuitively, that instead of oxygen-limited mitochondrial function altering cellular function, altered cell function triggered by hypoxia seems to alter mitochondrial function. Indeed, it was found that cellular ATP utilization is the primary factor influencing respiration rate in most cells, accounting for up to 50% of the control over the process, while the ETC account for only 0-15% [**40** Brown 1990a],[**41** Brown 1990b].

Suppression of mitochondrial oxygen consumption in the range of 1-3% O_2 is referred to as oxygen conformance and is a well-documented phenomenon [**28**

Hochachka 1996]. When this occurs, an increase in glycolytic respiration is usually seen. Though much less efficient than the aerobic process, glycolysis can proceed quickly and makes ATP availably directly into the cytoplasm. Thus it can provide a significant amount of ATP for a cell in the short term. However, glycolysis also uses glucose much more rapidly that aerobic respiration. In conditions where *both* oxygen and nutrient availability are limited (such as ischemia, or severe hypoxia in cells with a high energy demand) glycolytic glucose insufficiency can result in ATP depletion, loss of osmotic balance, and necrosis, as predicted by the traditional view of hypoxia [**42** Eguchi 1997].

That the oxygen-dependent chemical reaction in the aerobic metabolic pathway is not oxygen-limited when cells begin to exhibit a response to hypoxia indicates that nutritional oxygen (i.e. oxygen as a simple metabolic substrate) cannot be responsible for the changes in cell behavior. However, such adaptive behaviors are clearly a direct response to changes in oxygen concentration, implying that oxygen must be involved in affecting behavior by some other oxygen-sensitive pathways. Thus, it is clear that beyond simply serving as a nutrient, oxygen must also play a role in cell signaling events. This role, and the mechanisms by which it is facilitated, will be discussed in the following section.

1.2 Oxygen's Role in Cell Signaling

The ability of cells to react/adapt to low oxygen tension implies the existence of cellular mechanisms for sensing oxygen and subsequently transmitting signals to alter cell behavior. One of the earliest examples of such signaling to be discovered was the ability of low pO_2 to alter the ionic conductance of cells within the carotid body in the

carotid artery, triggering electrical signaling of the central nervous system to affect breathing and arterial tone [**43** López-Barneo 1988]. Another such oxygen-sensitive response is the upregulation of erythropoietin (EPO), the hormone responsible for red blood cell maturation, in oxygen deficient kidney and liver cells, also investigated in the mid eighties [**44** Bondurant 1986],[**45** Schuster 1989]. Following these observations, the subsequent, pervading assumption held that oxygen sensing in the body was accomplished primarily by such variously-distributed, specialized cells. However, work in the early 1990's by the Semenza group uncovered a universal oxygen-sensing/signaling mechanism common to all nucleated cells in humans and well conserved in most vertebrates. This mechanism was determined to be the primary means by which all cells regulate oxygen homeostasis, adapting energy consumption to oxygen supply and avoiding excessive ROS formation. Furthermore, continued research over the ensuing two decades has slowly revealed how low oxygen tension and the cellular behaviors that it drives are an ordinary and indispensible part of many cell functions and of normal organismal development. As tissue engineering and regenerative medicine perspectives take an increasingly prominent position in the advancement of medical therapies, it will be essential to consider oxygen's role not only as a nutrient but as a potent signaling molecule, influencing a myriad of cell behaviors.

1.2.1 Hypoxia Inducible Factors: The Master Regulators of Response to Hypoxia

Hypoxia-inducible factor-1 (HIF-1), first identified by Semenza and Wang in 1992 [**46** Semenza 1992], is an oxygen-regulated transcription factor, commonly referred to as the master regulator of hypoxia. Since its discovery, two other HIF-family proteins,

HIF-2 and HIF-3, have been identified. Beyond simply helping cells cope with reduced oxygenation, HIF proteins have been found to drive important cell behaviors involved in embryonic development, cell commitment and maturation, and healing, as well as pathologies such as cancer. As HIF-proteins appear to regulate the majority of observable changes in cell behavior in response to reduced oxygen tension, the presence of cellular HIF activity has the potential to be more instructive regarding cell behavior than measuring local oxygen concentration.

1.2.2 HIFs: Discovery

The observation of oxygen conformance in mitochondria suggested a widespread mechanism of oxygen sensing common to all cells [**28** Hochachka 1996]. Using DNase I protection assays to examine the mechanism of EPO responsiveness to oxygen in human hepatoma cells, Semenza et al. first identified a 256-base-pair region in the EPO gene that bound at least two anemia-induced nuclear factors and which conferred hypoxia inducibility when transiently expressed in other genes [**47** Semenza 1991]. Further examination of this region delineated the essential 50-nucleotide enhancer sequence, which was termed the hypoxia responsive element (HRE) and identified a nuclear factor, HIF-1α, which exhibited hypoxia-inducible binding to the HRE [**46** Semenza 1992]. In the hepatoma cells, presence of a functional HRE resulted in a seven-fold increase in EPO production in response to hypoxia (1% O_2).

Maxwell et al. soon showed that the HRE elicited hypoxia-responsive transcription in a number of other cell types as well [**48** Maxwell 1993]. Human fetal lung fibroblasts, human skin fibroblasts, human monocyte/macrophage cells, monkey

renal fibroblasts, pig retinal epithelial cells, rat aortic endothelial cells, Chinese hamster lung fibroblasts, Chinese hamster ovary cells, mouse renal adenocarcinomas, and mouse erythroleukemias were transiently transfected with a plasmid containing the HRE enhancer fused to a broadly active promoter and the α_1-globin gene as a reporter. In 1% oxygen, 11 of the 12 tested lines demonstrated a 3- to 11- fold induction of α_1-globin production, similar to the original observations in hepatomas [**48** Maxwell 1993]. This implied that the same hypoxia-responsive nuclear factor responsible for HRE binding and EPO upregulation in hepatomas must be present in a range of cell types and may represent a widespread mechanism for response to hypoxia. Indeed, Wang and Semenza observed that a number of mammalian cell types which did not express the EPO gene still exhibited binding of HIF-1 to DNA and that the binding site was the same conserved HRE sequence [**49** Wang 1993a]. Weiner et al. later demonstrated HIF-1 expression in every mammalian tissue they tested: brain, kidney, liver, heart, placenta, pancreas, and skeletal muscle tissue in mice, rats, and humans [**50** Weiner 1996]. Subsequent investigation has found that HIF-1 and its oxygen-sensitive regulator mechanism are conserved in all aquatic and terrestrial vertebrates [**51** Rytkönen 2011].

1.2.3 HIFs: Structure

HIF-family proteins are heterodimeric transcription factors comprising a constitutively-expressed and stable β subunit and one of three constitutively-expressed α subunits, subject to post-transcriptional, oxygen-dependent regulation. The β subunit is also known as the aryl hydrocarbon receptor nuclear translocator (ARNT). The α subunits are termed HIF-1α, HIF-2α, and HIF-3α, with HIF-1α being the most prominent

and most well-studied (though the importance of non-redundant activities regulated by HIF-2α is becoming more well-elucidated).

Both α and β subunits have been identified as members of the basic Helix-Loop-Helix PER-ARNT-SIM (bHLH-PAS) family of transcription factors [**52** Wang 1995]. Kewley et al. review the biology of this family of proteins [**53** Kewley 2004]. bHLH-PAS transcription factors are often signal-regulated and bind to non-traditional variants of the classic E-box enhancer. In the case of HIF heterodimers, the specific recognition sequence is the HRE found in the promoter region of target genes. The conserved portion of this recognition sequence is 5'-(A/G)CGTG-3' [**54** Semenza 1996]. The PAS domain is named for three proteins in which the domain was originally identified: Period Circadian Protein (PER), ARNT, and Single-Minded Protein (SIM). Signals mediated by PAS domains in various organisms include redox state, xenobiotic metabolism, light detection, and oxygen balance [**55** Taylor 1999].

Members of the bHLH-PAS family must dimerize to become functional and are defined by two major domains: 1) a bHLH domain near the N-terminus, termed the N-terminal transactivation domain (NTAD), responsible for nonspecific dimerization [**56** Murre 1989],[**57** Reisz-Porszasz 1994],[**58** Ema 1996],[**59** Jiang 1996a],[**60** Kobayashi 1997], with the basic region being the site of DNA binding [**61** Ferré-D'Amaré]; and 2) a PAS homology domain which establishes dimerization partner specificity and target gene specificity [**55** Taylor 1999],[**62** Pongratz 1998],[**63** Crews 1999]. In addition, HIF-α subunits contain an oxygen-dependent degradation domain (ODD), while HIF-1α and HIF-2α contain a C-terminal transactivation domain (CTAD) which interacts with

transcriptional co-activators to help initiate transcription [**64** Jiang 1997],[**65** Huang 1998],[**66** Ema 1999],[**67** O'Rourke 1999],[**68** Maynard 2003]. While HIF-β is known to interact with a number of other bHLH-PAS proteins, HIF-1α dimerizes almost exclusively with HIF-β. In humans, HIF-1α is encoded by the HIF1A gene, HIF-2α is encoded by the endothelial PAS domain protein 1 (EPAS1) gene, and HIF-3α is expressed as multiple splice variants of the HIF3A gene [**52** Wang 1995], [**68** Maynard 2003],[**69** Makino 2002].

1.2.4 HIFs: Transcriptional Activity

HIF-α is constitutively produced in the cytoplasm where it is rapidly degraded in the presence of oxygen. When oxygen concentrations drop and HIF-α levels rise, the protein is translocated to the nucleus where it is free to dimerize with HIF-β [**70** Chilov 1999]. Translocation may be partially dependent upon mitochondrial succinate [**71** Brière 2005]. In the nucleus, the HIF heterodimer binds to HRE sequences in target genes and recruits the CREB-binding protein/p300 (CBP/p300) transcriptional coactivator complex to initiate transcription [**66** Ema 1999],[**72** Arany 1996],. Both HIF stability and the ability of HIF dimers to interact with the CBP/p300 complex are regulated in an oxygen-dependent manner.

1.2.5 HIFs: Regulation

Following its discovery, it was known that HIF-1α was regulated by oxygen but was not itself responsible for oxygen sensing. Due to their direct chemical interactions with molecular oxygen, COX and heme proteins were first suggested as likely oxygen-sensing candidates [**28** Hochachka 1996]. (It was later shown that HIF-α can be

stabilized even in the absence of functional ETC machinery, including COX [**73** Brunelle 2005].) In 2001, however, it was discovered that a member of the conserved family of prolyl-4-hydroxylases (PHDs) [**74** Epstein 2001],[**75** Bruick 2001], specifically prolyl 4-hydroxylase 2 (P4H2) [**76** Berra 2003], was the cellular oxygen sensor and regulator of oxygen-dependent degradation of HIF-α. Since then, several other mechanisms of HIF regulation, either directly or indirectly dependent on oxygen, have been identified or suggested.

1.2.5.1 Regulation of HIF-α Protein Stability

Activation of HIF-1 is oxygen-dependent and is regulated by stability of the HIF-1α protein subunit. Both HIF-1α and HIF-1β messenger ribonucleic acids (mRNAs) are constitutively expressed intracellularly, but HIF-1α protein levels are nearly undetectable in normoxic cells, even when HIF-1α is overexpressed. In hypoxic cells, high levels HIF-1α are observed, but HIF-1β levels are unaffected. Both intracellular levels of HIF-1α and DNA binding of HIF-1 rapidly decrease upon re-introduction to normoxia [**77** Huang, 1996].

Examination of HIF-1α by Ratcliffe et al. revealed a region of the protein between amino acids 530 and 652, the ODD, which conferred oxygen-dependent repression when transferred to a reporter gene system [**78** Ratcliffe 1998]. They suggested that the mechanism of regulation may be mediated by proteolytic degradation. It was later found that P4H2 was responsible for hydroxylating HIF-1α within this region [**76** Berra 2003]. Specifically, it was shown that P4H2 hydroxylates two key proline residues, proline 564 [**79** Ivan 2001] and proline 402 [**80** Masson 2001],

in the ODD which allows for its recognition by the E3-ubiquitin ligase complex. Activity of the HIF PHD family of enzymes is dependent on Fe^{2+}, α-ketoglutarate (2-oxoglutarate), and ascorbic acid as co-factors and O_2 as a cosubstrate. In the case of HIF-1α, P4H2 catalyzes a dioxygenase reaction in which one oxygen atom is inserted into the proline residue and the other is inserted into α-ketoglutarate to form succinate and CO_2 [**81** Schofield 2004]. Thus P4H2 serves as the global, cellular oxygen sensor. In the presence of oxygen, P4H2 mRNA is upregulated [**74** Epstein 2001] and the hydroxylation reaction with HIF-1α proceeds. When oxygen is limited, the reaction does not take place and HIF1α is not hydroxylated. In addition, the protein, OS-9 can interact with both HIF-1α and P4H2 to promote degradation [**82** Baek 2005]. The requirement of Fe^{2+} as a cofactor explains the ability of iron chelating agents, such as cobalt chloride and desferoxamine, to induce a hypoxic response in cells.

Hydroxylated HIF-1α is recognized by the von Hippel-Lindau tumor suppressor protein (pVHL), the β-domain of which interacts with the hydroxylated moieties in the HIF-1α ODD. The α-domain of pVHL then recruits elongin B, elongin C, cullin-2, and ring-box 1 to form a complex which covalently links a chain of ubiquitin moieties to the ODD. Polyubiquitinated HIF-1α docks with the 26S proteasomal complex which selectively degrades ubiquitinated proteins [**83** Maxwell 1999],[**84** Ohh 2000]. The protein, SSAT2, helps to stabilize the interaction of pVHL with elongin C thus facilitating ubiquitination of HIF-1α. [**85** Baek 2007]. Degradation by this pathway is rapid; cytoplasmic HIF-1α is nearly undetectable under normoxic conditions, and the half-life of stabilized HIF-1α is approximately 5 minutes upon cellular reoxygenation.

The canonical pathway of HIF protein regulation, then, is as follows: In the presence of oxygen, P4H2 hydroxylates HIF-1α, which can than be recognized by pVHL and quickly degraded by the E3-ubiquitin ligase complex. In the absence of oxygen, hydroxylation of HIF-1α does not occur and intracellular levels of the molecule increase.

1.2.5.2 Regulation of HIF-α Transcriptional Activity

The transcriptional activity of HIFs can also be regulated in an oxygen dependent manner. HIF-α contains a nuclear localization signal in its CTAD, allowing stable HIF-α to rapidly bind to nuclear pore proteins and translocate into the nucleus [**86** Kallio 1998]. Once there, it is free to pair with HIF-β to form a functional HIF dimer. Ema et al. found that the CTAD of HIF-α in the nucleus interacts with CBP/p300 to initiate transcription of target genes [**66** Ema 1999]. A key asparagine residue in this region (asparagine-803 in HIF-1α and aspargine-851 in HIF-2α) can be hydroxylated by another hydroxylase-domain protein, termed factor inhibiting HIF (FIH), in the presence of oxygen [**87** Lando 2002a]. The modification sterically inhibits HIF-α from interacting with CBP/p300, necessary components of the transcription machinery [**88** Lando 2002b]. P4H2 has a K_m for oxygen that is approximately 3 times greater than FIH; therefore, in moderately reduced oxygen conditions in which HIF-α is beginning to be stabilized due to declining P4H2 activity, FIH can still repress HIF activity by inhibiting DNA binding [**89** Koivunen 2004].

As both major mechanisms for regulating HIF activity are hydroxylase-dependent, it is clear that hydroxylases are central to cellular hypoxic responses. It is not surprising then that, like HIF proteins themselves, the HIF regulatory hydroxylases also appear to

be highly conserved in vertebrates. Figure 1.3 summarizes how hydroxylase-domain proteins act in regulating HIF.

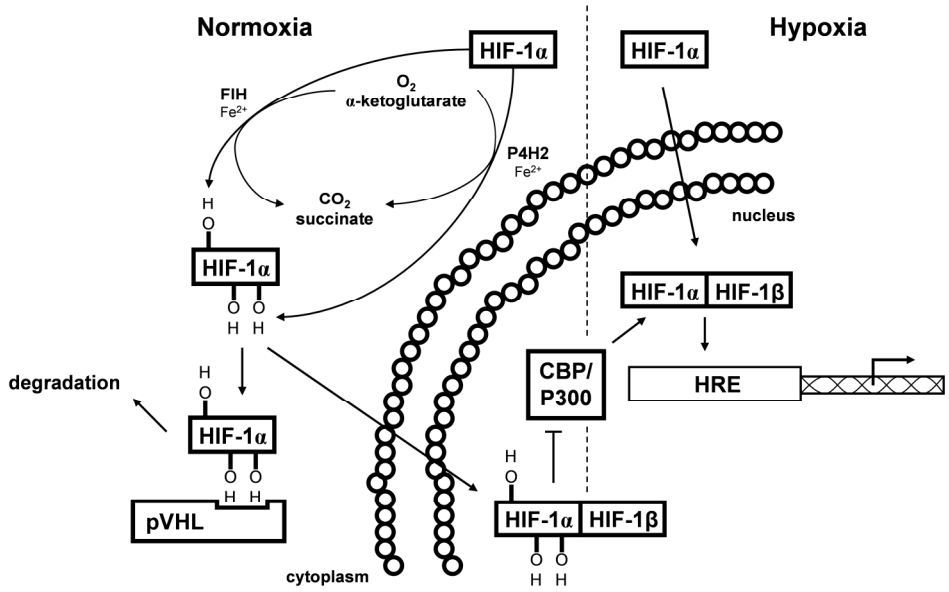

Figure 1.3 Oxygen-dependent mechanisms of HIF regulation. In normoxia, HIF-1α is constitutively expressed but protein levels are kept low by rapid ubiquitination and proteosomal degradation. Activity of any non-degraded HIF-1α is suppressed by the failure of the p300 co-activator to bind. In hypoxic conditions, oxygen dependency of both hydroxylases, P4H2 and FIH, prevents HIF-1α modification, inhibiting degradation and allowing for dimerization and binding of co-activators.

1.2.5.3 Additional Factors in HIF regulation

Though there seems to be limited redundancy in HIF regulation, several factors other than PHDs can influence HIF activity in both oxygen-sensitive and oxygen-independent manners. Specifically, agents which have the ability to affect HIF mRNA stability, PHD catalytic activity, pVHL affinity/polyubiquitination, and complexing of HIF/BCP/p300/HRE can modulate HIF activity. Several miRNAs and mRNA-destabilizing proteins have been shown to interfere with HIF-α mRNA stability [**90** Taguchi 2008],[**91**

Bruning 2011],[**92** Chamboredon 2011]. It has also recently been shown that the protein RACK-1 can bind to HIF-α and elongin C to recruit an E3 ubiquitin protein-ligase complex in lieu of pVHL [**93** Liu 2007]. This process is not dependent upon oxygen. ROSs also appear to play a role in HIF regulation, presumably by oxidizing hydroxylase-bound Fe^{2+} and abrogating its ability to serve as a cofactor in hydroxylating reactions [**94** Pan 2007]. SIRT-3 was shown to help destabilize HIF-α by inhibiting ROS production [**95** Finley 2001]. It is interesting to note that ROSs contribute to stabilizing HIF, as one of the major behaviors regulated by HIF is oxygen conformance of the mitochondria. Reducing oxidative phosphorylation in conditions of low oxygen presumably help limit excessive ROS production which would lead to cell damage. It is not surprising to find, then, that several metabolic intermediates of the citric acid cycle have also been reported to inhibit hydroxylase activity, including citrate, isocitrate, malate, oxaloacetate, pyruvate, succinate, and fumarate, [**96** Kaelin 2008]. Luo et al. also found that pyruvate kinase isoform M2 (PKM2), the enzyme that catalyses the final step in glycolysis, can function as a coactivator of HIF-α [**97** Luo 2011]. PKM2 can associate directly with HIF-1/2α and p300 to enhance their binding to HREs. Additionally, the mammalian target of rapamycin (mTOR) protein has been shown to enhance HIF activity, and this enhancement could be inhibited by rapamycin [**98** Semenza 2003],[**99** Land 2007]. Finally, very recent studies have suggested that epigenetics are involved in the regulation of HIF, with DNA and histone modifications altering accessibility and transcribability of HIF target genes [**100** Tanimoto 2010],[**101** Mimura 2011],[**102** Xu 2012],[**103** Vanharanta 2013],[**104** Nguyen 2012].

1.2.6 Gradation of HIF Response

The sensitivity of P4H2 to changes in oxygen concentration also imparts a graded responsiveness of HIF-1 to O_2. Jiang et al. exposed HeLa cells to oxygen concentrations ranging from 0% to 20% and measured levels of both HIF-1 subunit proteins as well as HIF-1 DNA binding [**105** Jiang 1996b]. As expected, the HIF-1α subunit was dramatically responsive to oxygen concentration. Between 20% and 6% oxygen, HIF-1α levels and DNA binding modestly increased as oxygen concentration decreased. However, below 6% oxygen both HIF-1α and HIF-1 DNA binding increased exponentially to reach maximal values at 0.5% oxygen. Half-maximal responses were observed between 1.5 and 2% oxygen. Thus, the majority of HIF-1 activity takes place over a physiologically relevant range of oxygen (0 - 5%), with the largest response occurring at physiologically hypoxic levels (0.5 - 1.5%).

Bracken et al. tested the graded response of HIF-1 in a similar set of experiments with a variety cell lines: HEK293T, HeLa, COS-1, HepG2, CACO-2, and PC12 cells [**106** Bracken 2006]. In every case, they also found an exponential increase in HIF-1α protein levels as oxygen was decreased from 5% to <1%. However, though HIF-1 activity, as measured by reporter protein production, was also maximal below 1% oxygen, the response did not always match HIF-1α protein levels. In addition to differences in maximal reporter protein production levels between cells types, they noted two categories of response. Some cells gradually increased reporter protein production as oxygen decreased from 10% to <1%. Others required an oxygen concentration of <2% before exhibiting a dramatic increase in reporter protein production, which much more

closely coincides with changes in HIF-1α levels. This indicates that hypoxia is better defined by cellular response than by absolute oxygen concentration.

1.2.7 Kinetics of HIF Response

The rate of HIF degradation/stabilization is also important to the responsiveness of its activity. Traditional immunoprecipitation assays reveal a half-life for HIF-α of approximately 5-8 minutes in normoxic conditions [**65** Huang 1998],[**107** Jaakkola 2001],[**108** Jeong 2002]. Using a firefly luciferase reporter protein fused to the HIF-1α gene, Moroz et al. reported a half-life of 4-6 minutes for the factor [**109** Moroz 2009]. However, though HIF-α is very unstable in normoxia, HIF-α mRNA is constitutively expressed and the protein is constantly produced. Additionally the K_m of P4H2 for O_2 is just above the concentration of O_2 in air. This high value ensures that even a small decrease in oxygen is likely to have a significant effect on P4H2 activity [**110** Hirsila 2003]. Thus HIF-1 can be both a highly-sensitive and rapidly-responsive initiator of hypoxia response.

Wang and Semenza studied the kinetics of HIF-1α protein stabilization and DNA binding in hepatoma cells exposed to 1% oxygen for 0-4 hours [**111** Wang 1993b]. They found that HIF-1 activity was first detectable within 15 minutes, with 8% maximal activity at 30 minutes, 50% maximal activity between 1 and 2 hours, and maximal activity at 4 hours. After rapid re-exposure to 20% oxygen, HIF-1 activity was reduced to 34% within 5 minutes and was eliminated by 15 minutes. The group also showed that binding of stabilized HIF-1 to DNA occurred rapidly, with 77% binding within 1 minute

and 100% binding within 5 minutes. Likewise, DNA binding decay occurred with a $t_{1/2}$ of 1 minute upon reoxygenation of the cells.

More recently, Jewell et al. used tonometers to rapidly equilibrate suspensions of HeLaS3 cells to various oxygen conditions and study the time-course of HIF-1α accumulation and degradation [**112** Jewell 2001]. Presence and DNA binding of nuclear HIF-1α was detected within 2 minutes of hypoxic exposure, with nuclear HIF-1α protein levels reaching a maximal value by 1 hour. Within 2 minutes of reoxygenation, DNA binding was reduced while nuclear HIF-1α protein levels were reduced within 4-8 minutes and undetectable by 32 minutes. These studies point to the capability of both rapid onset and rapid cessation of hypoxic signaling by the HIF mechanism.

1.2.8 Transcriptional Targets of HIFs

The primary role of HIF-mediated transcriptional regulation is to promote cell survival in acute hypoxia and cellular adaptation to prolonged hypoxia. As a rapid response to hypoxia, HIF mediates global changes in metabolism in order to reduce overall cellular ATP consumption. A traditional view of hypoxia held that lack of oxygen would inhibit oxidative phosphorylation, limiting the production of ATP which would be rapidly depleted if normal cell activities continued. As discussed, more detailed analyses suggest that oxidative phosphorylation is not limited under normal physiological hypoxia, but reduced oxygen concentrations affect its efficiency, resulting in higher levels of premature electron loss from the ETC and greater ROS formation. In order to avoid cellular ROS damage, HIF mediates the reduction of oxidative phosphorylation and the activation of glycolytic metabolism. However, because glycolytic metabolism cannot

sustain the level of ATP production achieved by oxidative phosphorylation, HIF also mediates cell-wide reduction of ATP-intensive activities to avoid depletion.

HIF additionally mediates cell behaviors which function to adapt a cell to prolonged hypoxia or to remediate the hypoxic state. For instance, HIF-induced upregulation of EPO helps to increase the number of oxygen-carrying red blood cells in the local vicinity. Such hypoxia-driven behavioral response are often observed during embryonic development, where the local microenvironmental oxygen concentration helps to inform cells about their relative bodily location and direct the behavioral sequences that are required for normal organismal growth. It is not surprising, then, to find that HIF functioning is mandatory to embryogenesis, with absence of HIF-1 function being embryonic lethal [**113** Maltepe, 1997],[**114** Iyer 1998],[**115** Ryan 1998]. $Hif1a^{-/-}$ mice die at embryonic day 9 due to vascular and cardiac defect/deformity [**114** Iyer 1998],[**116** Melillo 1995].

Because of the number of processes that are linked to cell metabolism, and therefore at least indirectly dependent upon oxygen, HIF has the potential for enormous regulatory oversight in cells. To date, over 100 genes have been identified as direct targets of HIF-1/2 [**117** Loboda 2010]. These genes are involved in any number of cell processes, including energy metabolism, transcriptional regulation, cell cycle and growth, viability and apoptosis, transport, signaling, migration, matrix and barrier function, paracrine activity, and differentiation [**81** Schofield 2004],[**118** Semenza 2000],[**119** Ke 2006]. A list of well-known HIF targets are presented in Table 1.2. Furthermore, because HIFs govern transcription of a large number of other transcription

factors, the number of genes that are indirectly regulated by HIFs is much larger. In fact, by some estimates, as many as 5% of the genes in the human genome are HIF-regulated in hypoxic conditions [**98** Semenza 2003]. In gene expression profiles performed in arterial endothelial cells, Manalo et al. found that the largest group of genes up-regulated by HIF-1 included transcription factors, with cytokines/growth factors, receptors, and other signaling proteins also displaying significant upregulation [**120** Manalo 2005]. Genes downregulated in hypoxia are generally involved in cell growth and proliferation [**120** Manalo 2005],[**121** Goda 2003]. Using chromatin immunoprecipitation and comparing results to genome-wide transcript profiling, other groups likewise found a large number of genes to be up- and downregulated in hypoxia, but reported that only upregulated genes appeared to contain an HRE sequence in the promoter [**122** Mole 2009],[**123**Schodel 2011]. This implies that direct transcriptional regulation by HIF is accomplished almost entirely by gene upregulation (in fact over 20% of genes upregulated in hypoxia were direct HIF targets [**122** Mole 2009]), while down regulation is accomplished indirectly. Indeed, of 191 genes downregulated in hypoxia in five different cell types, Ortiz-Barahona et al. found none of them to be directly targeted by HIF in all five cell types [**124** Ortiz-Barahona 2010].

Table 1.2 Direct transcriptional targets of HIF-1.

Function	Gene/Gene Product	Function	Gene/Gene Product
Glucose Metabolism	Adenylate kinase 3	**Vasomotor Regulation**	Adrenomedullin
	Aldolase A/C		Atrial natriuretic peptide
	Carbonic anhydrase-9		Endothelial nitric-oxide synthase
	Enolase-1		Endothelin-1
	Glucose transporter-1/3		Heme oxygenase-1
	Glyceraldehyde-3-phosphate dehydrogenase		Inducible nitric-oxide synthase
	Hexokinase-1/2		Nitric oxide synthase 2
	Lactate dehydroxygenase A		Tyrosine hydroxylase
	6-Phosphofructo-2-kinase/fructose-2,6-bisphosphate-3		α_{1B}-adrenergic receptor
	Phosphofructokinase L	**Erythropoiesis and Iron Metabolism**	Ceruloplasmin
	Phosphoglycerate kinase-1		Erythropoietin
	Pyruvate kinase M		Multidrug-resistance P-glycoprotein
Survival, Growth, and Apoptosis	Bcl-2/adenovirus E1B 19kD-interacting protein-3		Transferrin
	Calcitonin-receptor-like receptor		Transferrin receptor
	Endoglin	**Matrix Function/ Metabolism**	Collagen prolyl hydroxylase
	Insulin-like growth factor-2		Ecto-5′-nucleotidase
	Insulin-like growth-factor-binding protein-1/3		Intestinal trefoil factor
	Nip3-like protein X		Matrix metalloproteinases
	p21		Procollagen prolyl hydroxylase-α1
	Transforming growth factor-α		
	Wilms' tumour suppressor		
	α-Fetoprotein	**Cell Migration**	Chemokine receptor CXCR4
Angiogenesis	Endothelial-gland-derived vascular endothelial growth factor		c-Met
	Leptin	**Transcriptional Regulation**	DEC1
	Plasminogen-activator inhibitor-1		DEC2
	Transforming growth factor-β3		ETS1
	Vascular endothelial growth factor A		p35srj
	Vascular-endothelial-growth-factor receptor-1		

Compiled from references in **81** Schofield 2004, **118** Semenza 2000, and **119** Ke 2006.

1.2.9 Cell Type Variation in HIF Responses

HIF-mediated responses to hypoxia also display heterogeneity between cell types [**125** Stroka 2001],[**126** Chi 2006],[**127** Gardener 2008],[**128** Brachen 2006],[**129** Lendahl 2009]. Benita et al. examined hypoxia-responsive genes in 7 different cell types and found wide variability in HIF activity [**130** Benita 2009]. Monocytes displayed 486 genes that were differentially expressed in hypoxia while HeLa cells displayed 2119 such genes. Of these genes, 159 and 555, respectively, displayed an HRE sequence in the promoter region. Furthermore, only 17 genes responded to hypoxia in all of the studied cell types. The group concluded that a small subset of HIF direct-target genes, generally involved in the shift from oxidative to glycolytic metabolism and cessation of cellular growth/proliferation, represent the "core" HIF response to hypoxia. Genes that displayed variable responsiveness to hypoxia between cell types were less likely to contain an HRE sequence, suggesting that cell-type variation in gene expression is controlled indirectly by HIF.

Secondary factors that are involved in HIF indirectly-regulated pathways are often affected by a cell's phenotype and current physiologic context. This helps to explain how cellular responses to hypoxia can vary despite similar levels of HIF mRNA expression in most hypoxic cells. For instance, while most cells undergo inhibition of proliferation in hypoxic conditions, vascular endothelial cells are often triggered to divide and migrate under hypoxia as part of the angiogenic response. Likewise, Bcl2/adenovirus E1B 19 kDa protein-interacting protein 3 (BNIP3) and p53 contribute to HIF-regulated apoptotic cell death, while B-cell lymphoma 2 (Bcl-2) family proteins can

promote HIF-regulated cell survival in hypoxia [**127** Gardener 2008]. Because cellular activity can impact the effect of HIF-signaling, it is reasonable to predict that cells whose primary functions involve energy-intensive activities will be more negatively impacted by hypoxia, while cells with low energy requirements should be tolerant of hypoxia. Indeed, this appears to be the case: neurons, pancreatic β-cells, and cardiomyocytes are all highly oxygen dependent, with their primary functions (de/re-polarization, muscle contraction, and insulin secretion, respectively) being severely diminished in hypoxic conditions. Alternatively, articular chondrocytes have very low metabolic requirements and tolerate prolonged hypoxic exposure for the majority of their mature life cycle.

Of recent interest has been how the various HIF isoforms contribute to differential hypoxic responses in different cell types. While HIF-1 is expressed in all metazoan cells, HIF-2 is restricted to specific cell types in vertebrates [**131** Semenza 2011a]. Furthermore while HIF-1 and HIF-2 exhibit some of the same target genes, they can also mediate regulation of different cell functions without overlap. This means that because both HIFs recognize the same HRE sequence in target genes, HRE and PHD binding affinity for HIF-1 versus HIF-2 can influence which responsive cell behaviors are elicited in hypoxia [**132** Kenneth 2008]. While HIF-1 globally regulates genes involved in glycolytic metabolism and complex patterns of genes affecting cell survival versus apoptosis decisions, HIF-2 is only expressed in certain cells of the kidney, liver, pancreas, lung, heart, intestine, and epithelium and does not contribute to affecting glycolysis [**117** Loboda 2010],[**133** Hu 2003]. HIF-2 is prominently expressed in the vascular endothelium during embryonic development and may contribute to maintenance of

normal vascular architecture. It has also been shown to be the primary HIF isoform mediating transcriptional regulation of octamer-binding transcription factor 4 (Oct4), which is crucial to stem cell self-renewal, and transforming growth factor β (TGF-β) [**134** Raval 2005],[**135** Covello 2006]. HIF-3 acts as an antagonist to HIF-1 and HIF-2 by forming a functionally inactive dimer with HIF-β [**136** Makino 2001]. Elucidating the different expression profiles, activities, and roles of the HIF isoforms in different cells/tissues remains an active area of cellular research [**128** Brachen 2006].

1.2.10 HIF: Implications for Identifying Hypoxia

Given the broad array of cellular behaviors that HIFs can mediate, and knowing that physiological hypoxia is a normal and often required condition in organismal growth, development, and activity, it is clear that identification of hypoxic status is of import to biomedical research. However, identifying hypoxia, especially on the cellular level, is tricky. Krohn et al. adroitly explain:

> *"Hypoxia is therefore a phenomenologic concept. There is no specific value of O_2Hb [oxyhemoglobin] concentration, % Hb saturation by oximetry, or tissue partial pressure, PO2 measured with electrodes, that results in a transition from normoxia to hypoxia… The biologic consequences of hypoxia depend on duration and the needs of individual cells…"* [**137** Krohn 2008]

Hypoxia, therefore, may be best defined in terms cell behavioral responses. The following section offers a discussion of current techniques for detecting hypoxia at the tissue and cellular levels, highlighting advantages and disadvantages of each, and

proposes that a fluorescent HIF reporter system is particularly well suited for identifying hypoxia in 3D tissue cultures and engineered tissue constructs *in vitro*.

1.2.10.1 Current Methods for Detecting Hypoxia

Current strategies for identifying hypoxia are typically aimed at either tissue- or cell-level detection. At the tissue level, evaluation usually consists of measuring or analyzing some biomolecule present in the blood or interstitial fluid that is differentially affected in hypoxic conditions. At the cell level, stains or markers are often used to detect intracellular changes indicative of hypoxia. Hypoxia detection strategies can also be categorized by whether they measure environmental conditions (oxygen concentration) or biochemical conditions (behavioral changes).

1.2.10.1.1 Indirect Measures of Hypoxia

Many indirect techniques for imaging hypoxia at the tissue level have come from cancer research, where hypoxia in tumors has been found to be associated with poor outcomes. Magnetic resonance imaging (MRI) can be used to distinguish between oxygenated hemoglobin and deoxyhemoglobin, giving an indication of local oxygen availability in the vasculature of a given tissue [**138** Kim 2005],[**139** Leontiev 2007]. While this technique can be used to assess temporal changes in relative tissue oxygenation, it is not capable of providing quantitative information. MRI can also be used to measure increases in tissue lactate, which builds up as a result of increased glycolytic metabolism. Both of these approaches measure downstream consequences of hypoxia, which can exhibit some lag and also persist for a time even after normoxia

has been restored. MRI can also be used to measure pO_2 directly, using an oxygen-sensitive reporter perfluorocarbon injected into the site of interest [**140** Mason 1993],[**141** Zhao 2004]. This technique is dependent upon adequate perfluorocarbon perfusion of the study tissue. However, for routine *in vitro* studies, use of MRI is impractical. Furthermore, these techniques focus on identifying hypoxia on a tissue-wide scale and may not have the resolution to identify hypoxia on the cellular level.

Various oxygen probes are also used to detect hypoxia. Microelectrodes can precisely measure the local oxygen concentration down to a very small scale, and may offer quantitative information about the oxygen conditions at a specific location, even at the cellular level [**142** Vaupel 1991],[**143** Collingridge 1999],[**144** Kim 2003],[**145** Mason 2003]. However, they require O_2 for detection, meaning that as oxygen concentrations become very small, readings become less reliable. Fluorescent needle type oxygen probes contain a fluorophore which is quenched in the presence of oxygen, eliminating the variability of readings at low oxygen levels [**146** Jorge 2006]. However, oxygen probes of any kind provide only very local information about oxygen concentration and require a large number of evaluations to obtain meaningful spatial information about oxygen distribution. Furthermore, any such probe requires placement in the tissue, leading to damage and inflammatory responses that can alter local tissue oxygen levels.

Nitroimidazoles represent a more direct method for identifying hypoxia. Nitroimidazoles can act as oxygen mimetics, accepting terminal electrons from the ETC. Their affinity for electrons is less than O_2, so that under normal oxygen conditions only low levels of nitroimidazoles are reduced. These molecules are only singly reduced and

can still be easily oxidized by O_2. However, under hypoxic conditions, without competition from oxygen, nitroimidazoles become doubly reduced, forming alkylating agents that react indiscriminately with cellular macromolecules, thus trapping nitroimidazole within the cell [**137** Krohn 2008]. For tissue-wide analysis, the nitroimidazole can be radiolabeled for positron emission tomography (PET) [**147** Adamsen 2005]. Antibodies to the nitroimidazole, pimonidazole (commonly available as Hypoxyprobe-1), have also been prepared. This allows for immunohistochemical staining and analysis of samples for the identification of hypoxia down to the cellular level [**148** Varia 1998],[**149** Olive 2000],[**150** Nordsmark 2003]. A primary disadvantage of histological analyses is that they require the sacrifice of the tissue/construct under study. Therefore, it is not possible to monitor the hypoxic status of the sample over time or in response to changing conditions.

Another approach is to predict the occurrence of hypoxia by computational modeling [**151** Gross 2007],[**152** Cheema 2008],[**153** Buchwald 2009]. Models provide the ability to draw predictive conclusions about expected oxygen concentrations and gradients without the need for cell culture. However, while modeling is a powerful tool, results are only as powerful as the assumptions on which the model is based, which in turn are guided by current knowledge of the system being modeled. Therefore, an incomplete understanding of cellular processes can lead to models which do not accurately recapitulate observed phenomena.

The methods represent indirect approaches to detecting hypoxia. In these techniques, indicators of hypoxia are evaluated but the immediate effector of response

to hypoxia, HIF, is not. Alternatively, direct HIF detection may be a better determinant of hypoxia within a cell as it is the mediator which transitions a cell's status from "normal" to "hypoxic".

1.2.10.1.2 Direct Measures of Hypoxia: HIF Detection

Direct detection of HIF is perhaps a more telling indicator of whether or not a cell is experiencing hypoxic stress than measurements of oxygen or detection of metabolites involved in secondary hypoxia responses. HIF-1 stability is highly sensitive to oxygen concentration with a graded and rapid response to hypoxia. Thus, intracellular levels of HIF-1 both directly correspond to a cell's immediate state of oxygenation and are predictive of imminent biochemical cellular responses that occur as HIF activity affects transcription. Real-time polymerase chain reaction (RT-PCR) can be performed to quantify changes in HIF-α mRNA levels; however, as HIF-α is constitutively expressed in most cells, this is not a good indication of transition of a cell to a hypoxic state. Alternatively, the HIF-α protein itself can be identified. This is commonly done by immunohistochemical/immunofluorescent staining, which can indicate HIF localization in a tissue, or by Western blotting which allows for quantification by densiometry. These methods directly measure a cell's hypoxic status. However, they do suffer from a number of drawbacks. First, the short half-life of HIF-α makes accurate capture and determination of protein levels difficult. Secondly, basal and elevated HIF-α levels can vary among cell types, meaning that specific concentrations of HIF-α do not always correspond directly to a consistent level of transcriptional changes in a cell. Most importantly, however, is that both immunostaining and Western blotting protocols

require the sacrifice of the tissue of interest. This means that repeated analysis of hypoxic status within the same sample cannot be performed. Thus by these methods, it is difficult to develop a temporal profile of the hypoxic response within a cell.

An alternative approach to HIF protein detection is the use of a reporter system. Several groups have detailed the use of an engineered vector containing repeats of the HRE enhancer and a minimal promoter to allow for hypoxia-induced expression of a fused gene. Given the appropriate reporter protein, this approach conveniently allows for the kinetics and magnitude of HIF-mediated effects on transcription to be observed. Furthermore, if the reporter protein is non-toxic to the cell and is easily detected, repeated observations of the same sample can be made.

The majority HIF reporter vectors detailed in the literature have been constructed as potential targeted gene-therapies for cancer treatment or diagnostic tools for the identification of hypoxia in tumors. Shibata et al. prepared a vector containing five HRE repeats from the human VEGF gene coupled to a minimal cytomegaloviral (CMV) promoter with luciferase as a reporter gene [**154** Shibata 2000]. They reported a 500-fold increase in luciferase expression in response to hypoxia in transfected cells. This type of vector was suggested as a means to selectively express a therapeutic agent (in lieu of the luciferase reporter gene) in tumors which are generally hypoxic compared to normal tissues [**154** Shibata 2000],[1**55** Payen 2001]. Indeed, a similar vector containing a suicide gene (herpes simplex virus thymidine kinase) under HRE control was used to induce tumor regression in mice [**156** Koshikawa 2000]. Similarly, Harada et al. used a HRE-luciferase reporter system to observe changes in the

number of hypoxic cells within a tumor to evaluate the effectiveness of cancer drugs [**157** Harada 2005].

The recent characterization and marketing of a number of genes whose products are stable fluorescent proteins has also allowed for the construction of imagable hypoxia reporter systems. Vordermark et al. reported the suitability of green fluorescent protein (GFP) as a reporter gene product for identifying HIF activity at oxygen concentrations as low as 0.02% [**158** Vordermark 2001]. Serganova et al. transfected C6 glioma cells with an HRE-GFP reporter vector and observed green fluorescence, indicating HIF-mediated transcriptional activity, in tumor masses comprised of the cells [**159** Serganova 2004]. They noted the particular usefulness of this approach for determining dynamics and spatial heterogeneity of HIF-1-specific transcriptional activity [**159** Serganova 2004].

A fluorescent reporter of HIF activity appears to be a relevant and useful tool for determining whether or not a cell is hypoxic and investigating different microenvironmental conditions that can result in HIF-induced changes in cell behavior. Such a system identifies cellular hypoxia in terms of cell behavior and offers a good estimate of the expression of other direct HIF targets. The method also avoids a number of the problems inherent in other hypoxia detection techniques, such as the need to sacrifice the study sample. However, very little use of such a system outside of tumor hypoxia has been reported. As discussed, low oxygen conditions can be common in the human body and can be necessary to drive normal and appropriate biological processes. As researchers make increasing efforts to simulate *in vivo* conditions in their

in vitro studies, there is an apparent need to understand how environmental signals, like oxygen tension, in a cell's physiological environment contribute to affecting its function. Use of a fluorescent reporter system to identify HIF activity and correlate it to other relevant changes in cell behavior should begin to fulfill this need.

1.3 Regulating Hypoxia to Affect Cell Behaviors in Transplantation Therapies

The loss or failure of tissues and organs due to damage and disease is one of the most prevalant and expensive problems encountered in medicine today [**160** Laschke 2006]. Since it was officially defined by the National Science foundation in 1987, the field of tissue engineering has offered the promise of addressing this issue through development of functional replacement tissues that are transplanted into the recipient [**161** Langer 1993]. With the subsequent discovery and utilization of embryonic and adult stem cells, tissue engineering has slowly become encompassed under the umbrella of "regenerative medicine", which, as defined by Mason and Dunnill, "…replaces or regenerates human cells, tissues or organs to restore or establish normal function" [**162** Mason 2008]. By this definition, any cell-transplantation therapy qualifies as regenerative medicine. Regenerative medicine combines the use of cells, materials, and bio-physical/chemical stimuli in a rational effort to produce functional tissues that are closely analogous to native tissues for the treatment of defects or disease. A key feature of regenerative medicine is the harnessing of innate properties and capabilities of cells that are difficult, if not impossible, to reproduce artificially. The cellular genome contains all of the inherent instructions required to run the myriad biological processes that together result in a living organism. Through evolution, these

have developed into a highly regulated and enormously complicated pattern of conserved and emergent cell behaviors that allow for survival and reciprocal interaction with the world. Tissue engineers, then, have the difficult task of applying, in an intelligent manner, what information has been learned about these preprogrammed cell functions in order to drive desired cell behaviors while restricting undesired ones in an effort to develop therapies for tissue restoration.

It has become increasingly noted that for cell transplantation and tissue engineering endeavors to succeed, the *in vitro* conditions in which tissue growth/fabrication takes place will need to closely mimic the native physiological environment. Differences between the conditions that cells encounter in culture and in the body can lead to discrepancies between *in vitro* and *in vivo* results. One of the most non-physiological conditions encountered by cells in routine cell culture is elevated exposure to oxygen. In atmospheric culture conditions, cells are exposed to nearly 21% O_2, whereas oxygenation of a typical tissue in the body is much lower. Therefore, investigators using standard culture conditions may not observe the same responses from cells as might typically be seen *in vivo*. As more research is performed at physionormal oxygen concentrations, it will be important to monitor the hypoxic status of cells in culture and observe the effects of reduced oxygen on cell behavior. Furthermore, tissue engineering is often concerned with the production of 3D tissues, which differ widely from the monolayers typical of standard culture. Because oxygen delivery occurs by diffusion from the media *in vitro*, oxygen gradients can easily form in 3D tissues, thus exposing cells to heterogeneous oxygen conditions. Because of this,

oxygen tension in many tissue engineered constructs may exert a significant, and potentially more complicated, effect on cell behavior than is typically considered.

A fluorescent hypoxia reporter system, described in the present work, provides a means for evaluating hypoxia and its effects in different cell systems. Though its role in signaling has become much better understood, "hypoxia" is still often viewed with a negative connotation, as it can lead to aberrant cell behavior and cell death. However, many beneficial behaviors, such as vascularization and wound healing, can also be triggered by hypoxia. Thus, hypoxia's role in cell transplantation and tissue engineering is phenomenological and context dependent. In the present work, it is hypothesized that for different 3D tissue systems, tissue dimensions and external oxygen concentration (both controllable culture parameters *in vitro*) contribute to the hypoxic status experienced by cells within the culture, and can work to promote desirable, hypoxia-induced behaviors or, alternatively, to inhibit cell function (Figure 1.4). This dual nature of hypoxia in cell-based, tissue engineering therapies, as well as the versatility of a fluorescent HIF reporter for use in its study, is highlighted in two systems which were the subject of the present work: islet-like β-cell clusters, and ADSC spheroids. In β-cell clusters, beneficial cell behavior is achieved by avoiding hypoxia, while in ADSC spheroids, hypoxia promotes the desired behavior. The importance of these systems as transplantation therapies as well as the role of hypoxia in each is discussed in the following sections.

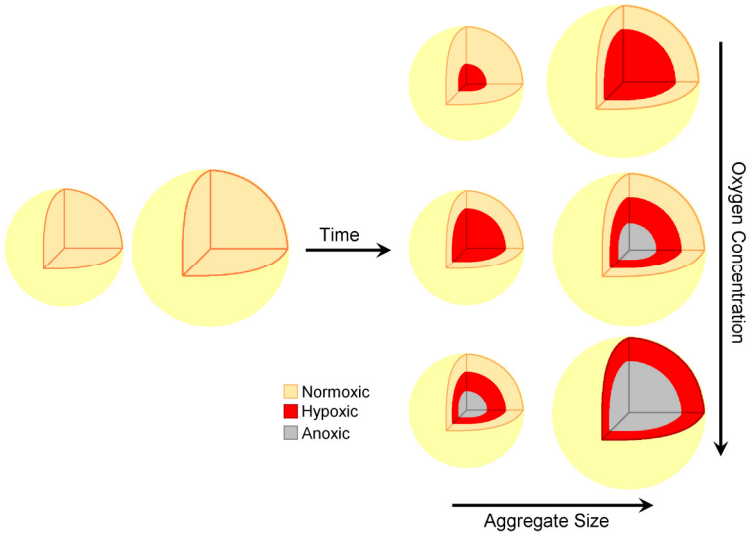

Figure 1.4 Schematic of development of hypoxia in 3D cultures. The extent of hypoxia within a cell aggregate should be affected by aggregate size and external oxygen concentration. To achieve the desired cell behavior, it may be possible to vary these parameters to optimize hypoxic status throughout the aggregate.

1.3.1 Encapsulated β-cells as a Treatment for Type I Diabetes Mellitus

Type 1 diabetes mellitus (T1DM) is a chronic inflammatory disease of the pancreas resulting in the body's inability to produce insulin. β-cells, the cells responsible for insulin production and secretion, reside within specialized tissue clusters called the islets of Langerhans found within the pancreas. In T1DM, the β-cells are destroyed, presumably through a dysfunctional autoimmune process. Without the insulin produced by β-cells, the body tissues are unable to take in and utilize glucose, the primary energy product of metabolism and the body's main energy source. If untreated, T1DM is fatal.

There are currently several treatment options for T1DM, offering the potential to improve patient prognosis considerably. Exogenous insulin administration via injection

is the most prevalent such option. By constantly monitoring blood glucose levels and administering insulin when needed, diabetic patient quality of life and life expectancy can be much improved. However, besides the discomfort of repeated blood drawl and hypodermic injection, this method also inadequately replicates what the body does naturally. In the body, islets are well perfused with blood and β-cells can continually monitor blood glucose levels and respond by secreting the appropriate amount of insulin. This continual monitor/secrete system is called responsive release, and it ensures that at any given moment the amount of insulin and glucose in the blood are appropriately balanced to achieve the correct physiological function. Exogenous supplementation of insulin, however, occurs in doses. Doses are administered periodically in amounts estimated to adequately process the glucose load of a meal over a given time period. Such periodic administration means that insulin concentration is not necessarily matched to glucose concentration at all times. Thus, exogenous insulin supplementation often fails to prevent the chronic, systemic complications of T1DM, such as retinopathy, glaucoma, neuropathy, and hypertension, over time.

In the normal physiological state, the body naturally secretes insulin in a responsive manner dependent upon blood glucose concentration at a given moment. It stands to reason, then, that an ideal method for treating T1DM would do the same. Because β-cells are specifically specialized to perform this task, transplantation of functional pancreatic tissue to replace compromised islets offers an appealing treatment approach. Transplantation was first attempted as a treatment for severe T1DM in 1966, with allotransplantation of a pancreas, duodenum, and kidney

concurrently [**163** Kelly 1967]. This and other subsequent early attempts offered poor outcomes due to complications from the invasive surgery and the requirement of immunosuppressive drugs to prevent organ rejection. Later transplantation attempts made use of the fact that islets represent only a small percentage of the total pancreatic mass but are sufficient for remediating T1DM. Islets were isolated and purified from donor pancreata and transplanted into recipients, greatly reducing surgical invasiveness but still requiring a life-long immunosuppressant regimen to prevent rejection. Besides issues with long-term immunosuppressant drug use, transplantation procedures also suffer from donor limitations. The islets from as many as three donors are required to satisfy the needs of single recipient. Thus, although positive outcomes have been achieved by islet transplantation, methods to improve the procedure and overcome limited tissue supply continue to be explored.

Encapsulation has been considered as means of overcoming the main shortcomings of islet transplantation. Encapsulation separates the transplanted tissues from the cells of the immune system and offers two benefits. First, possibility of immune rejection is greatly reduced so that immunosuppressive drugs are not required. Secondly, the avoidance of an immune response makes utilization of xenotypic tissue sources a potential way to overcome limited donor supply. Lim and Sun first evaluated the potential of this technique by encapsulating rat islets in semipermeable, cross-linked alginate [**164** Lim 1980]. They then examined viability and function of the islets *in vitro* and in chemically induced diabetic rats. They found that encapsulated islets exhibited glucose-stimulated insulin secretion (GSIS) similar to unencapsulated islets and could

restore normoglycemia in the mice for at least 20 days, compared to six day survival of mice receiving unencapsulated islets. More recent trials have shown xenotransplantation proof of concept, with alginate-encapsulated pig islets functioning to remediate hyperglycemia in diabetic monkeys [**165** Dufrane 2006a] and dogs [**166** Abalovich 2009] for several months without immune rejection. Elliott et al. even reported viability of alginate-encapsulated pig islets 9.5 years after transplantation into a human (function was lost after 14 months) [**167** Elliott 2007], thought a second group was unable to duplicate the result [**168** Tuch 2009]. However, limited duration of viability/function of encapsulated islets has largely restricted the overall success of transplantation therapies. Capsule material and nutrient delivery (especially oxygen) are the two major parameters that appear to most affect encapsulated islet performance.

1.3.1.1 Poly(Ethylene Glycol) as a Favorable Material for β-Cell Encapsulation

A majority of current encapsulation trials utilize hydrogels as the semipermeable matrix which separates β-cells from immune cells. Hydrogels are appealing for their ability to hold many times their volume in water, which provides a large aqueous environment for the encapsulated cells. Though alginate-based gels are traditionally the most utilized, poly(ethylene glycol) (PEG) hydrogels represent a promising alternative. A shortcoming of alginates has been their propensity to become fibrotically overgrown if not adequately purified [**169** Langlois 2009] and their batch-to-batch variability making comparisons between studies difficult. Recent direct comparisons have shown that, in these two respects, PEG yields superior performance [**170** Liu 2010]. In addition to

being highly biocompatible, PEG is also easily functionalized and non-degrading when covalently crosslinked. PEG hydrogels have already been shown to support a number of cell types including chondrocytes [**171** Bryant 2002],[**172** Rice 2004], osteoblasts [**173** Burdick 2002], valvular interstitial cells [**174** Benton 2009], and mesenchymal stem cells [**175** Nuttelman, 2004]. PEG network permeability, a function of mesh size, is also easily manipulated by varying macromer concentration and size in the photoactive solution [**176** Cruise 1998]. Lin-Gibson et al. provided a method for photopolymerizing PEG dimethacrylates (PEGDM) that had been prepared by microwave methacrylation of PEG [**177** Lin-Gibson 2004]. Using this method, Weber et al. showed that polymer mesh size was easily controlled by appropriate selection of initial macromer size [**178** Weber 2008] and that such hydrogels were suitable for sustaining β-cells [**179** Weber 2006]. Bryant et al. showed that neither the photoinitiator nor time of UV exposure used in the photopolymerization process was toxic to the cells [**180** Bryant 2000].

1.3.1.2 Hypoxia in Islet Encapsulation

Loss of function and/or viability is often observed in a significant percentage of cells following tissue isolation and encapsulation procedures. This has been especially noted of islets of Langerhans, transplanted as a treatment for T1DM [**181** De Vos 1997],[**182** Suzuki 1998],[**183** De Vos 1999]. While a variety of factors have been investigated, hypoxia has increasingly been implicated as the primary cause for this observed device failure, with insulin secretion by the pancreatic β-cells being particularly sensitive to changes in oxygen concentration [**184** Dionne 1989],[**185** Dionne 1993],[**186** de Groot 2003]. Low oxygen tension in explanted islets can be

directly attributed to their removal from the rich vasculature of the pancreas. Encapsulation exacerbates this problem in two ways: 1) by prohibiting islet revascularization and 2) by adding an additional barrier to oxygen transport. Outcomes in unencapsulated islet transplants have shown that diffusion of oxygen and nutrients to islets in well-perfused sites of the body prior to revascularization can be sufficient to maintain viability and function [**187** Shapiro 2000],[**188** Shapiro 2006]. A capsule, however, may hinder diffusion of oxygen to encapsulated tissues because of permeability limitations and increased diffusional distance [**189** Schrezenmeir 1994]. However, besides material and geometric considerations of capsule design, a variety of factors such as islet size [**190** Lehmann 2007],[**191** Cavallari 2007], rate of oxygen consumption [**192** Sweet 2002],[**193** Wang 2005], and site of implantation [**194** Dufrane 2006b] all play a part in determining how much oxygen may be available to any particular cell.

Oxygen insufficiency is known to inhibit β-cell function by decoupling glucose sensing from insulin exocytosis [**195** Zehetner 2008],[**196** Cantley 2009],[**197** Puri 2009]. Studies characterizing how size, encapsulation material, and external oxygen conditions affect the hypoxic status of islets as well as how techniques such as re-aggregation and hypoxic preconditioning contribute to hypoxic tolerance (if at all) are obviously important to optimizing implant function. However, direct characterization of hypoxia, in terms of HIF activity, in β-cells is scarcely reported. In the present work, use of a fluorescent HIF reporter was shown to facilitate such investigations, allowing for the determination of temporal and spatial profiles of hypoxia in 3D, islet-like clusters and

observation of how cluster size and external oxygen concentration contribute to hypoxia-mediated effects on cell function.

1.3.2 ADSC Spheroids as a Cell-Based Method to Drive Angiogenesis

Despite its promise, tissue engineering has offered relatively few clinical successes to date [**198** Griffith 2002],[**199** Ikada 2006]. Lack of vascularity has consistently been cited as the largest obstacle to the development of clinically relevant engineered tissues over the past several years [**160** Laschke 2006],[**200** Rauwkema 2008],[**201** Lovett 2009],[**202** Santos 2010],[**203** Novosel 2011],[**204** Horch 2012],[**205** Laschke 2012]. Most cells in the body reside within 100-200μm of a blood vessel, a distance which corresponds closely the theoretical limit of oxygen diffusion in a tissue [**206** Folkman 1973],[**207** Colton 1995]. For engineered tissues, which are avascular, this diffusional restraint limits the size of tissues that can be effectively transplanted. Following transplantation, local inflammation and healing processes at the implant site resulting from the surgical procedure can help to induce infiltration of host vessels into the implant. However, the rate of vessel progression is slow and interior cells of the implant often do not survive long enough to be vascularized. Several strategies for enhancing vascularization of engineered tissues have been described, including administration of pro-angiogenic growth factors, cell co-culture, and pre-vascularization. These strategies either attempt to promote angiogenesis, the sprouting of vascular branches from existing vasculature, or vasculogenesis, the *de novo* formation of microvessel networks from disorganized precursor cells.

Growth factors are known to be potent mediators of angiogenesis and vasculogenesis *in vivo*. VEGF is the most powerful stimulator of angiogenesis, often working in concert with basic fibroblast growth factor (bFGF) [**208** Carmeliet 2011]. When triggered by these growth factors, endothelial cells in existing vessel walls secrete matrix metalloproteinases (MMPs), branch off from the vessel, and begin to migrate in the direction of the growth factor source. Endothelial cells directly behind these migrating cells begin to proliferate rapidly, extending a new capillary sprout toward the tissue of need. Subsequent vessel maturation is important to reducing capillary leakiness and preventing vessel regression. Platelet-derived growth factor (PDGF), TGF-β, and angiopoietin 1 (Ang-1) are involved in vessel stabilization and maturation by reducing MMP secretion, stimulating matrix production, and recruiting supporting cells such as smooth muscle cells and pericytes [**200** Raukema 2008],[**209** Carmeliet 2000],[**210** Hirschi 2002].

In regenerative medicine applications, administration of angiogenic factors can help to stimulate blood vessel growth and promote more rapid vascularization of tissue implants. For this purpose, recombinant VEGF is often applied. VEGF can be administered by direction injection; however, high dose requirements due to VEGF instability and negative systemic side-effects, including ectopic blood vessel development and excessive capillary leak, make this delivery technique unfavorable [**160** Laschke 2006]. An alternative strategy has been to localize VEGF to the implant site by controlling its release from the implant itself, often a biomaterial scaffold that serves as the matrix component of an engineered tissue. Many demonstrations of

material-based constructs for VEGF delivery are reported in the literature, displaying a wide variety of release profiles and mechanisms [**211** Zisch 2003],[**212** Sokolsky-Papkov 2007],[**213** Übersax 2009],[**214** Fu 2010]. However, material-based delivery systems do face a number of hurdles. First, they require both a prior knowledge of the appropriate delivery dosage/duration and the ability to achieve this release profile from a material construct. Also, the maximal cumulative dose is predefined by the loading process during fabrication and cannot be augmented after implantation. Furthermore, few systems are capable of responding to cellular and other microenvironmental cues that would modulate delivery to match physiological need. Finally, the process of angiogenesis is driven by concurrent action of multiple factors each displaying different availability profiles which change over time; however, the appropriate relative profiles of many growth factors are not fully characterized in many cases, and most material-based growth factor delivery systems have difficulty incorporating and delivering multiple factors differentially.

1.3.2.1 Cell-Based Delivery for Therapeutic Angiogenesis in Tissue Engineering

A more recent technique has been to use cells as a growth factor source, an approach termed cell-based delivery. In cell-based delivery, a particular cell type is chosen for incorporation into the engineered tissue to promote tissue angiogenesis, either natively or by some inducing stimulus. Cell-based delivery techniques are attractive, as researchers are able to take advantage of natural biological mechanisms that cells already possess. This approach offers three key benefits [**200** Rauwkema 2008]. First, unlike most biomaterials, cells can participate in innate biological signaling

processes that regulate angiogenic factor secretion to maintain factor concentrations in the physiological range and adapt them to meet the requirements of different stages of vessel formation. Secondly, growth factors secreted from cells often interact with the extracellular matrix to form three dimensional microgradients which contribute to directing capillary arrangement [**215** Helm 2005]. Finally, cells may have the capability to produce and secrete a variety of different angiogenic factors, in physiological profiles, that act together to direct several stages of vessel migration, stabilization, and maturation [**205** Laschke 2012].

For cell-based delivery to be effective, a cell source must be chosen that is capable of producing the factors of interest and providing the appropriate signals within the implant microenvironment. The recently-characterized ADSCs represent a very promising cell population for the promotion of angiogenesis. ADSCs are readily isolated from lipoaspirates which can be collected through a minimally invasive procedure. The stem cell yield from adipose tissue is large, approximately 500 times greater than from bone marrow, where similar stromal cell populations were first identified [**216** Mizuno 2009]. Ease of culture and rapid expansion make ADSCs ideal for autologous use. ADSCs have also been shown to be capable of secreting a number of factors of relevance to angiogenesis in regenerative medicine, including VEGF; bFGF; hepatocyte growth factor (HGF); basic nerve growth factor (bNGF); angiogenin; Ang-1; insulin-like growth factor 1 (IGF-1); interleukins (IL)-6, -7, -8, -11, and -17; monocyte chemoattractant protein (MCP)-1 and -2; granulocyte/monocyte-, granulocyte-, and macrophage colony stimulating factors (CSF); tumor necrosis factor α (TNF-α), and stromal cell-derived

factor 1 (SDF-1) [**217** Kilroy 2007],[**218** Hong 2010],[**219** Rasmussen 2011]. Furthermore, ADSCs have shown the potential to differentiate into a variety of mature lineages of mesodermal and non-mesodermal origin, including adipogenic, chondrogenic, osteogenic, skeletal muscle, smooth muscle, cardiac muscle, epithelial, hepatocytic, pancreatic, and hematopoietic support cells [**216** Mizuno 2009]. Of particular relevance are studies indicating that ADSCs can differentiate directly into endothelial precursor and endothelial cells [**220** Planat-Benard 2004],[**221** Miranville 2004],[**222** Cao 2005],[**223** Colazzo 2010],[**224** Keerl 2010],[**225** Shi 2012].

In recent years, ADSCs have been shown to contribute to improved tissue repair in dermal wounds [**226** Kim, W.S. 2007],[**227** Lu 2008],[**228** Kim 2009],[**229** Nambu 2009], mouse ischemic hindlimbs [**221** Miranville 2004],[**222** Cao 2005],[**230**Nakagami 2005],[**231** Moon 2006],[**232** Kim, Y. 2007], and myocardial infarcts [**233** Miyahara 2006],[**234** Valina 2007],[**235** Cai 2009],[**236** Schenke-Layland 2009],[**237** Wang 2009]. Usually, the cells are directly injected into the deficient tissue as a dispersion, or a seeded into a tissue scaffold for implantation. The restorative effects of ADSCs have mostly been attributed to their enhancement of angiogenesis, which appears to be accomplished through one or more of the following mechanisms. First, current evidence supports a primary paracrine activity of ADSCs, with secretion of pro-angiogenic and anti-apoptotic growth factors contributing to enhanced tissue survival and increased capillary density. (VEGF and IGF-1, for instance, have been shown to function in both roles [**219** Rasmussen 2011].) ADSCs also secrete factors which can recruit circulating stem and endothelial precursor cells, as well as various support cells

such as fibroblasts and pericytes [**238** Takahashi 1999],[**239** Crosby 2000],[**240** Ceradini 2005],[**241** Nakao 2010]. In particular, SDF-1, appears to function in stem cell homing [**242** Askari 2003],[**243** Ceradini 2004]. Finally, as mentioned, ADSCs can differentiate into endothelial cells to directly integrate into developing vasculature. ADSCs also share many common characteristics with pericytes, cells which support the vascular endothelium and have been shown to contribute to superior angiogenesis and vessel stabilization when co-cultured with endothelial cells [**244** Traktuev 2008],[**245** Traktuev 2009]. Taken together, these properties suggest that ADSCs are capable of modulating the stem cell niche to create a local microenvironment that is highly primed to promote angiogenesis [**246** Gimble 2007].

1.3.2.2 Hypoxia and the Angiogenic Potential of ADSCs

In order to fully take advantage of the angiogenic potential of ADSCs for regenerative medicine, researchers will need to develop techniques to control and possibly amplify their pro-angiogenic behaviors. To this end, a better understanding of the stimuli that encourage these behaviors will be advantageous. In the body, ADSCs reside in a perivasacular niche with oxygen concentrations ranging from 2-8% O_2, an environment that has been described as locally hypoxic [**247** Matsumoto 2005],[**248** Pasarica 2009],[**249** Mohyeldin 2010]. This concentration encompasses the range over which HIFs are exponentially stabilized, suggesting that HIF activity plays an important part in regulating typical ADSC functions. Indeed, hypoxia appears to be one of the primary motivating factors promoting ADSC paracrine activity and affecting differential potential. Hypoxic culture of ADSCs has been reported to upregulate expression of

VEGF, bFGF, IGF-1, and HGF *in vitro* [**219** Rasmussen 2011],[**250** Rehman 2004],[**251** Rosová 2008], [**252** Lee 2009],[**253** Liu 2013]. In particular, the VEGF gene is known to contain HRE repeats in its promoter region, making it a direct target of HIF-1 [**254** Levy 1995],[**255** Liu 1995],[**256** Forsythe 1996]. In animal studies, hypoxic preconditioning of ADSCs resulted in superior survival, healing, and vascularity of ischemic skin flaps and myocardial infarcts in mice [**257** Tang 2009],[**258** Yue 2013]. Hypoxia has also been suggested to contribute to an increase in stem cell survival and to the secretion of pro-survival factors from stem cells [**259** Chacko 2010]. However, despite the fact that the potent angiogenic properties of ADSCs are largely regulated by hypoxia over physionormal oxygen tensions, relatively little work has focused on developing a better understanding of how cellular hypoxia in encountered by ADSC cultures. Furthermore, Abdollahi et al. have recently concluded that "…further study is needed to optimize the use of hypoxia as a stimulus for various stem cell functions, including its potential role in therapeutic angiogenesis" [**260** Abdollahi 2011].

Realization that oxygen is one of the key regulators of stem cell function has a profound significance on how current cell-based and tissue engineering applications using ADSCs can be further improved [**261** Zachar 2011]. While upregulation of angiogenic growth factors by genetic engineering has been shown to enhance the therapeutic outcomes with stem cells [**262** Geiger 2007], hypoxia can be used to a similar effect while eliciting a more global and complex cell response and avoiding potential concerns such as oncogene formation [**263** Baraniak 2010]. As discussed previously, oxygen diffusion in a 3D tissue is known to affect oxygen tension. Therefore,

in the present work, it is suggested that 3D and hypoxic culture can be used to illicit upregulation of angiogenic behavior in ADSCs. In addition to the potential paracrine effects, 3D culture has been shown to enhance survival of cells within a spheroid through contact-dependent signaling and upregulation of pro-survival factors [**264** Shweiki 1995],[**265** Bates 200],[**266** Gaedtke 2007],[**267** Bhang 2012a]. Furthermore, 3D culturing may serve to precondition the cells for hypoxic conditions encountered at the ischemic implant site [**268** Saleh 2011],[**269** Baraniak 2012]. Application of a fluorescent HIF reporter system allows for a unique characterization of hypoxia within 3D ADSC cultures which should serve as a supplement to the few investigations of hypoxia in ADSC spheroids. Furthermore, it is hypothesized that spheroid size and external oxygen concentration can be adjusted to affect hypoxic status of cells throughout a culture, and thus control the output of angiogenic factors. This hypothesis is investigated in the current work. Using culture size to control hypoxia for tissue engineering has not been previously reported in the literature and has implications for optimizing tissue designs for angiogenic cell-therapies in regenerative medicine.

Chapter 2

Correlating Hypoxia with Insulin Secretion Using a Fluorescent Hypoxia Detection System[1]

[1] M.L. Skiles, R. Fancy, P. Topiwala, S. Sahai, J.O. Blanchette. Correlating hypoxia with insulin secretion using a fluorescent hypoxia detection system. J Biomed Mater Res B Appl Biomater 2011, 97(1);148-55. (published) [**270** Skiles 2011a]

2.1 Abstract

A common obstacle to the survival of encapsulated tissue is oxygen insufficiency. This appears particularly true of encapsulated pancreatic β-cells. Our work investigates a fluorescent hypoxia detection system for early recognition of hypoxic stress in encapsulated pancreatic tissue. Murine insulinoma (MIN6) cells were engineered to produce a red fluorescent protein under the control of hypoxia-inducible-factor-1. Aggregates of these cells were encapsulated in poly(ethylene glycol) hydrogels at densities of 200,000, 600,000, and 1 million cells per capsule then incubated in either a 1% or 20% oxygen environment. Cell function was evaluated by daily measurement of glucose-stimulated insulin secretion. Encapsulated cells were also fluorescently imaged periodically over 72 hours for expression of the marker signal. Results indicate that oxygen insufficiency severely impacts insulin release from MIN6 cells, and that large aggregates are especially vulnerable to oxygen limitations. Our marker was found to be successfully indicative of hypoxia and could be used as a predictor of subsequent insulin release. Further work will be required to fully characterize signal dynamics and to evaluate *in vivo* efficacy. The method presented here represents a unique and valuable approach to detecting hypoxic stress in living tissues which may prove useful to a variety of fields of biological research.

2.2 Introduction

Loss of function and/or viability is often observed in a significant percentage of cells following tissue isolation and encapsulation procedures. This has been especially noted of islets of Langerhans, transplanted as a treatment for T1DM [**181** de Vos

1997],[**182** Suzuki 1998],[**183** de Vos 1999]. While a variety of factors have been investigated, hypoxia has increasingly been implicated as the primary cause for this observed device failure, with insulin secretion by the pancreatic β-cells being particularly sensitive to changes in oxygen concentration [**184** Dionne 1989], [**185** Dionne 1993],[**186** de Groot 2003].

Low oxygen tension in explanted islets can be directly attributed to their removal from the rich vasculature of the pancreas. Encapsulation exacerbates this problem in two ways: 1) by prohibiting islet revascularization and 2) by adding an additional barrier to oxygen transport. Outcomes in unencapsulated islet transplants have shown that diffusion of oxygen and nutrients to islets in well perfused sites of the body prior to revascularization can be sufficient to maintain viability and function [**187** Shapiro 2000],[**188** Shapiro 2006]. A capsule, however, may hinder diffusion of oxygen to encapsulated tissues by permeability limitations and an increased diffusional distance [**189** Schrezenmeir 1994]. For many commonly used materials, oxygen can easily permeate and diffuse within the capsule. Weber, et al. [**178** Weber 2009], for instance, have shown that the diffusion coefficients of small molecules within a poly(ethylene glycol) (PEG) hydrogel polymerized from 10 kDa macromers approach their values for diffusion in water. This implies that in terms of oxygenation, combined effects of capsule geometry and material may largely influence device success. However, beyond material and geometric considerations, a variety of factors such as islet size [**190** Lehmann 2007],[**191** Cavallari 2007], rate of oxygen consumption [**192** Sweet 2002],[**193** Wang 2005], and site of implantation [**194** Dufrane 2006b] all play a part in determining

how much oxygen may be available to any particular cell. As such, a method for quickly detecting hypoxia in individual living cells would provide obvious benefits to the field of cell encapsulation.

Our work reports the development of such a detection system. HIF-1, a heteromeric dimer, has previously been identified as central to cellular hypoxia response [**271** Semenza 2001]. In particular, presence of the HIF-1α subunit, necessary for HIF-1 activity, has been shown to increase exponentially in cells exposed to oxygen levels lower than 6% [**105** Jiang 1996b]. We have developed a transfer vector capable of inserting a gene coding for production of a red fluorescent protein under the control of HIF-1. In response to diminished oxygen availability, HIF-1α is upregulated, dimerizes with HIF-1β, and attaches to HREs in the genome, initiating transcription of native hypoxia response genes as well as the inserted red fluorescent protein gene. Signal can be observed in living cells under a fluorescent microscope.

To better characterize this marker, we have employed it in PEG-encapsulated murine β-cells. Covalently crosslinked PEG networks have been shown to provide a suitable environment for β-cell survival [**179** Weber 2006]. Among their favorable characteristics, PEG hydrogels are highly biocompatible, non-degrading, and readily functionalized. Within the hydrogels, hypoxia signal expression and cell function, as defined by GSIS, were compared in normoxic and hypoxic conditions. As a rapid indicator of hypoxia in living cells, we believe this detection system could prove useful not only in cell encapsulation but also in other fields in which hypoxia plays an important role, such as the directionalization of stem cell differentiation.

2.3 Materials and Methods

2.3.1 Materials

PEG (linear, M_n = 10,000 g mol^{-1}) and 1-Hydroxycyclohexyl phenyl ketone (99%) (Irgacure 184) were purchased from Sigma-Aldrich (St. Louis, MO, USA) and used as received. Methacrylic anhydride (94%) and reagent A.C.S. grade dichloromethane (≥ 99.5%), and anhydrous diethyl ether (≥ 99.5%) were also purchased from Sigma-Aldrich and used as received.

2.3.2 PEGDM Synthesis and Functional PEGDM Solution Preparation

Polymer was prepared in a manner similar to that described by Lin-Gibson et al. [**177** Lin-Gibson 2004]. Methacrylic anhydride and PEG were combined in a scintillation bottle at a molar ratio of 10:1 by addition of 0.308g of methacrylic anhydride to 2.0g of PEG. PEG was evenly melted by irradiating the bottle in a standard domestic microwave (1050 W) for 2 minutes, vortexing, then irradiating for another 5 minutes. This process allowed for covalent addition of a methacrylate group to each PEG chain end forming PEGDM. The heated solution was allowed to cool briefly before being re-dissolved in excess dichloromethane (~6 mL). PEGDM was precipitated out of solution in cold anhydrous diethyl ether and collected by vacuum filtration. After drying, PEGDM was dissolved in deionized water and transferred into cellulose ester dialysis tubing with a molecular weight cut-off of 1,000 Da (Spectra/Por Dialysis Membrane, Spectrum Laboratories, Los Angeles, California, USA). The solution was dialyzed against deionized water for 5 days to purify the product. Water was replaced every 24 hours. After

purification, the PEGDM solution was transferred into an appropriate container and placed in a freezer at -80°C overnight. The frozen solution was then lyophilized on a freeze-drier (Freezone 2.5, Labconco, Kansas City, MO, USA) for 4 days to obtain the final powder form. To prepare the photoactive PEGDM solution, PEGDM was dissolved in Hank's Balanced Salt Solution (HBSS, Invitrogen, Carlsbad, CA, USA) to form a 10 wt% solution. Irgacure 184 was added at 0.025 wt% as a photoinitiator. The final solution was sterilized by filtration through a 0.2 μm syringe filter and stored in the dark. Crosslinking was achieved by exposure of the desired volume of photoactive PEGDM solution to long wavelength UV light (352 nm). Upon exposure, degradation of Irgacure 184 results in production of free radicals which attack the vinyl carbon-carbon double bonds of the methacrylate end groups resulting in covalent crosslinking of PEG chains and formation of the hydrogel.

In their work, Lin-Gibson et al. noted near stoichiometric conversion of PEG (M_n = 1,000 and 4,000) to PEGDM after 5 minutes of reaction with methacrylic anhydride at a 1:10 molar ratio (96% and 99% methacrylation, respectively, with no significant difference) [**177** Lin-Gibson 2004]. Initial monomer size was not observed to impact resultant percent methacrylation. The procedure described in our work for the preparation and purification of PEGDM is identical to a similar procedure used by Weber et al. for 10 kDa PEG monomers [**179** Weber 2006]. Their group reports 95 ± 3% methacrylation of PEGDM prepared by this method as determined by ^{1}H NMR. Byproducts of the microwave methacrylation reaction are methacrylic acid, which

should be easily removed during purification, and un-methacrylated or mono-methacrylated PEG which should only comprise a small percentage of the final product.

2.3.3 Cell Culture

MIN6 cells are an immortalized mouse pancreatic β-cell line exhibiting GSIS comparable to native mouse β-cells. Cells were cultured in RPMI 1640 medium (Invitrogen) supplemented with 10% fetal bovine serum (Invitrogen), 1% penicillin-streptomycin (Invitrogen), and 0.5μg/mL Fungizone (Invitrogen). Cells were plated on 75 cm^2 treated tissue culture flasks and incubated at ambient oxygen levels at 37°C and 5% CO_2 in humid conditions.

2.3.4 Dissolved Oxygen Studies

Nitrogen-purged programmable incubators were used to maintain constant oxygen levels for cellular studies (Napco Series 8000 WJ, Thermo Electron, USA). All "high" oxygen studies were maintained at 5% CO_2 and 20% oxygen. All "low" oxygen studies were maintained at 5% CO_2 and 1% oxygen. To determine the corresponding dissolved oxygen content in culture medium during incubation, measurements were taken with a dissolved oxygen probe (Pasport Xplorer GLX and Pasport Dissolved Oxygen Sensor, PASCO, Roseville, CA, USA). The probe was calibrated with deionized water at 25°C. Then, 2 mL of RPMI 1640 growth medium was placed into the well of a 24-well suspension plate, the probe was inserted, and the plate was incubated for at least 12 hours. The media remained uncovered and unagitated throughout study of both high and low oxygen conditions. Incubator temperatures were maintained at 37°C. To

determine if dissolved oxygen concentration was measurably impacted by cellular utilization of oxygen, 1 million dispersed MIN6 cells were seeded into a well and allowed to incubate in 2 mL of medium while dissolved oxygen concentration was measured. Concentrations were again recorded for both high and low oxygen conditions.

2.3.5 Encapsulation of Cells

Cultures of MIN6 cells were trypsinized and counted with a hemocytometer on a Nikon Eclipse T*i* microscope (Nikon, Tokyo, Japan). A range of densities were seeded into 6-well suspension plates in a total volume of 2 mL of growth medium: 100,000 cells/mL, 300,000 cells/mL, and 500,000 cells/mL. Dissociated β-cells have been shown to rapidly lose viability and function, but can spontaneously reaggregate if allowed [**272** Matta 1994]. Therefore, cells were incubated at 37°C and 20% oxygen on a rotational shaker at 100 rpm for 24 hours to allow for aggregate formation.

To prepared vessels for capsule polymerization, clear, 1mL syringes were placed tip up in a rack and decapitated to remove the tapered point. Capsules were formed in two steps. Bottom halves of capsules were prepared first, by addition of 20 µL of photoactive PEGDM solution into the tips of standing syringes followed by photopolymerization by UV irradiation for 10 minutes. Then, cells that had been aggregating for 24 hours were centrifuged at 200 rpm for 2 minutes and medium was removed. Aggregates were re-suspended in 20 µL of photoactive PEGDM solution, with care taken to not dissociate the aggregates. This volume was added into the syringe on top of previously polymerized capsule bottom and polymerization was continued for an additional 10 minutes. In this manner, settling of suspended aggregates in their

respective aliquot resulted in a finished capsule with aggregates fixed in the medial plane. Finished capsules were cylindrical in shape, approximately 6 mm in diameter and 2 mm thick. Capsules were ejected from the syringe tubes, washed with HBSS, and placed in 24-well suspension plates in 1 mL of growth media.

2.3.6 Characterization of Aggregate Sizes

Representative images of aggregates at Time 0 (initial time of encapsulation) were analyzed for each of the three cell densities prepared using Nikon NIS-Elements imaging software. Long axis diameter and shortest orthogonal diameter were determined. Average aggregate diameter and standard deviation were calculated from long-axis measurements. A shape factor was also calculated as the ratio of the short-axis to long-axis diameter for each aggregate. The number of aggregates determined to be large (diameter > 150 µm) and extremely large (diameter > 250 µm) were additionally determined and reported along with the average size of large and extremely large aggregates.

2.3.7 Insulin Release Studies

To assess degree of device function, GSIS from encapsulated aggregates was measured over two weeks. Capsules containing 200,000, 600,000 and 1 million aggregated cells were studied. One day after encapsulation, culture medium was removed and 1 mL of a low concentration buffered glucose solution (1.1 mM) was introduced to each well. Capsules were incubated for one hour before removal of this solution and addition of a high concentration buffered glucose solution (16.7 mM).

After an hour of incubation, samples from the high glucose solution were removed for later analysis and capsules were returned to culture medium. These conditions were used to replicate a starved-state/fed-state cycle. One set of capsules was then returned to incubation in the high oxygen condition while the second set was placed in low-oxygen incubation. Glucose stimulation was repeated in this manner every 24 hours for 2 weeks. At the end of the study, insulin concentration in samples was determined via mouse insulin ELISA assay (Mercodia, Upsalla, Sweden). Capsules of each cellular density were studied in identical experimental setups.

2.3.8 Construction of the Hypoxia Marker Virus

A schematic of the mechanism of hypoxia signaling is shown in Figure 2.1. The marker virus is a recombinant adenovirus generated using the pAdEasy-1 system (QBiogene, Montreal, Canada). The red fluorescent protein is a destabilized variant of the DsRed protein. The destabilized protein (termed DsRed-DR) has a portion of mouse ornithine decarboxylase fused to the C-terminus of the DsRed protein which contains a PEST sequence. The DsRed-DR sequence was removed from its vector and inserted into the multiple cloning site of the AdEasy transfer vector under the control of a minimal SV40 promoter with a trimer of the HRE sequence from murine lactate dehydrogenase (LDH). A transfer vector with the LDH HRE SV40 promoter was generously donated by Dr. Rachel Cowen (University of Manchester, UK). The HRE trimer upstream of the SV40 promoter allows hypoxia-dependent transcription of the DsRed-DR protein. After insertion of the DsRed-DR sequence, the transfer vector was allowed to undergo homologous recombination with the pAdEasy vector to produce the recombinant

adenoviral genome which was linearized, transferred and amplified according to the manufacturer's specifications. Following purification of the virus, a plaque assay was performed to determine the concentration of the resulting HRE DsRed-DR viral stocks which allowed infection at specified multiplicities of infection (MOI). This value was determined to be 3.7 x 10^7 plaque-forming units per microliter.

Figure 2.1 Schematic of a novel hypoxia detection system in living MIN6 cells. In response to hypoxia, HIF-1α is stabilized and dimerizes with HIF-1β. This unit initiates transcription at HREs in target genes producing hypoxia-response proteins as well as the fluorescent DsRed-DR protein.

2.3.9 Fluorescent Hypoxia Detection Studies

Cells were infected at an MOI of 100 by addition of the vector to the medium just prior to the 24 hour aggregation incubation period. They were then encapsulated as described in the methods and imaged on an inverted fluorescent microscope with an excitation wavelength of 556 nm at a time denoted as Time 0. One set of capsules was returned to the high oxygen condition while a second set was incubated in the low oxygen condition. Capsules were then re-imaged approximately every 10 -12 hours for 2 to 3 days. Capsules containing 200,000, 600,000, and 1 million aggregated cells were studied. Growth medium was replaced every 24 hours.

2.3.10 Statistical Analysis

For capsules prepared at each of the described cell densities, mean insulin secretion at the high and low oxygen conditions were compared. An unpaired Student's t-test assuming unequal variances and with $\alpha = 0.05$ was used to determine significance of differences between each condition. Significance of differences in size and shape factor between groups was also determined by the same test. Some measured insulin concentrations were at the maximum detectable limit of the performed assay. For these samples, the maximum detectable value (an absorbance of 4.0 at 450 nm) was used. Reported means calculated with inclusion of an estimated maximum value are indicated by '$^{+}$'.

2.4 Results

2.4.1 Dissolved Oxygen

Dissolved oxygen concentrations in RPMI 1640 medium incubated in high and low oxygen conditions overnight are shown in Figure 2.2A After 13.5 hours, medium in the high oxygen condition exhibited a dissolved oxygen concentration of 3.9 mg/L. This value was reached within the first 1.5 hours of incubation. Medium in the low oxygen condition displayed a dissolved oxygen concentration of 0.6 mg/L after 13.5 hours while showing a more gradual decline to this value. A dissolved oxygen concentration of 3.9 mg/L, which represents the end concentration reached in the high oxygen condition, was reached within 15 minutes in the low oxygen trial.

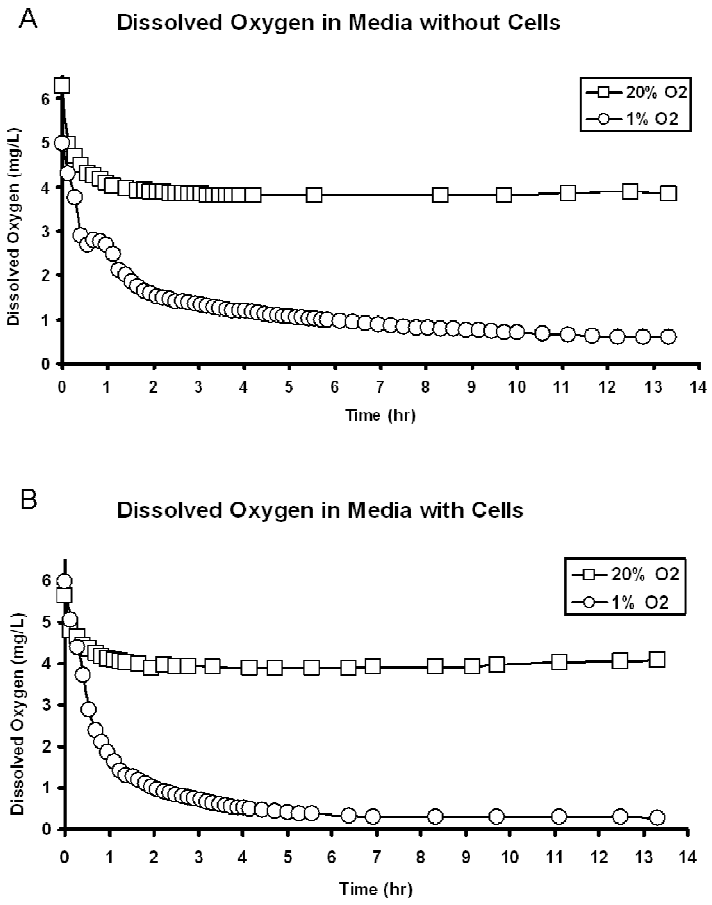

Figure 2.2 A) Dissolved oxygen concentrations measured in 2 mL of growth medium incubated at 37°C in 20% and 1% oxygen. B) Dissolved oxygen concentrations measured in 2 mL of growth medium containing 1 million MIN6 cells incubated in high and low oxygen conditions.

In the second trial, 1 million MIN6 cells were added to the media in both high and low oxygen conditions. Figure 2.2B shows the dissolved oxygen concentrations obtained from these trials. Media containing 1 million cells displayed a dissolved oxygen concentration of approximately 4.0 mg/L after 13.5 hours in high oxygen incubation. This showed no decrease from the value observed in the high oxygen condition in the absence of cells. However, after 13.5 hours of low oxygen incubation, media containing

1 million cells displayed a dissolved oxygen concentration of 0.2 mg/L. This value is approximately one-third of the value observed for media free of cells in the low oxygen condition.

2.4.2 Aggregate Sizes

Capsules were imaged immediately following polymerization to ensure that cells were fully encapsulated and to determine the size of encapsulated aggregates. Centrifugation and re-suspension of cells during the encapsulation procedure was not observed to cause dissociation of aggregates. At each encapsulated density, the bulk of aggregates had a diameter of 75-150 µm. At every density, at least one exceptionally large aggregate (> 250 µm) was observed. These were more frequent in higher density capsules, with 4 to 5 being observed in each capsule containing 1 million cells. Capsules containing 1 million aggregated cells additionally displayed significant association of averaged-sized aggregates to form larger fused aggregate networks.

Four representative images of encapsulated aggregates for each density were analyzed to better characterize aggregate size. Table 2.1 shows average aggregate size for aggregates formed at each of the seeded densities. The number and size of large and exceptionally large aggregates are also given, along with average aggregate size excluding large aggregates. Differences in average aggregate size between all groups, though small, were found to be significant ($p<0.05$). When excluding aggregates larger than 150 µm, which were less prevalent and displayed greater variability in size, aggregates formed from 200,000 cells still displayed a statistically significant difference in size from aggregates formed from 600,000 ($p = 0.002$) and 1 million ($p = 0.0003$) cells,

though the differences in average size was small. Aggregates formed in the 600,000 and 1 million cell conditions did not display a significant difference in average size when excluding large aggregates. In evaluating shape, aggregates were best described as elliptical. Average shape factor was determined to be 0.72 and any difference in shape factor among aggregates from different cell densities or between aggregates of different sizes was not significant.

Table 2.1 Analysis of MIN6 aggregate sizes

Cell Density (per capsule)	Size ($\bar{x}$, µm)	#>150 µm	%>150 µm	#>250 µm	%>250 µm	Size ($\bar{x}$, µm) <150 µm	Range (µm)
200k	75.7*± 29.7	5	1.63	2	0.65	73.0*± 20.1	17.3-322.6
600k	80.1*± 33.4	9	1.67	2	0.37	77.4*± 21.1	22.4-519.0
1M	96.4*± 67.2	34	11.8	4	1.39	80.6± 30.0	27.4-835.2
*Difference in value between groups is significant, $p < 0.05$.							

2.4.3 Glucose-Stimulated Insulin Secretion

GSIS was measured at high and low oxygen for each of the cell densities prepared. In high oxygen conditions, capsules containing 200,000 aggregated cells displayed an average (n = 4) insulin release of 6.4† µg/L (± 3.1 µg/L) at the end of two weeks. Insulin release from capsules containing 600,000 (n = 3) and 1 million cells (n = 4) was reported on average to be 10.7 µg/L (± 0.9 µg/L) and 8.2† µg/L (± 3.2 µg/L), respectively, at the end of two weeks. For all three high-oxygen trials, insulin release remained relatively consistent and undiminished over the 14 day period. In 1% oxygen, cells encapsulated at a density of 200,000 exhibited insulin release of 0.6 µg/L (± 0.4 µg/L), cells encapsulated at a density of 600,000 exhibited insulin release of 0.3 µg/L (± 0.1 µg/L), and cells encapsulated at a density of 1 million exhibited insulin release of 2.1

µg/L (± 0.7 µg/L), after 14 days. In each case, drastic reduction in insulin release was observed by as early as day 2. Figures 2.3A, B, and C show high-oxygen and low-oxygen insulin release from capsules containing 200,000, 600,000, and 1 million aggregated cells, respectively.

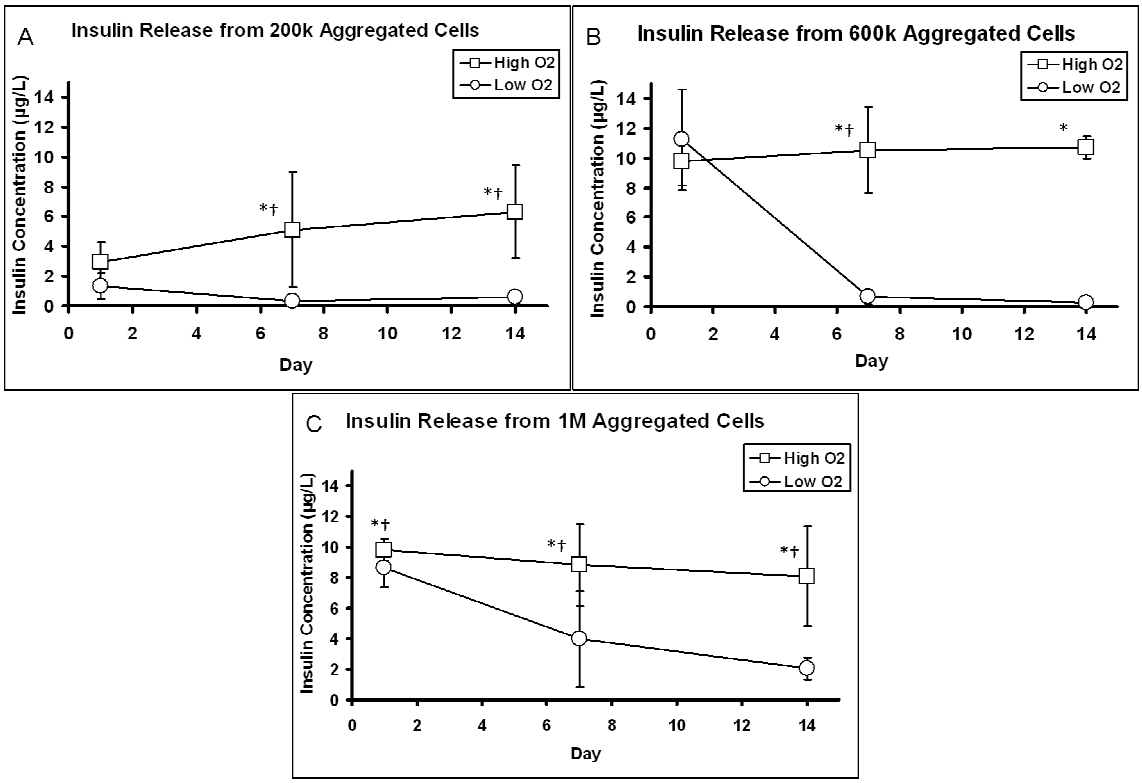

Figure 2.3 Daily one hour insulin release over 2 weeks from capsules containing (A) 200,000, (B) 600,000, and (C) 1 million aggregated MIN6 cells incubated in 20% or 1% oxygen. Statistical significance of differences between high and low oxygen insulin secretion values is indicated by '*', where $p < 0.05$. Data points denoted by '†' include at least one estimated maximum value in determination of the mean.

Comparison of the low and high oxygen conditions showed no significant difference in mean insulin secretion on Day 1 for all three trials. However, on Days 7 and 14, secretion in the low-oxygen condition was found to be significantly lower than in the high-oxygen condition for each cell density tested. ($p = 0.04$ and 0.02, $p = 0.01$

and 0.0008, and p = 0.03 and 0.02 for Days 7 and 14 for capsules containing 200,000, 600,000, and 1 million cells, respectively.)

2.4.4 Fluorescent Detection of Hypoxia

After incubation with the hypoxia marker vector for 24 hours, capsules containing 200,000, 600,000, and 1 million aggregated MIN6 cells were incubated in either high or low oxygen. Capsules were fluorescently imaged over 96 hours with red signal indicative of hypoxic stress. For capsules incubated in high oxygen conditions, signal was not detected in aggregates smaller than 250 µm over the three day study period (Figure 2.4a1, b1, c1, d). Signal was observed in aggregates of all sizes within 20 hours in capsules incubated in low oxygen conditions (Figure 2.4a2, b2, c2). In both low and high oxygen conditions, aggregates larger than 250 µm displayed signal in core regions. With extended time, signal in low oxygen aggregates expanded to include the entire aggregate, but remained localized in the aggregate core in high oxygen capsules (Figure 2.4e, f). The largest aggregates (> 700 µm) exhibited localized interior signal at the time they were encapsulated, immediately following the 24 hour aggregation period (Figure 2.4 g). In continued hypoxic conditions, maximum signal expression was reached by 48 hours and was sustained thereafter with maintenance of the low oxygen condition.

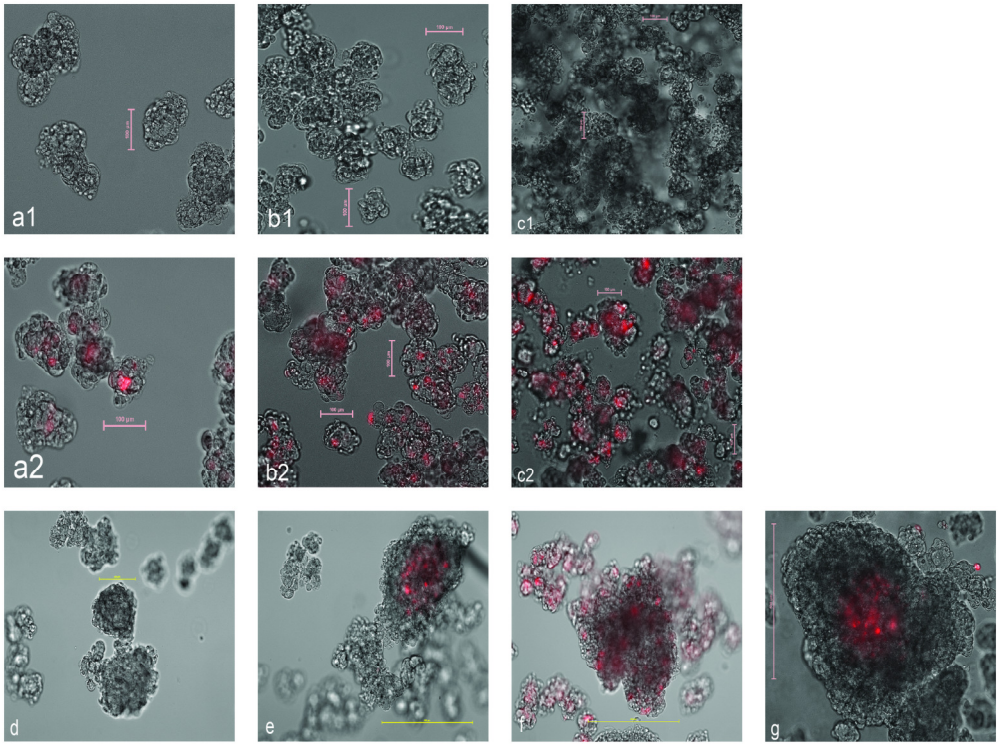

Figure 2.4 Fluorescently imaged aggregates from capsules containing 200,000 (a, bar=100µm), 600,000 (b, bar=100µm), and 1 million (c, bar=100µm) cells incubated in high (1) and low (2) oxygen conditions for 20 hours. At 20 hours in high oxygen, 250 µm aggregates (d, bar=100µm) did not display signal, but 500 µm aggregates showed centralized signal (e, bar=500µm). At 20 hours in low oxygen, 500 µm aggregates displayed ubiquitous signal (f, bar=500µm), though signal onset also occurred in core regions. Exceptionally large aggregates (~700 µm shown) displayed central signal at Time 0 (g, bar=500µm). Fusion of smaller aggregates was noted in capsules with higher cell densities (b1,c1,b2,c2).

2.5 Discussion

As early as 1980, transplanted encapsulated pancreatic tissue was shown to have potential to alleviate diabetes [**164** Lim 1980]. However, long-term success of such devices has remained elusive, with oxygen insufficiency suspected as a primary cause. Currently, most studies evaluating hypoxia in tissues do so indirectly, by quantifying functional changes in response to varying oxygen levels, or after the fact by

immunostaining fixed histological sections. However, the former approach does not easily account for the fact that functional changes may not be exhibited uniformly by all cells within a capsule, while the latter cannot indicate cellular responses at the time of occurrence nor retain viability of the tissue of interest. On the other hand, knowing the minimum cellular oxygen requirement, one could attempt to determine whether that value is met within a capsule, as has been done with microelectrode measurement of oxygen concentration [**273** Carlsson 1998] and computational modeling [**151** Gross 2007],[**153** Buchwald 2009],[**274** Dulong 2007]. However, although providing a good estimate, models are time consuming to develop and employ and must be re-adapted to any change in material or geometrical configuration. Furthermore, they still cannot take into account every factor affecting oxygen concentration throughout a capsule as some are not yet even fully understood. As an alternative approach, our fluorescent hypoxia marker system allows individual, living cells to report when they initiate a hypoxic stress response. This method both obviates the need to measure oxygen concentration and allows hypoxic conditions to be detected quickly, and potentially remediated, prior to tissue necrosis.

The hypoxia marker was evaluated in MIN6 aggregates encapsulated at different densities within crosslinked PEGDM hydrogels. No toxic effects should be expected from the method of encapsulation used in this work. Acrylated or methacrylated PEG as an encapsulation matrix has been shown to be supportive of a range of cell types. PEG itself is highly biocompatible while the Irgacure 184 photoinitiator has been shown to have no influence on viability at low concentrations [**180** Bryant 2000]. Bryant et al. also

showed that 10 minutes of UV irradiation was likewise not detrimental to cell viability, and report that this length of exposure is within the clinically acceptable range [**180** Bryant 2000]. Low-speed centrifugation prior to encapsulation did not result in aggregate disruption.

Results from both our functional studies and hypoxia detection studies are in good agreement with the published literature. Exposure of MIN6 aggregates to hypoxic conditions elicited an observable fluorescent response within 20 hours. Though future work will focus on timing of signal initiation, extremely large aggregates (> 500 µm) displayed central signal at the time of encapsulation. This indicates that signal onset occurs fairly quickly and agrees with Moritz et al. who found that response to hypoxia was observed in as little as 6 hours [**275** Moritz 2002]. We also observed reduction in insulin secretion under hypoxic conditions, with effects beginning as early as day 2. Similar results have been widely reported [**184** Dionne 1989],[**185** Dionne 1993],[**186** de Groot 2003].

When comparing signal expression and insulin secretion between capsules containing differing densities of cells, density of seeding did not appear to directly influence hypoxic signaling; at 1% oxygen all aggregates appeared to display signal, while at 20% oxygen signal was only seen in core regions of the largest aggregates. Thus aggregate size appears to exert more influence over aggregate oxygenation than overall cell number. As noted, though small, differences in average aggregate size between the tested cell densities were determined to be significant. However, it is unlikely that these average size differences contribute much to differences in signal expression and

insulin secretion (73 µm and 80 µm aggregates, for instance, did not exhibit differences in hypoxia signal expression and likely secreted insulin similarly). The percentage of large and exceptionally large aggregates present in the differing populations, on the other hand, may have contributed more significantly. In capsules containing 1 million cells, aggregates 150 µm or larger represented nearly 12% of aggregates while making up less than 2% of aggregates in 200,000- and 600,000-cell capsules. Additionally, twice as many exceptionally large aggregates (>250 µm) were observed in 1 million-cell capsules. At this size, aggregates began to display hypoxia signaling in core regions, even in a 20% oxygen environment, again, consistent with findings by other groups [**184** Dionne 1989],[**275** Moritz 2002]. Thus, hypoxia signaling and insulin secretion were only indirectly affected by seeding density in capsules containing 1 million cells, insomuch that large aggregates were more prevalent. We point out that in our work it was desirable to observe the behavior of both large and small aggregates. However, in studies where stricter control of aggregate size may be important, consistency in size may be achieved by aggregating cells at a density of 100,000 cells per mL and then pooling aggregates to attain the desired number of cells per capsule.

Close observation of insulin secretion data may point to a tempting hypothesis – a greater percentage of large aggregates with hypoxic core regions explains an apparent "diminishing returns" in insulin secretion, where capsules containing 1 million cells incubated in high oxygen secreted statistically similar amounts of insulin as capsules containing 600,000 cells. Indeed, such an effect has been reported by Suzuki et al. [**182** Suzuki 1998]. However, as noted, a number of the measured high-oxygen insulin

concentrations were at the maximal detectable limit of the assay and were estimated in calculations to be the maximal value. Because of this, accurate comparisons between the different seeding density groups cannot be made. However, the effect of these estimated values is not so detrimental to a comparison between the high and low oxygen conditions, on which this study is primarily focused. Even with relatively large standard deviation in some cases (attributable to small variability in cell number, precision of the assay, and the nature of insulin secretion), cells in high oxygen conditions secreted an amount of insulin that was, as calculated, significantly higher than cells in low oxygen conditions on Days 7 and 14. Because any true secretion value could only be the same or higher than the estimated value reported in this work, the difference between levels of insulin secreted in high and low oxygen conditions would only be increased by knowledge of the more accurate value. Thus our approach does not impact any conclusion drawn by a comparison of the functional effects of a 20% or 1% oxygen environment.

We report that hypoxia signaling was observed within 24 hours of exposure to low oxygen conditions while a drop in GSIS became apparent by day 2. In this sense, hypoxic signaling was predictive of future device function. Furthermore, signal onset was rapid enough to allow time for a remediating response prior to cell loss. Additional study will be required regarding signal extinction, though preliminary observations show that extinction occurs within 48 hours after re-exposure to the high oxygen condition. We hope that with modification of MOI, this system may be tuned to achieve real-time signaling. As a real-time indicator of hypoxia, the marker system might be particularly

useful to study of encapsulated tissues *in vivo*. Strength of emission will determine if signal is detectable, but we would expect utility at least in small animal models with an implantation site near to the skin. A possible modification in order to increase *in vivo* applicability could be to substitute a bioluminescent marker for the DsRed-DR gene used in this work. Though quantification of either type of signal is difficult, current work is focused on measuring HIF-1α levels to compare to fluorescent intensities and determining threshold intensities corresponding to specific cellular responses.

Finally, though in this work MIN6 cells were particularly suited to demonstrating our method of hypoxia detection, we believe that the marker system may be favorably utilized in other cell types as well. We have recently, for instance, observed marker expression in native islets of Langerhans isolated from Balb/c mice. In this regard, degree of HIF-1 expression may vary among tissue types and will have large implications as to whether the marker could be considered for use [**275** Moritz 2002]. Nonetheless, recent works suggesting the role of hypoxia in directing stem cell differentiation offer another exciting field in which our method of hypoxia detection could be helpfully employed [**260** Abdollahi 2010],[**276** Ma 2009],[**277** He 2010]. We hope to investigate such applications in future work.

Chapter 3

Identifying HIF Activity in 3D Cultures of Islet-Like Clusters[2]

[2]M.L.. Skiles, N.B. Wilder, S. Sahai, J.O. Blanchette. Identifying HIF activity in three-dimensional cultures of islet-like clusters. Int J Artif Organs 2013, 36(3);175.83. (published) [**278** Skiles 2013]

3.1 Abstract

Purpose: Hypoxia is a major cause for failure of encapsulated islet grafts. 3D re-aggregation and hypoxic preconditioning are used to help overcome this obstacle. However, it is still difficult to identify hypoxic cells in a 3D system. We evaluate the efficacy of a fluorescent system for detecting HIF-1 activity in live β-cells. Identification of HIF-1 activity and correlation with insulin secretion and viability will allow for more informed implant construction and better prediction of post-transplantational function.

Methods: MIN6 cells were infected with the marker virus and rotationally cultured to form clusters. Clusters were encapsulated in PEG hydrogels and incubated in 20%, 2%, or 1% O_2. Gels were imaged daily for hypoxia marker signaling and for morphological observation. Daily GSIS was quantified by insulin ELSIA and cell viability was assessed by LIVE/DEAD staining.

Results: Clusters cultured in 2% and 1% O_2 displayed high levels HIF activity compared to 20% O_2 clusters. 20% O_2 clusters maintained viability and achieved a smooth, islet-like morphology by Day 14. Clusters in 2% and 1% O_2 failed to associate cohesively and showed reduced viability. As a whole, constructs cultured in 20% O_2 exhibited 10-fold higher GSIS than constructs in 2% and 1% O_2.

Conclusions: Our marker is an effective approach for identifying cellular hypoxia in 3D cultures. β-cell clusters in 2% and 1% O_2 are similarly affected by reduced oxygen tension, with HIF-1 activity correlating to reduced GSIS and impaired cell/cluster morphology. Simultaneous aggregative culture and hypoxic conditioning may not be beneficial to β-cell transplantation.

3.2 Introduction

Cell-based therapies for treatment of T1DM remain hindered by dramatically-reduced oxygenation of excised and transplanted islets [**279** Davalli 1995],[**280** Carlsson 2001],[**281** Miao 2006]. While alleviating some of the difficulties associated with tissue transplantation, encapsulation can further decrease oxygen tension in the graft [**186** de Groot 2003],[**282** Cornolti 2009]. To reduce hypoxia-related loss of function, methods such as hypoxic preconditioning [**283** Semenza 2011b],[**284** Lo 2012] and islet dissociation/re-association (to produce smaller, more β-cell dense clusters) have been suggested [**191** Cavallari 2007],[**285** Schuit 2001]. Still, further advancement in islet transplantation will depend upon quick and accurate detection of the hypoxic state, an understanding of the cellular impact of and response to hypoxia, and an ability to remediate the hypoxic condition or avoid it in the first place.

Most cells exhibit substantial changes in gene expression as an adaptive response to oxygenation below 5 or 6%. A majority of these changes involve upregulation of genes by activity of HIF-1, a heterodimeric bHLH-PAS family transcription factor whose presence in the cell is tightly regulated by oxygen. Specifically, the HIF-1α subunit is subject to rapid degradation under normoxic conditions, but is exponentially stabilized as oxygen becomes limited [**105** Jiang 1996b]. HIF responses serve to adapt the cell for survival in a low oxygen environment by, among other things, switching the cell to glycolytic metabolism, promoting local angiogenesis, inhibiting apoptosis, and reducing oxygen-intensive cellular activities [**286** Cassavaugh 2011]. In the insulin-secreting β-cells of the pancreas, HIF-1-induced

switching to glycolytic metabolism has been shown to decouple glucose sensing from insulin exocytosis resulting in a dramatic impairment of insulin secretion from hypoxic islets [**195** Zehetner 2008],[**196** Cantley 2009],[**197** Puri 2009].

Determining if and when insulin-producing cells become hypoxic is clearly important in predicting their performance. However, identifying hypoxic cells, especially within 3D islet and islet-like cluster cultures, can be difficult. Measuring oxygen partial pressure and modeling oxygen diffusion/consumption may help identify regions of low local oxygen concentration but do not identify any behavioral changes in the cells. A complimentary technique is to identify HIF-1 activity, which represents a behavioral response to hypoxia whatever the specific oxygen concentration. Due to its activity as a transcription factor and its short half-life (in normoxia, 4-8 minutes) [**109**Moroz 2009],[**287** Yu 1998], direct detection of HIF-1 without compromising the cell and/or construct is difficult or impossible. Furthermore, HIF responses are not homogeneous across cell types, with degree of stabilization and upregulated target genes varying between and within tissues [**48** Maxwell 1993],[**128** Brachen 2006],[**129**Lendahl 2009]. Therefore we employ a fluorescent reporter gene system which indicates HIF activity in oxygen-stressed cells rather than HIF abundance. We have previously reported the convenience of this approach for identifying hypoxic cells in β-cell clusters and allowing HIF activity to be monitored in the same sample over time [**270** Skiles 2011a].

In the present work, we sought to compare HIF activity in aggregated, encapsulated murine β-cells to other cell properties that are impacted by hypoxia, such

as morphology, viability, and GSIS. While atmospheric oxygen concentrations are common in cell culture, they are not representative of an implant microenvironment; therefore, we examined β-cell behavior in normal culture conditions (20% O_2) as well as a pair of more physiological oxygen concentrations commonly used for hypoxic preconditioning (2% and 1% O_2). Given the high oxygen requirement of β-cells, elevated HIF activity would be expected to correlate to decreased insulin secretion and possibly loss of viability. Such results would show the utility of the marker to predict functional changes in encapsulated β-cells and to evaluate the consequences of various oxygen conditions.

3.3 Materials and Methods

3.3.1 Cell Culture

MIN6 cells were cultured in RPMI 1640 medium (Mediatech, Manassas, VA) supplemented with 10% fetal bovine serum (PAA, Dartmouth, MA), 1% penicillin-streptomycin (Mediatech), 0.5 μg/mL amphotericin B (Mediatech), and 7 mM D-(+)-glucose (Sigma-Aldrich, St. Louis, MO). Cultures were maintained in standard incubation conditions at 37 °C, 5% CO_2, and high humidity. For experimental use, the cells were trypsinized prior to confluence, counted, and seeded into the wells of a 12-well suspension culture plate at a density of 400,000 cells per well in 1.7 mL of media.

3.3.2 Hypoxia Marker

For marker studies, the cells were infected with a hypoxia marker virus prior to encapsulation, as previously described [**270** Skiles 2011a]. Briefly, the marker virus was

added to each well of dispersed cells at an MOI of 100 immediately following cell trypsinization and seeding. The marker is a recombinant adenovirus generated by the pAD-Easy-1 system (QBiogene, Montreal, Canada) that introduces a gene coding for a destabilized variant of the red fluorescent protein, Ds-Red-DR under the control of a minimal SV40 promoter and trimer of the HRE sequence. In an infected cell, hypoxia-stabilized HIF-1 binds to the HRE and allows for hypoxia-induced transcription of the Ds-Red-DR gene and subsequent fluorescent signaling.

Following introduction of the virus, dispersed cells were incubated in rotational culture at 100 rpm for up to 36 hours to allow for infection and for formation of islet-like clusters. Clusters were then encapsulated and immediately imaged, and the gels were divided into three groups for rotational culture in either a 20%, 2%, or 1% oxygen environment. Oxygen concentration was controlled through use of Napco Series 8000 incubators (Thermo Fisher, Waltham, MA) with automated nitrogen purging for maintenance of a set oxygen percentage. Following placement in the appropriate incubator, gels were fluorescently imaged daily followed by replacement of media.

As a positive control, cells were infected with a modified marker virus containing a CMV promoter in place of the HRE trimer, allowing for constitutive expression of the marker signal, regardless of oxygen status. As a negative control, uninfected cells were also fluorescently imaged.

We have previously measured dissolved oxygen content of media incubated in 1% O_2 and observed that 24 hour incubation is sufficient to achieve a steady, equilibrated concentration [**270** Skiles 2011a]. Therefore, in the present study, low-

glucose media and high-glucose buffer solutions to be added to gels incubated in 2% and 1% O_2 conditions were pre-equilibrated to 2% and 1% O_2, respectively, for 24 hours prior to use.

3.3.3 PEGDM Synthesis and Cell Encapsulation

PEGDM was synthesized from linear, 10 kDa PEG (Sigma-Aldrich) as previously described [**270** Skiles 2011a], following a protocol adapted from Lin-Gibson et al. [**177** Lin-Gibson 2004]. Briefly, microwave methacrylation of PEG was carried out by irradiating a 10:1 molar ratio solution of methacrylic anhydride (Sigma-Aldrich) and PEG in a standard domestic microwave for 5 minutes to form PEGDM. This was dissolved in excess dichloromethane (Sigma-Aldrich) then precipitated in cold, anhydrous diethyl ether (Sigma-Aldrich) and collected. The precipitate was dissolved in deionized water and dialyzed against the same for 3 days for purification. Purified PEGDM powder was collected by lyophilization.

A photoactive, PEGDM solution was prepared for the formation of hydrogels. PEGDM was dissolved in HBSS (Mediatech) to form a 10 wt% weight solution and Irgacure 2959 (Ciba, Basel, Switzerland) was added to 0.025 wt% as a photoinitiator. The solution was sterile-filtered prior to use.

Cell clusters were encapsulated in a two-step process. First, the bottom half of the hydrogel was formed by pipetting 20 µL of photoactive PEGDM solution into a narrow cylindrical tube. The tube was exposed to UV light (365 nm, ~7 mW/cm^2) for 8 minutes to initiate cross-linking. During this time, previously aggregated MIN6 clusters were removed from their wells and centrifuged for 4 minutes at 210 g. The media was

removed and the clusters were gently resuspended in 20 µL of photoactive PEGDM solution. This volume was added on top of the first 20 µL volume and cross-linking was completed by an additional 8 minute UV exposure. The hydrogels were then ejected, rinsed in HBSS, and placed in a 24-well plate in 1 mL of media for incubation.

3.3.4 Glucose-Stimulated Insulin Secretion

To evaluate GSIS from encapsulated MIN6 clusters, gels were prepared with each containing aggregates formed from a total of 400,000 cells. Freshly-formed gels were divided into three groups and placed in 24-well plates in 1 mL of low-glucose media (2 mM) each. For the first day, all plates were incubated in rotational culture at 20% O_2. After 24 hours, the media was removed and replaced with a buffered, high-glucose solution (16.7 mM) for one hour. This solution was removed and frozen for future analysis and replaced with 1 mL of low-glucose media. Plates were then placed in rotational culture at 20%, 2% or 1% O_2. Thereafter, gels were stimulated in the same manner every 24 hours. Insulin concentration in media samples was quantified by mouse insulin ELISA (Mercodia, Winston-Salem, NC) following the manufacturer's protocol.

3.3.5 Viability

To assess viability of encapsulated cells, an esterase activity and plasma membrane permeability assay (LIVE/DEAD, Invitrogen, Grand Island, NY) was performed. MIN6 cells were aggregated and encapsulated as described and placed in 20%, 2% or 1% oxygen incubation in 1 mL of media each. Every 24 hours, one gel from each incubator

was removed and stained with LIVE/DEAD reagent for 30 minutes following the manufacturer's protocol. Media was replaced in the remaining gels and they were returned to incubation. Stained gels were then briefly rinsed with HBSS and fluorescently imaged. Viable cells were indicated by a green cytoplasmic staining and dead cells were indicated by red nuclear staining. For cells incubated in 2% and 1% O_2, media pre-equilibrated to 2% and 1% O_2, respectively, was used.

3.3.6 Imaging and Statistical Analysis

Fluorescent imaging was performed on a Nikon Eclipse T*i* (Nikon Instruments, Melville, NY) inverted, fluorescent microscope. For fluorescent capture, care was taken to ensure that consistent lamp intensity and exposure settings were maintained and that fields were representative of the whole gel. In marker studies, the same gels were tracked over time. Image analysis was performed in NIS-Elements AR 3.0 (Nikon) software. For quantitative GSIS studies, a minimum of three replicate samples were analyzed. Results are reported as mean ± standard deviation. Differences between values were assessed by a student's t-test assuming unequal variances with statistical significance occurring when $p < 0.05$ (indicated in the results with an asterisk, '*').

3.4 Results

3.4.1 Encapsulation and Cell Morphology

Clusters of aggregated MIN6 cells were formed by 36 hour rotational culture of 400,000 cells in low-adherence 12-well culture plates. Previous studies indicated that clusters larger than 300 µm experience core hypoxia even at 20% oxygen conditions,

and that few clusters of this size would be formed in rotational culture of 400,000 cells [**270** Skiles 2011a]. For each well, all clusters were collected and encapsulated in a single hydrogel, placed in 20%, 2% or 1% oxygen conditions, and periodically imaged over 2 weeks. Hydrogels were cylindrical, approximately 2 mm high and 5 mm in diameter when swollen, with clusters distributed throughout (Figure 3.1).

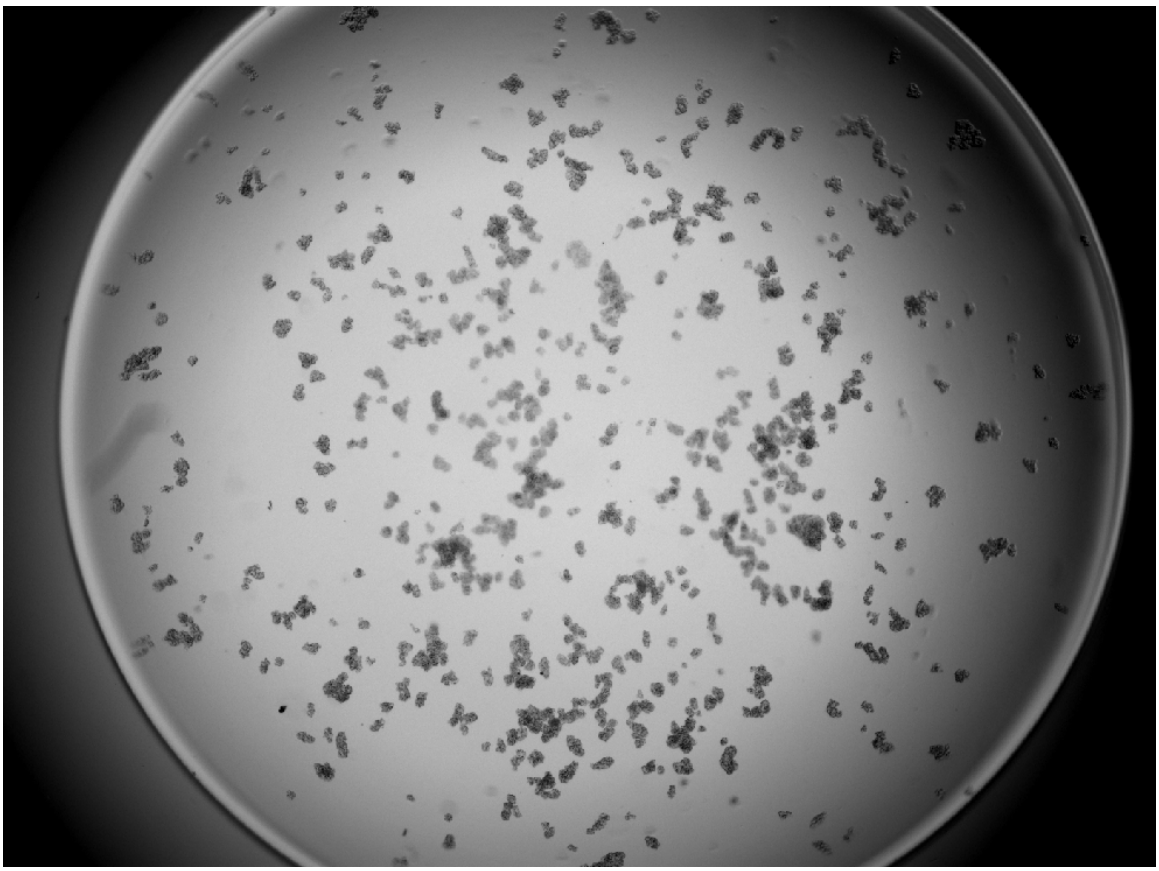

Figure 3.1 400,000 MIN6 cells aggregated to form islet-like clusters and encapsulated in a 40 µL PEGDM hydrogel. Bar = 1 mm.

Initially after formation, the cells were associated into small, irregularly-shaped clusters with individual cells remaining discernable. By 4 days, 20% O_2 clusters were clearly distinguishable from Day 1 clusters, with Day 7 clusters displaying a more regular,

ovoid shape and a smooth surface morphology akin to native islets. Individual cells within the cluster could not be distinguished. In 1% or 2% oxygen, clusters did not achieve a smooth, round morphology by 4, 7 or 14 days and individual cells were still β-cells discernable within the clusters. Clusters in 20% oxygen could be distinguished from those in 1% or 2% oxygen by 4 days, though not sooner. After 2 weeks, clusters incubated in 20% oxygen were large, round and healthy looking with a clear islet-like appearance while clusters incubated in 2% and 1% oxygen appeared unchanged or irregular and necrotic (Figure 3.2).

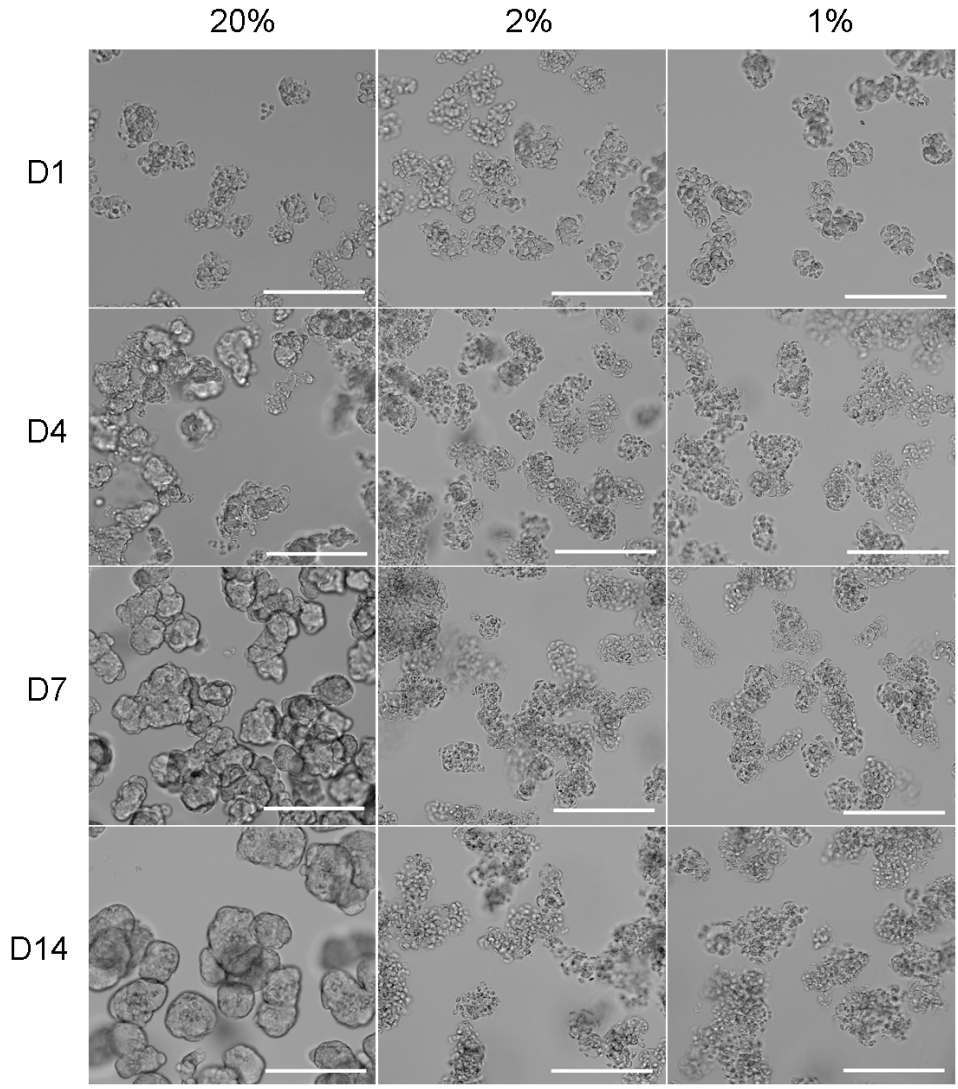

Figure 3.2 Brightfield microscopy images of islet-like clusters for the analysis of morphology over 2 weeks in 20% O_2, 2% O_2, or 1% O_2. Clusters incubated in 20% O_2 attained a morphology similar to that of primary islets by 1 week and retained that morphology thereafter. Clusters incubated in 2% and 1% O_2 never achieved a primary islet-like morphology, with loosely associated cells and irregular aggregate morphology.

3.4.2 Hypoxia Marker

To correlate hypoxia with cellular activity of HIF-1, a fluorescent reporter system was employed. Transient infection with the marker virus allowed the cells to produce a red fluorescent protein under the control of active HIF-1. If present, this signal was easily detected by fluorescent microscopy. At the time of encapsulation (Time 0), no cells were observed to display fluorescent signal. At the given capture settings, Clusters incubated in 20% oxygen exhibit few or no cells displaying fluorescent signal at the given capture settings over the course of the study. Clusters incubated in 2% and 1% O_2 showed a dramatic increase in number and intensity of fluorescing cells beginning on Day 1 compared to 20% O_2 clusters (Figure 3.3). Intense signal in 2% O_2 slightly preceded such signal in 1% O_2. Maximum signal intensity was reached on Day 2 or 3. Signal pervasiveness and intensity appeared similar between 2% and 1% O_2 clusters. Fluorescence was heterogeneous throughout signaling clusters, with signal clearly identifiable in individual cells. Though signaling cells appeared somewhat randomly distributed in the clusters, fluorescence was often observed in central cells of larger clusters. In control studies, all CMV-DsRed-DR infected cells displayed rapid, intense fluorescent signaling indicating efficacy of the system and high rate of infection. Uninfected cells displayed no fluorescence.

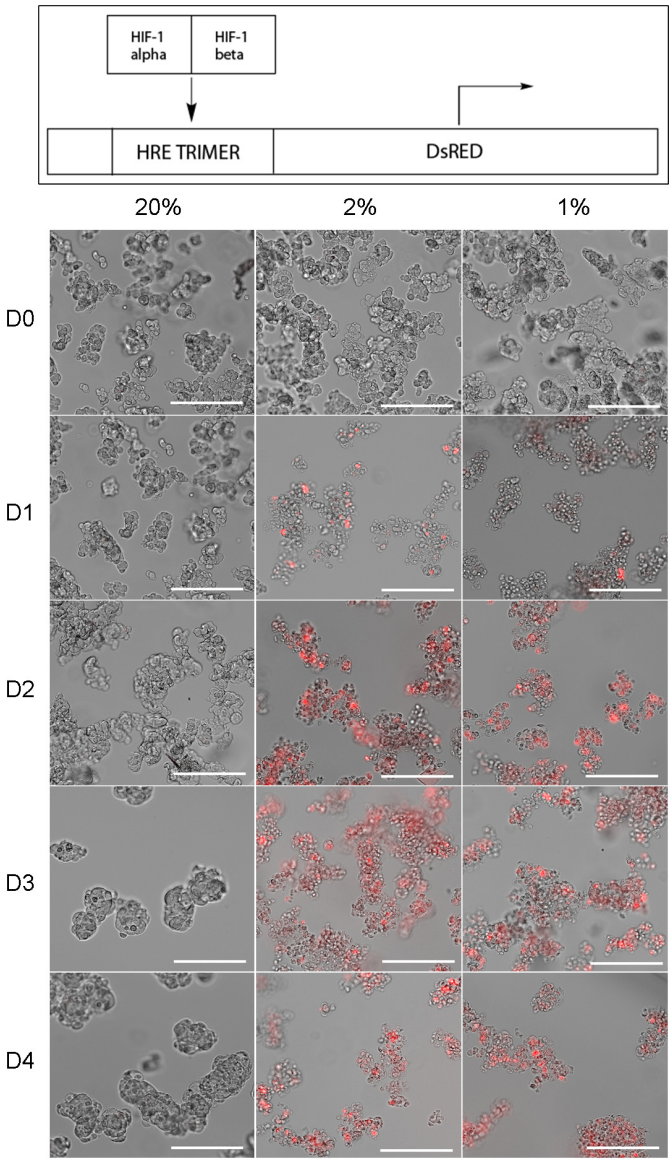

Figure 3.3 (Top) Schematic of HIF-induced cellular fluorescence used to identify HIF activity in this study. At sufficiently low oxygen concentrations, HIF-1α is stabilized, dimerizes with HIF-1β and binds to the HRE sequence, initiating transcription of the target gene, in this case Ds-Red-DR. (Bottom) Hypoxic signaling in islet-like clusters of MIN6 cells infected with the hypoxia marker virus for HIF-activated fluorescence. Clusters incubated in 20% O_2 displayed little or no fluorescence through the study. Clusters incubated in 2% and 1% O_2 expressed signal by Day 2 with fluorescence located throughout all clusters.

3.4.3 Glucose-Stimulated Insulin Secretion

We assessed the secretory activity of MIN6 clusters incubated in 20%, 2%, and 1% O_2 for comparison to HIF-1 activity as indicated by the fluorescent marker. These results are graphically represented in Figure 3.4.

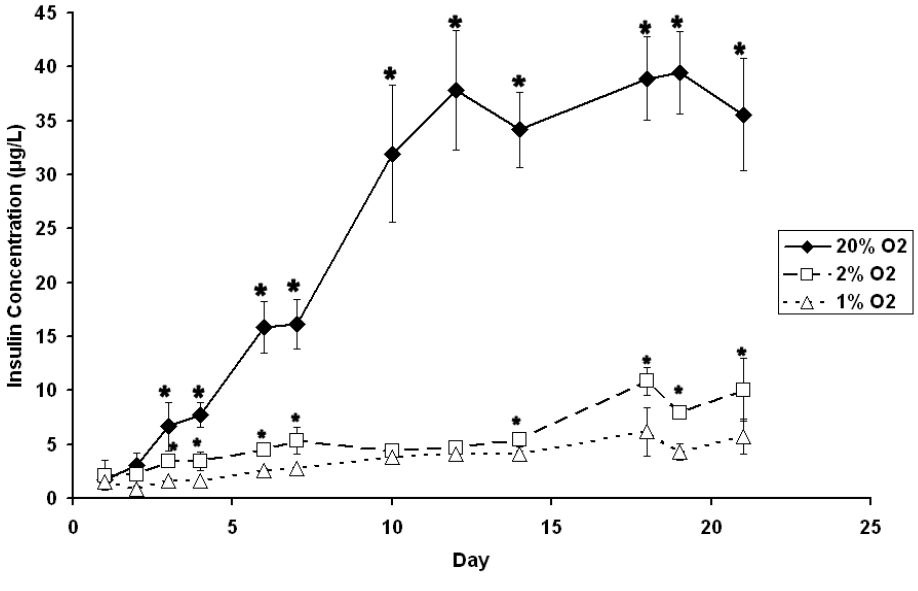

Figure 3.4 GSIS in clusters of MIN6 cells cultured in 20%, 2%, or 1% O_2 (mean ± standard deviation, n = 3). Large asterisks indicated significant difference between 20% O_2 and both low-oxygen conditions. Small asterisks indicate significant difference between 2% and 1% O_2 samples ($p < 0.05$).

Consistent with islet-like morphological arrangement and minimal indication of HIF-1 activity, clusters incubated in 20% oxygen displayed high levels of insulin secretion. Continued increase in secretion was observed from Day 1 through Day 12. This correlates well with the timeframe over which primary islet-like size and morphology were achieved. On Day 12 insulin secretion plateaued, with 37.8 ± 5.5 µg of insulin secreted during the 1 hour stimulation period. In clusters incubated in 1% and 2% O_2,

very little increase in secretion from Day 1 was observed over the course of the study. Statistical significance between secretion from 20% clusters and secretion from low-oxygen clusters was seen by Day 3, the time by which hypoxia signaling reached a maximum. Secretion from clusters incubated in 2% O_2 was slightly higher than secretion from clusters incubated in 1% O_2. On Day 12, one-hour secretion from clusters incubated in 2% and 1% O_2 was measured to be 4.7 ± 0.2 µg and 4.1 ± 0.1 µg, respectively, equating to 8 to 9 times less insulin than by clusters in 20% O_2. As reported, these secretion results represent the overall insulin-producing capability of constructs incubated in their respective oxygen condition.

3.4.4 Viability

The viability of cells within the encapsulated clusters was examined via a Live/Dead esterase activity/plasma membrane integrity assay (Figure 3.5). On Day 1, nearly 100% viability was observed in cells from all three oxygen conditions. Cells incubated in 20% O_2 maintained this level of viability throughout the 14 day study. Loss of viability in a small number of cells was first observed on Day 2 in gels incubated in 1% oxygen and on Day 4 in gels incubated in 2% oxygen. Through the remaining two weeks of the study, the appearance of non-viable cells slowly increased in both of these conditions; however, overall viability appeared to remain high.

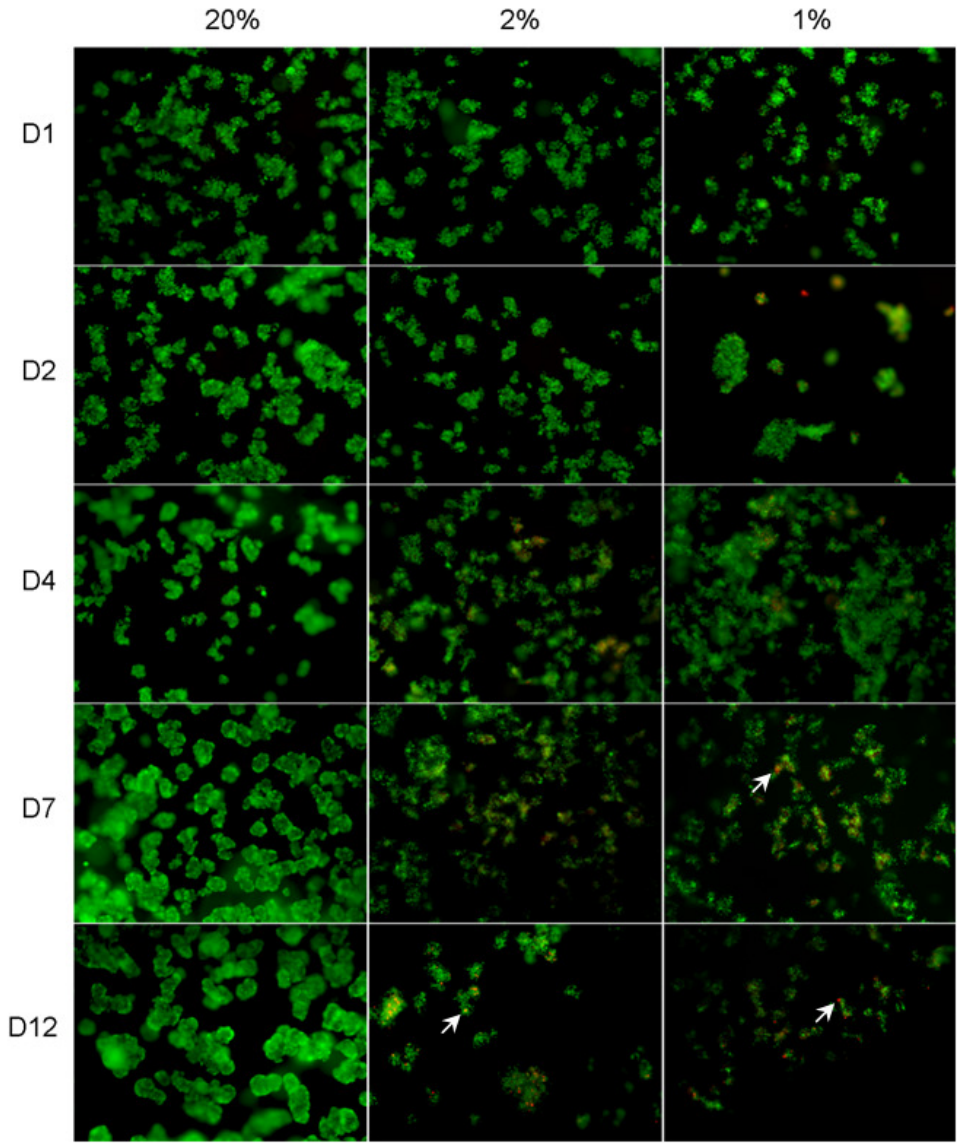

Figure 3.5 Analysis of viability in clusters of MIN6 cells. Cells incubated in 20% O_2 appear completely viable (green staining) over two weeks. Clusters incubated in 2% and 1% O_2 both displayed some cell death (red staining, indicated with white arrows) within clusters by Day 4. Numerous cells appeared to be non-viable in these conditions by Day 14, though total viability was estimated to remain above ~75%.

Consistent with morphological observations, green cytoplasmic staining, indicating viable cells, expanded and intensified in 20% O_2 clusters over the same timeframe in which they adopted a primary islet-like morphology. That these clusters were healthy and functional is supported by their high, sustained GSIS. Alternatively, green cytoplasmic staining in 2% and 1% O_2 clusters was unchanged or increasingly diminished indicating a reduced cytoplasmic volume and reduced esterase activity. This corresponded to both evidence of active HIF-1 and poor GSIS. Representative non-viable cells are indicated by the arrows in the figure. Though useful as an indicator of change in viability between clusters incubated in 20% O_2 and those incubated in hypoxic oxygen conditions, percent viability within the clusters was not able to be accurately quantified due to the 3D nature of the cultures and difficulty in distinguishing neighboring cells.

3.5 Discussion

That low oxygen tension has a profoundly negative impact on insulin secretion from pancreatic β-cells, both *in vitro* and *in vivo*, has been widely documented[**184** Dionne 1989],[**185** Dionne 1993],[**186** De Groot 2003],[**280** Carlsson 2001]. However, the difficulty in assessing when a cell becomes hypoxic (i.e. begins to respond to hypoxia) on a cellular level within 3D aggregates has hindered better understanding of whether various physiological/culture conditions will illicit a detrimental hypoxic response. Many common approaches to "identifying" hypoxia involve direct or indirect measurement of oxygen partial pressure or dissolved oxygen concentration. However, these methods suffer from a number of drawbacks, including invasiveness and potential

tissue/construct damage, insufficient resolution for cellular-scale detection, consumption of oxygen in the detection process, requirement for tissue/construct sacrifice, reliance upon expensive equipment, and/or poor precision [**288** Springett 2007],[**289** Grist 2010]. Furthermore, these methods focus on measurement of oxygen concentration but not cellular activity in response to that concentration.

Alternatively, the method discussed in this work identifies activity of the primary regulator of intracellular response to hypoxia, HIF-1, and in this sense may be considered to truly identify hypoxic status. This method has the added benefit that signaling and detection do not impact viability and that the tissue/construct need not be sacrificed in the detection process, as is required in histological analysis, allowing for the same population to be examined over time. Our marker can be easily applied to monolayer culture, micromass culture, and tissue culture within 3D scaffolds to investigate the potential impact on oxygenation resulting from each of these conditions. Furthermore, because the signal protein is a direct target of HIF-1, this system is ideal for examining the relationship between culture conditions and various other HIF-induced responses.

HIF-activated pathways have been recognized as the primary mechanisms by which low, intracellular, oxygen concentration is translated to a program of transcriptional responses which result in loss of β-cell function. We therefore undertook the current work based on an interest in using identification of intracellular HIF-1 activity as an indicator of activation of these downstream pathways. We employed a previously-developed fluorescent marker system to indentify HIF-1 activity

in living cells which we compared to a number of physiological and functional events known to be impacted by hypoxia. We showed that marker signal was induced by hypoxic incubation and that signal corresponded to irregular cell association and morphology, inability of clusters to achieve primary islet-like organization, and dramatic decline in GSIS. Furthermore, hypoxic signal was apparent by Day 2, prior to the time at which a difference in morphology of GSIS was detectable, highlighting the use of this system as a predictor of cell viability and function.

Luther et al. report that unencapsulated clusters of MIN6 cells cultured in 20% oxygen achieve a size and conformation similar to primary islets after 7 days [**290** Luther 2005]. In the present study, we report that encapsulated MIN6 clusters achieve primary islet-like size and appearance by Day 7 when cultured at 20% oxygen but not at 2% or 1% oxygen. Alternatively, MIN6 clusters incubated in 1% and 2% oxygen displayed hypoxia marker signal expression, indicative of HIF activity, and failed to achieve the tight, round morphology found in primary islets. Individual cells within the clusters remained more distinguishable suggesting loose cell interactions rather than the tight interactions seen in clusters at 20% oxygen. Proper function of pancreatic β-cells is heavily dependent upon cell-to-cell contact [**291** Hauge-Evans 1999],[**292** Lin 2011],[**293** Luther 2006]. HIF-1-induced repression of cell adhesion proteins such as E-cadherin through upregulation of lysyl oxidase LOX, LOXL2, SIP1 and Snail provides an appealing explanation for this poor association [**294** Schietke 2010],[**295** Evans 2007].

HIF-1 also impacts insulin secretion directly by hindering metabolic pathways required for insulin exocytosis [**283** Semenza 2011b]. Secretion of insulin from

pancreatic β-cells is highly coupled to glucose sensing through aerobic mitochondrial pathways [**296** Lee 2008]. In β-cells with active HIF-1, these pathways are switched off resulting in severely blunted GSIS. We found that β-cell clusters incubated in atmospheric oxygen conditions (20%) did not exhibit impaired GSIS, despite the hindrances to oxygen diffusion that encapsulation and 3D tissues provide. However, when cultured in low physiological levels of oxygen, the cells exhibited clear HIF activity and impairment of GSIS in both 2% and 1% O_2.

Current studies suggest that there may be benefits to dissociating islets and re-forming them into islet-like clusters, primarily to reduce cluster diameter and improve oxygen transport [**285** Schuit 2001],[**191** Cavallari 2007]. Indeed, large diameter clusters can experience internal hypoxic gradients with central cells experiencing significantly different oxygen conditions than peripheral cells. In previous studies, we reported that central cells in clusters larger than approximately 300 μm displayed increased HIF activity via the reporter gene, even in 20% O_2 [**270** Skiles 2011a]. Clusters smaller than this size did not exhibit the increase in 20% O_2 and exhibited more uniform HIF activity in 2% and 1% O_2. Thus it is likely that severe oxygen gradients are not developed in clusters of the size examined in the current study. Another approach to improve post-transplantational function of β-cells is hypoxic preconditioning prior to implantation in order to prime them for the reduced oxygenation of the implant site [**283** Semenza 2011b],[**284** Lo 2012]. Our results suggest that simultaneous aggregation and hypoxic conditioning do not result in maintenance of islet-like morphology or GSIS and that the two techniques should be applied individually or sequentially.

3.6 Conclusions

It is clear that identifying cellular hypoxia will be beneficial to the advancement of cell-based diabetes therapies. Our marker, indicating HIF-1 activity, represents an ideal means of making such an identification. With this tool, we hope to establish correlations between β-cell oxygenation in 3D systems and β-cell function. Having shown its usefulness in a model system, we intend to apply this marker to future studies in isolated mouse islets. Here, we will be able to make predictions about implant function at various implantation sites with differing degrees of oxygenation. We will also examine the correlations between HIF-1 activity, cell binding protein production during re-aggregation, and GSIS in 3D culture systems. We feel that our marker system represents a convenient, non-invasive method of indicating intracellular HIF-1 activity that can serve as a much-needed tool for identifying hypoxia and examining its effects in current and future cell-based delivery endeavors.

Acknowledgements:

We thank the lab of Dr. Melissa Moss of the Chemical Engineering Department at the University of South Carolina, Columbia for shared use of equipment and the Medical University of South Carolina Instrument Resource Facility for assistance with histology. Special thanks to Dr. Kristi Anseth at the University of Colorado, Boulder for the generous donation of the MIN6 cell line.

This research was funded through grants from the National Science Foundation (EPS 0903795) and the National Institutes of Health (P20 RR-016461).

Chapter 4

Use of Culture Geometry to Control Hypoxia-Induced VEGF Secretion from ADSCs: Optimizing a Cell-Based Approach to Drive Vascular Growth[3]

[3]M.L. Skiles, S. Sahai, L. Rucker, J.O. Blanchette. Use of culture geometry to control hypoxia-induced VEGF secretion from ADSCs: optimizing a cell-based approach to drive vascular growth. Tissue Eng Part A (submitted, in revision)

4.1 Abstract

ADSCs possess potent angiogenic properties and represent a source for cell-based approaches to delivery of bioactive factors to drive vascularization of tissues. Hypoxic signaling appears to be largely responsible for triggering release of these angiogenic cytokines, including VEGF. 3D culture may promote activation of hypoxia-induced pathways, and has furthermore been shown to enhance cell survival by promoting cell-cell interactions while increasing angiogenic potential. However, the development of hypoxia within ADSC spheroids is difficult to characterize. In the present study we investigated the impact of spheroid size on HIF-1 activity in spheroid cultures under atmospheric and physiological oxygen conditions using a fluorescent marker. Hypoxia could be induced and modulated by controlling the size of the spheroid; HIF-1 activity increased with spheroid size and with decreasing external oxygen concentration. Furthermore, VEGF secretion was impacted by the hypoxic status of the culture, increasing with elevated HIF-1 activity, up to the point at which viability was compromised. Together, these results suggest the ability to use 3D culture geometry as a means to control output of angiogenic factors from ADSCs, and imply that at a particular environmental oxygen concentration an optimal culture size for cytokine production exists. Consideration of culture geometry and microenvironmental conditions at the implantation site will be important for successful realization of ADSCs as a pro-angiogenic therapy.

4.2 Introduction

Therapies that stimulate regeneration of damaged tissues in the body or restore deficient tissues with bioengineered replacements represent an appealing and emerging technology. Such therapies often involve the implantation of cells or tissue into an ischemic wound environment, necessitating rapid vascularization for survival and integration of the implant. Indeed, diffusional mass transfer limitations restrict the potential size of engineered tissues and remain one of the biggest challenges to their clinical success [**201** Lovett 2009],[**203** Novosel 2011]. New strategies to enhance angiogenesis are required to overcome these hurdles.

Strategies that harness the angiogenic potential of cells have shown promising results in recent studies. Fibroblasts [**297** Levenberg 2005],[**298** Kunz-Schughart 2006] and mesenchymal stem cells (MSCs) [**232** Kim 2007],[**299** Blasi 2011],[**300** Halfon 2011] can significantly contribute to endothelial network formation and maintenance of microvasculature. Dispersed mesenchymal stromal cells implanted in dermal wounds [**252** Lee 2009],[**301** Nie 2011] and ischemic tissue [**302** Kang 2010],[**303** Bhang 2011] increased local levels of angiogenic cytokines and promoted increased capillary density. Of the potential cell candidates to be utilized for cell-based delivery, ADSCs appear particularly well suited for use in regenerative medicine due to their relative abundance and ease of culture as well as their ability to differentiate into relevant cell types in musculoskeletal tissue engineering (e.g., osteoblasts, chondrocytes, vascular smooth muscle cells).

The manner of cell transplantation to an injury site can impact transplant performance. Cells injected as a dispersion have reduced cell-cell and cell-matrix interactions which are important in sustaining pro-survival pathways and suppressing apoptosis [**265** Bates 2000],[**303** Bhang 2011]. Alternatively, 3D cultures retain these interactions, while also providing reduced oxygen tension within the cell mass which may prime the cells for the ischemic implantation site [**267** Bhang 2012a],[**268** Saleh 2011],[**269** Baraniak 2012], enhancing therapeutic effect. For example, cord blood MSCs implanted as 3D spheroids upregulated expression of anti-apoptotic and angiogenic proteins, downregulated expression of proapoptotic proteins, and showed superior integration into newly forming vessels in ischemic mouse hind limbs compared to dispersed cells [267 Bhang 2012a].

Oxygen gradients that form within 3D tissues are not necessarily detrimental. In particular, hypoxia is responsible for initiating angiogenesis *in vivo* [**304** Shweiki 1992],[**305** Germain 2010] through activation of HIFs and subsequent upregulation of bioactive factors such as VEGF [**256** Forsythe 1996],[**306** Maxwell 2002],[**307** Fong 2009],[**308** Rey 2010]. HIF proteins are dimeric transcription factors of the bHLH-PAS family each composed of an α and β subunit [**52** Wang 1995]. The α subunit undergoes oxygen-dependent hydroxylation, marking it for proteosomal degradation. When local oxygen concentrations are not adequate for hydroxylation to occur, the subunit is stabilized, pairs with a β subunit, and is free to bind to HREs found in the promoter region of a number of genes involved in adapting the cell for survival in low oxygen.

Thus, oxygen tension in 3D cell masses can contribute to activation of HIF-regulated pathways which benefit the cells. For instance, stabilization of HIF and VEGF upregulation in growing avascular tumors is well known to promote tumor vascularization [**309** Brahimi-Horn 2001],[**310** Semenza 2012b]. Similarly, endothelial cells cultured as spheroids were found to express higher levels of HIF-1α mRNA than those cultured as a monolayer under the same oxygen conditions [**311** Bhang 2012b]. Additionally, hypoxia is known to play a role in regulating cell differentiation. During formation of vascularized endochondral bone, regional hypoxia leads to HIF activation and VEGF upregulation and is integral for the formation of a cartilage template and synchronization of ossification with angiogenesis [**312** Zelzer 2004],[**313** Araldi 2010]. Thus it is clear that identifying approaches to regulate desirable, HIF-activated signaling in ADSCs could provide new avenues towards creation of vascularized tissue and repair of critical size defects in bone.

The present study investigates the ability to control VEGF secretion from ADSCs by regulating hypoxic status. The effects of culture dimensions and incubator oxygen tension (atmospheric conditions as well as a pair of hypoxic levels) on angiogenic potential of ADSC spheroids are examined. HIF activity within the spheroids, identified using a previously-described fluorescent marker system [**270** Skiles 2011a], was compared to levels of VEGF secretion from the cells. The impact of pelleting and hypoxia on cell viability and morphology were examined by staining and histological analysis. Results from this study provide insight into the nature of hypoxia in 3D

cultures and may suggest a relevant approach for tailoring the release of angiogenic factors from ADSCs for improved vascularization of engineered tissues.

4.3 Materials and Methods

4.3.1 Cell Culture

Passage 1 human ADSCs isolated from lipoaspirates were purchased from Invitrogen (Carlsbad, CA) and cultured in Complete MesenPRO RS™ reduced-serum medium supplemented with a penicillin-streptomycin solution (Mediatech, Manassas, VA; final concentration: 115 IU/mL penicillin, 115 µg/mL streptomycin). This medium was also used throughout all experiments. For passaging, cells were kept in a humidified atmosphere of 95% air and 5% carbon dioxide at 37°C. Medium was changed three times a week. At approximately 80% confluence, the cells were trypsinized and sub-cultured at a ratio of 1:4 until reaching passage 6, as recommended by the supplier. All data included in these studies were obtained from cells between passages 3 and 6. Maintenance of ADSC stemness was verified by cell-surface staining and flow cytometry. Purchased, P1 cells were > 95% positive for stem cell surface markers CD44 and CD105. Fluorescent antibody labeling for each (CD44: eBioscience, San Diego, CA; CD105: Biolegend, San Diego, CA) revealed > 95% staining for both markers at P6 (Figure 4.1).

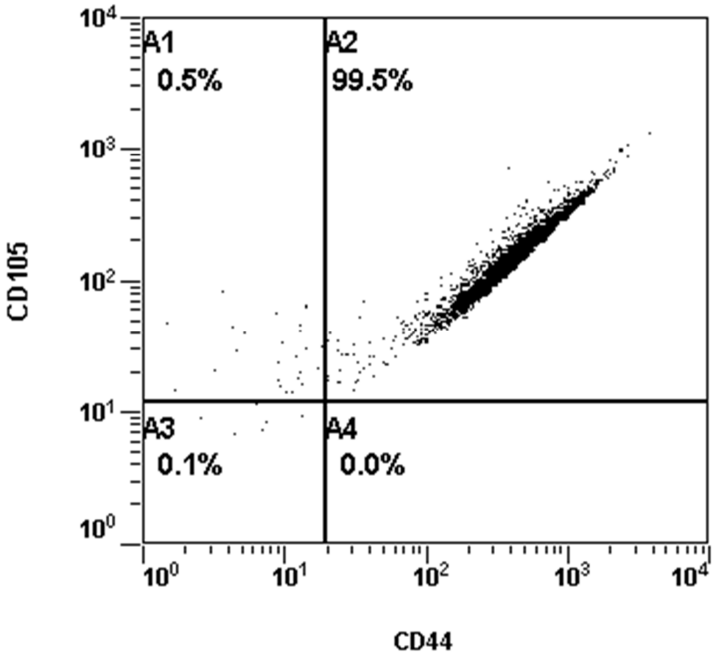

Figure 4.1 Flow cytometry analysis of cell surface markers CD44 and CD105 in P6 ADSCs. The cells were still >95% positive for both markers at passage 6, indicating maintenance of stemness.

Nitrogen-purged, programmable incubators (Napco Series 8000, Thermo Electron, Waltham, Massachusetts) were used to maintain low oxygen levels for hypoxic culture studies. For 2% and 1% oxygen studies, all media, buffers, and fixatives to be used with the cells were kept in vented tubes in the corresponding incubator overnight prior to use to equilibrate the solutions to the appropriate oxygen concentration.

4.3.2 Hypoxia Marker Virus

We have previously described the recombinant adenovirus used in this study to identify HIF activity [**270** Skiles 2011a]. Briefly, the virus was generated using the pAdEasy-1 system (QBiogene, Montreal, Canada) by inserting into the vector a

destabilized variant of the red fluorescent protein, DsRed, (termed DsRed-DR) under the control of a minimal SV40 promoter and an HRE trimer. Previous ADSC studies have indicated approximately 100% infection efficacy using an MOI of 80 (data not shown), which was utilized in these studies.

4.3.3 ADSC Infection and 3D Culture Formation

At approximately 80% confluence, ADSCs were trypsinized, centrifuged, resuspended in growth medium and counted. For HIF activity tracking studies, hypoxia marker virus was added to suspended cells and gently mixed for 30 minutes. ADSC spheroids of four different sizes were prepared by centrifugal pelleting. Five thousand (5k), 10,000 (10k), 20,000 (20k), or 60,000 (60k) cells were pipetted into 0.5 mL, screw-cap microcentrifuge tubes and centrifuged at 500 rcf for 2 minutes. Spontaneous aggregation of the pelleted cells into cohesive spheroids occurred during overnight incubation at 37°C. Spheroids of each size were then divided into three groups for incubation in 20%, 2%, or 1% O_2. While in incubation, the tube caps were loosened slightly to allow for gas transfer. Medium was changed daily.

Spheroids for HIF activity tracking studies were encapsulated in polyethylene glycol (PEG) by methods identical to those that have been published previously [**270** Skiles 2011a]. For reference, a video demonstration of this method by the authors is suggested [**314** Skiles 2011b].

4.3.4 Quantification of Secreted VEGF

For secretion studies, spheroids were cultured in a volume of media based on cell number. 60k, 20k, 10k, and 5k spheroids were cultured in 900µL, 300µL, 150µL, and 75µL of medium, respectively. 60,000 cells grown in monolayer were also cultured at each oxygen concentration in 1mL of medium. Every 24 hours, the medium was removed from each sample and replaced with fresh medium. Media samples were stored at -80°C prior to analysis. Levels of VEGF in media samples were determined by ELISA (Abcam, Cambridge, MA) following the manufacturer's instructions. For each group, 6 independent samples were analyzed.

4.3.5 Analysis of Cell Viability and Morphology

Cell viability in ADSC spheroids was examined using a LIVE/DEAD cytotoxicity/viability assay (Invitrogen) and by histological examination. The LIVE/DEAD kit was used according to the manufacturer's instructions to identify esterase activity in live cells and loss of plasma membrane integrity in dead cells. For histological analysis of morphology, spheroids were first fixed overnight in a 4% paraformaldehyde solution. The spheroids were then embedded in 2% agar, paraffin processed, and cut into 5µm sections. Sections were stained with hematoxylin and eosin and imaged.

4.3.6 Fluorescent Cell Imaging and Image Analysis

Imaging for spheroid size determination and fluorescent detection of the hypoxia marker was performed on a Nikon Eclipse T*i* inverted fluorescent microscope (Nikon Instruments, Melville, NY) and image processing and analysis was performed in NIS-

Elements software (Nikon Instruments). Identical camera and microscope settings were used for each capture within a study. Spheroids were imaged immediately following encapsulation and then every 24 hours thereafter. Histological sections were imaged on a Nikon Optiphot-2 microscope (Nikon) fitted with a Zeiss AxioCam MRc camera (Carl Zeiss, Oberkochen, Germany).

For determination of spheroid sizes, the cross-sectional area of spheroids was measured in the software from representative, central-plane images of spheroids from each size group and the diameter of a circle with an equivalent area was calculated. Results are reported as the mean ± standard deviation of 6 independent samples. To roughly quantify hypoxia marker signal, a fluorescent signal threshold intensity was applied to representative images from each group. The area of signal meeting or exceeding the threshold value was compared to the total spheroid area as calculated from the image. The threshold value was chosen such that no signal was detected in monolayer cells incubated in 20% O_2, as levels of HIF-1α in these cultures were below detectable limits by western blotting in previous studies [**315** Sahai 2012].

4.3.7 Statistical Analysis

All values are reported as mean ± standard deviation of replicate samples. Statistical significance of differences between samples was determined by a two-tailed student's t-test assuming unequal variances ("**" indicates statistical significance at $p \leq 0.01$, "*" indicates statistical significance at $p \leq 0.05$).

5.4 Results

4.4.1 Pelleted ADSCs form Spherical, 3D Cultures of Reproducible Size

Following centrifugation, ADSCs formed a small plaque at the tip of each microcentrifuge tube. After overnight incubation, the cells had spontaneously condensed into round spheroids with a diameter dependent upon the initial number of cells. Figure 4.2A shows representative spheroids of each size at Time 0. ADSC spheroids were cohesive and consistently sized within each group. In Figure 4.2B the average diameter for spheroids from each study group at Time 0 (white bar) and at Day 4 (black bar) is shown. Minimum spheroid diameter was achieved by Day 4 with no further condensation observed thereafter. 5k, 10k, 20k and 60k spheroids were 362 ± 10 µm, 454 ± 21 µm, 557 ± 20 µm, and 811 ± 37 µm in diameter, respectively, immediately after formation. Spheroids diameters on Day 4 were 282 ± 6 µm, 379 ± 8 µm, 469 ± 16 µm, and 714 ± 15 µm, respectively. The ratio of spheroid size on Day 4 to initial spheroid size was similar for all size groups, ranging from approximately 78% for 5k spheroids to 88% for 60k spheroids. Differences in culture oxygen concentration did not appear to have an effect on spheroid condensation.

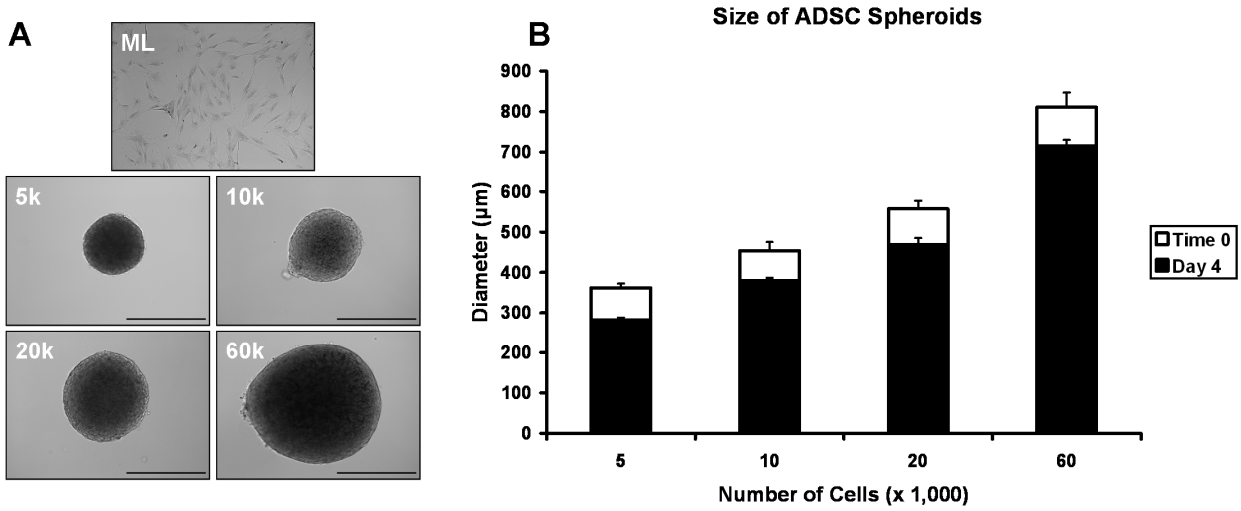

Figure 4.2 Diameter of spheroids formed by centrifugally pelleting different numbers of ADSCs. Initial spheroid size could be reliably controlled by adjusting the number of cells pelleted (white bars). Spheroids continued to condense for several days following initial formation before reaching a final minimal diameter by Day 4 (black bars). Bar = 500µm.

4.4.2 Spheroid Size and External O_2 Concentration Affect Regional Hypoxic Signaling

The degree of HIF activity in ADSC spheroids as indicated by red fluorescent signaling of the HIF marker is shown in Figure 4.3. In spheroids of all sizes, HIF activity increased as incubator oxygen concentration decreased. With decreasing oxygen, signal onset was more rapid and signal area and intensity were increased. Signal also increased with spheroid size. 5k spheroids incubated in 20% O_2 displayed little or no signal over 5 days. Increasingly more signal was seen in 20% O_2 spheroids as spheroid diameter increased. For each oxygen concentration, signal onset was more rapid and signal area and intensity were higher as spheroid diameter increased. In general, signal was first observed in central regions of the spheroids and remained most intense there.

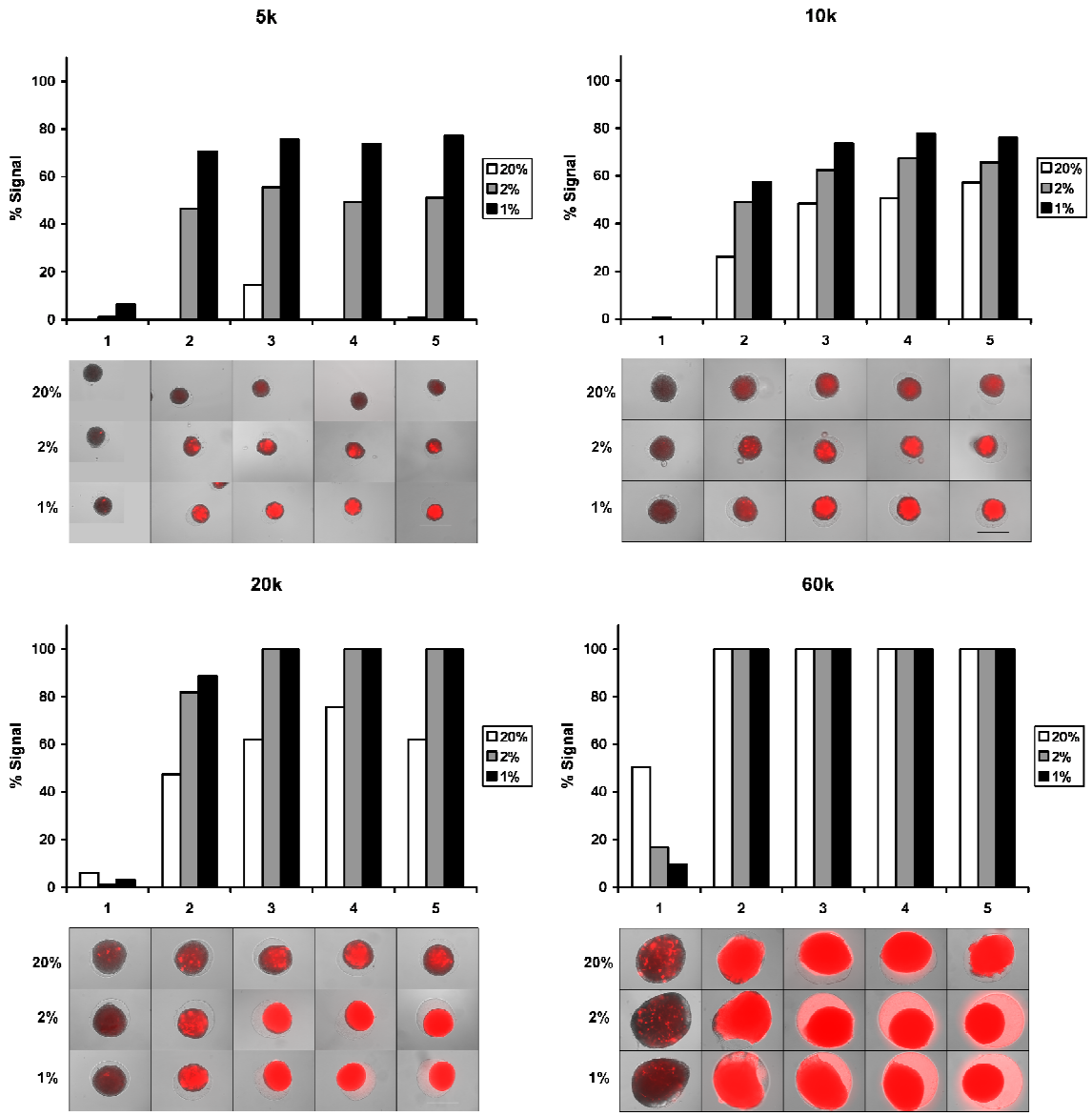

Figure 4.3 Fluorescent DsRed signaling as an indicator of HIF activity in 5k (top left), 10k (top right), 20k (bottom left), and 60k (bottom right) ADSC spheroids incubated in 20%, 2% or 1% O_2. The relative extent of signaling is quantified in the graph above each set of figures by applying a signal intensity threshold value. The voided region caused by spheroid condensation can be seen as a ring in the hydrogel around the culture in some images. Bar = 500µm.

To roughly quantify the prevalence of HIF activity throughout the spheroids, the intensity threshold was applied to each image to identify regions exceeding it. The areas of these regions were compared to the total spheroid cross-sectional area as determined in the software (graphs in Figure 4.3).

The capture settings used in Figure 4.3 resulted in some spheroids with high levels of HIF activity being overexposed. In this case, differences in signal intensity between overexposed spheroids could be resolved by reducing the camera exposure time (Figure 4.4). Though useful in identifying differences in HIF activity in spheroids that exceeded the dynamic range of capture at the given settings, apparent signal intensities measured from those images cannot be compared to intensities in Figure 4.3.

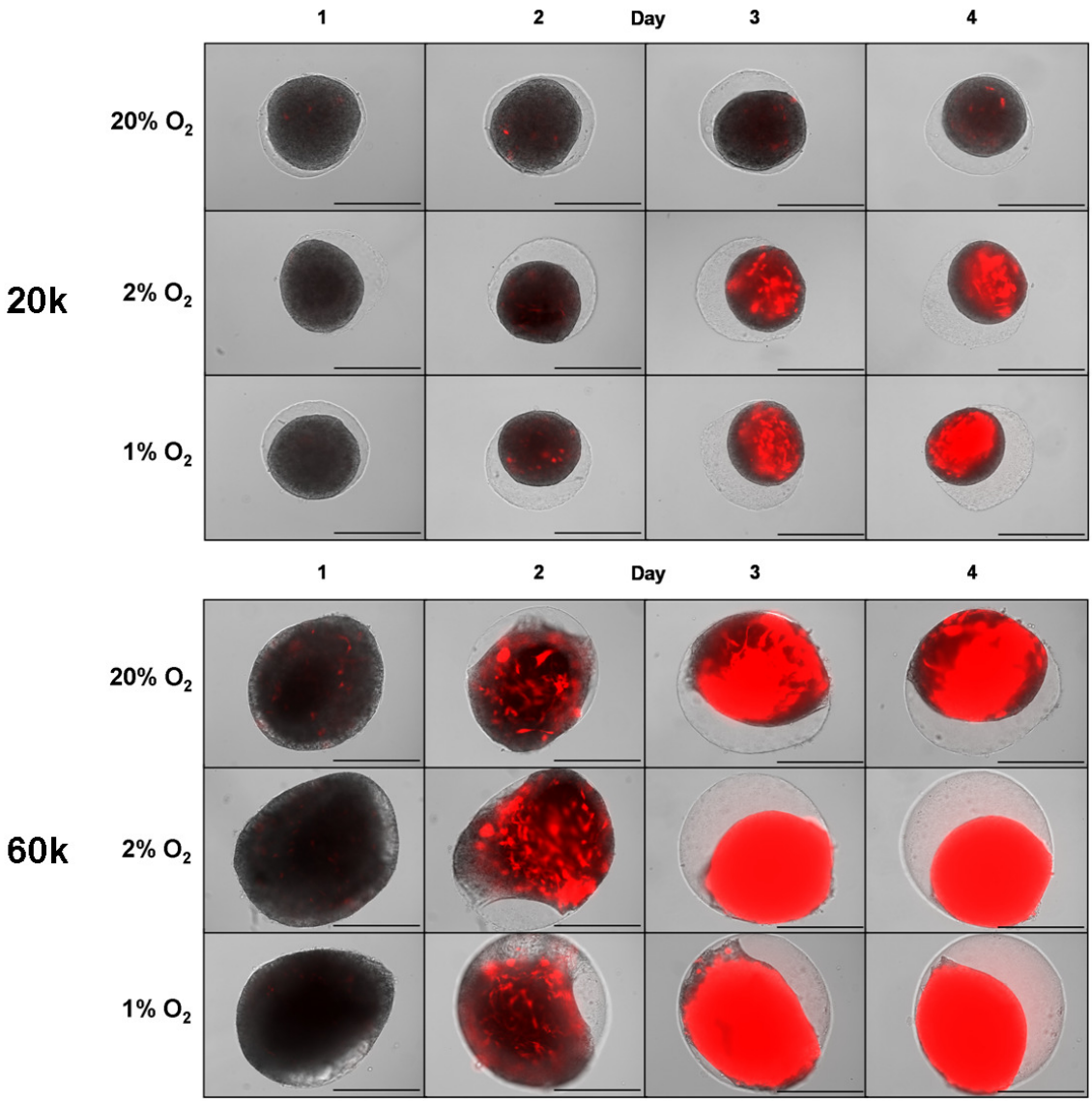

Figure 4.4 Fluorescent HIF reporter signal displayed at 1/5 the exposure length as in Figure 4.3 for 20k and 60k spheroids. Differences in signal intensity between samples that were lost due to over-saturation are better resolved at the lower exposure. Overexposure is still observed in 60k Day 3 and 4 spheroids. Bar = 500µm.

4.4.3 Degree of Hypoxia Impacts VEGF Secretion Profile

Figure 4.5 displays per-cell VEGF secretion from ADSCs in monolayers and spheroids cultured under different oxygen concentrations. The calculated mean values and standard deviations are reported in Table 4.1.

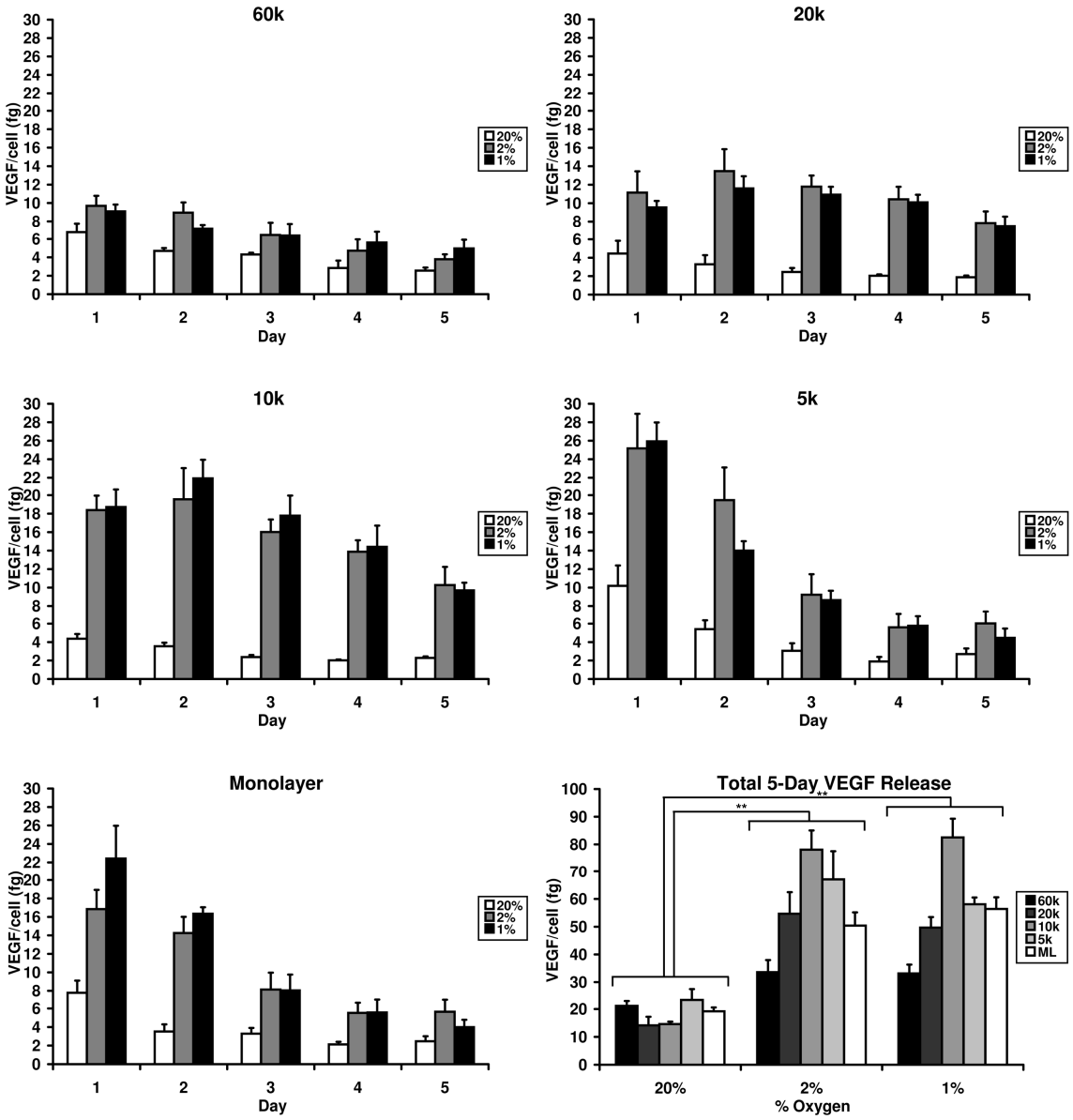

Figure 4.5 Levels of daily and total per-cell VEGF release from ADSC monolayers and 5k, 10k, 20k, and 60k spheroids incubated for 5 days in 20%, 2%, or 1% O_2.

VEGF (fg)

%O_2	Size	Day 1	2	3	4	5	Total
20%	ML	7.8 ± 1.3	3.5 ± 0.8	3.3 ± 0.6	1.9 ± 0.3	2.3 ± 0.5	18.8 ± 1.4
2%	ML	16.8 ± 2.1	14.2 ± 1.7	8.1 ± 1.8	5.1 ± 1.0	5.2 ± 1.2	49.5 ± 4.6
1%	ML	22.1 ± 3.5	16.4 ± 0.7	8.0 ± 1.7	5.1 ± 1.3	3.2 ± 0.6	54.8 ± 4.1
20%	5k	10.2 ± 2.2	5.4 ± 1.0	3.1 ± 0.8	1.9 ± 0.5	2.7 ± 0.6	23.2 ± 4.3
2%	5k	25.2 ± 3.7	19.5 ± 3.6	9.2 ± 2.2	5.6 ± 1.4	6.0 ± 1.4	63.9 ± 7.7
1%	5k	25.9 ± 2.0	14.0 ± 1.0	8.6 ± 1.0	5.8 ± 1.0	4.5 ± 1.0	58.9 ± 1.6
20%	10k	4.4 ± 0.5	3.5 ± 0.4	2.4 ± 0.2	2.0 ± 0.1	2.3 ± 0.2	14.6 ± 0.9
2%	10k	18.4 ± 1.6	19.6 ± 3.5	16.0 ± 1.4	13.9 ± 1.2	10.3 ± 2.0	78.1 ± 6.9
1%	10k	18.7 ± 1.9	21.9 ± 2.0	17.8 ± 2.2	14.4 ± 2.3	9.7 ± 0.8	82.5 ± 6.8
20%	20k	4.5 ± 1.4	3.3 ± 1.0	2.5 ± 0.4	2.0 ± 0.1	1.9 ± 0.2	14.1 ± 3.1
2%	20k	11.1 ± 2.3	13.5 ± 2.4	11.8 ± 1.2	10.4 ± 1.4	7.8 ± 1.3	54.7 ± 7.8
1%	20k	9.5 ± 0.7	11.6 ± 1.3	10.9 ± 0.8	10.1 ± 0.8	7.5 ± 1.0	49.7 ± 3.8
20%	60k	6.7 ± 1.0	4.7 ± 0.3	4.3 ± 0.2	2.8 ± 0.8	2.5 ± 0.3	20.6 ± 1.2
2%	60k	9.7 ± 1.1	8.9 ± 1.1	6.4 ± 1.4	4.7 ± 1.2	3.8 ± 0.5	34.0 ± 4.8
1%	60k	9.1 ± 0.7	7.1 ± 0.5	6.4 ± 1.3	5.6 ± 1.2	5.0 ± 0.9	33.9 ± 2.9

Table 4.1 Mean values and standard deviation of VEGF release from ADSC cultures. Statistical significance of differences between groups is indicated in Table 4.2.

Released VEGF values represent total release over the 24 hours prior to the stated time point. For each culture size, cells secreted significantly more VEGF when cultured in 2% or 1% O_2 than in 20% O_2, while little significant difference was observed between 2% and 1% O_2. In 2% and 1% O_2 culture, monolayers and 5k spheroids displayed significantly elevated VEGF secretion on Day 1 followed by a sharp decline through Day 5. Under the same conditions, 10k and 20k spheroids displayed a much more sustained elevation in VEGF secretion over 5 days, with peak secretion occurring on Day 2. 60k spheroids showed minor elevation of VEGF secretion on Day 1 which decreased over the remaining days. Total 5-day secretion was similar in 2% and 1% O_2 culture, which were both significantly higher than 20% O_2 culture. Total per-cell VEGF

release increased from monolayers to 5k spheroids and from 5k to 10k spheroids then decreased from 10k to 20k spheroids and from 20k to 60k spheroids. Statistical significance of differences in VEGF release between the different study groups can be found in Table 4.2.

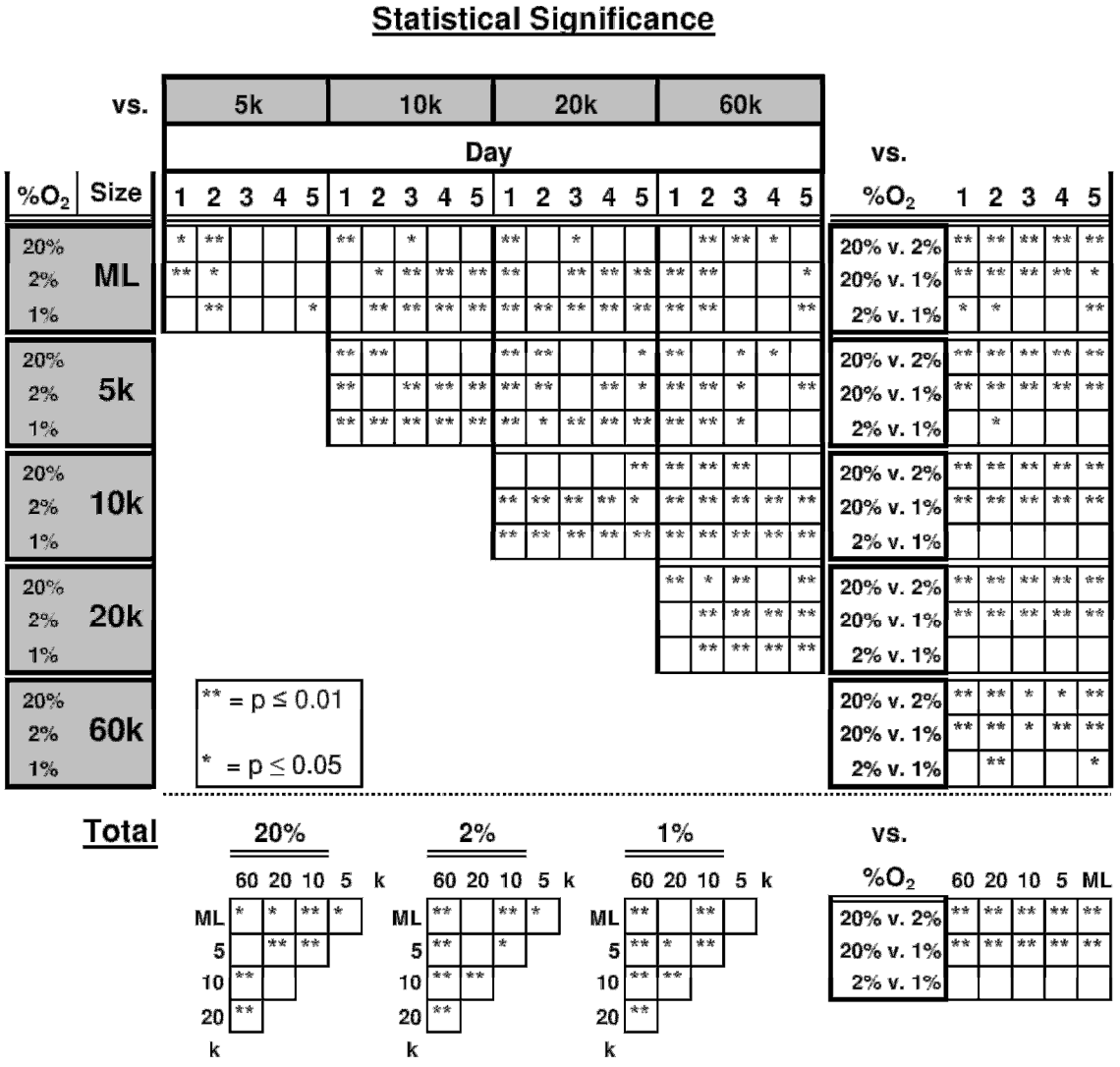

Table 4.2 Table indicating statistical significance of differences in mean VEGF release from the cultures under study. '**' indicates statistical significance at $p \leq 0.01$. '*' indicates statistical significance at $p \leq 0.05$.

5.4.4 Impact of Hypoxia on Morphology and Viability

The morphology of stained spheroid sections is shown in Figure 4.6a-h. On Day 1, all spheroids appeared cellular and cohesive throughout (a-c). After 5 days of culture in 20% O_2, little morphological change was observed in most spheroids, though 60k spheroids did display a small central region of cells exhibiting cytoplasmic swelling (h). In 2% O_2, the region with cytoplasmic swelling in 60k spheroids was much larger and some cellular discontinuity was observed (g). In 1% O_2, the 60k spheroids exhibited noticeable central tissue loss and a discontinuous core. Cells that did inhabit the central region all expressed cytoplasmic swelling (f). The 10k and 20k spheroids cultured in 2% and 1% O_2 for 5 days exhibited only minor morphological changes in some central cells but little or no loss of tissue. These spheroids cultured in 1% O_2 are shown in Figures 4d and 4e.

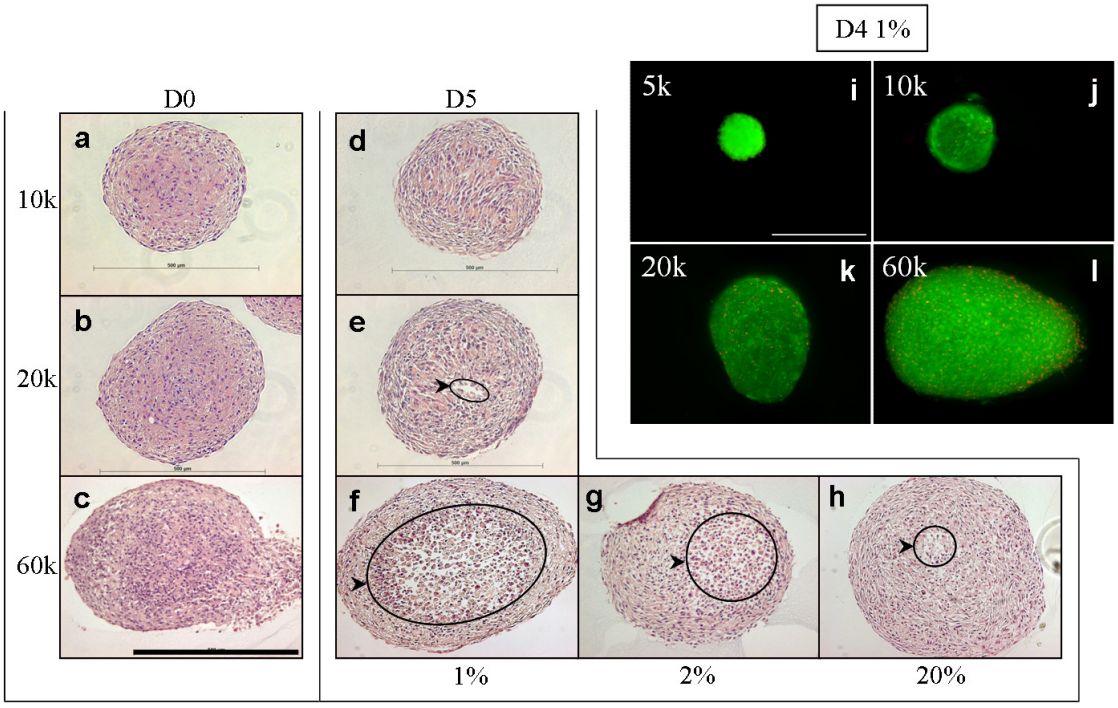

Figure 4.6 a-h) H&E staining of ADSC spheroid sections. Immediately following formation, spheroids showed high cellularity and cohesion (a-c). Cytoplasmic swelling and loss of cellular cohesion (circled regions) of central cells increased significantly with decreasing culture oxygenation in 60k spheroids (f-h). 10k and 20k spheroids incubated in 1% O_2 for 5 days showed little morphological change, though cellular discontinuity was seen in a small central region of some 20k spheroids (d & e). Inset: i-l) Live/Dead viability assessment of ADSCs in 5k (i), 10k (j), 20k (k), and 60k (l) spheroids cultured at 1% O_2 for 4 days. Green fluorescence indicates a viable cell while red, nuclear fluorescence indicates a non-viable cell. Bar = 500µm.

A LIVE/DEAD viability stain showed that on Day 1, no dead cells were observed in 5k, 10k, and 20k spheroids and only a small number were observed in 60k spheroids. As seen in Figure 4i-l, on Day 4 no dead cells were observed in 5k spheroids and only a small number of dead cells were observed in 10k spheroids. 20k and 60k spheroids displayed relatively more non-viable cells, though these still appeared to represent a small percentage of overall cells. All dead cells were located in peripheral regions of the spheroids.

4.5 Discussion

In this work, we examined the degree of HIF activity in ADSCs cultured as spheroids of different sizes in atmospheric and reduced-oxygen conditions. We found that HIF activity increased in spheroids in a size-dependent manner and with decreasing culture oxygenation. As a well-defined HIF target, we expected VEGF to be secreted at levels that increased correspondingly with HIF activity. VEGF release profiles could be altered by changing the spheroid size, with 10k spheroids cultured in 2% or 1% O_2 secreting most efficiently. That spheroids larger than 10k secreted VEGF less efficiently despite having greater HIF activity may be due in part to loss of cell viability as hypoxic severity increases, as is supported by the histology. Our results indicate that culture geometry can be used a means to control cell function and stress the need to carefully consider tissue size and expected oxygen concentration at the implant site when engineering a therapeutic graft in order to maximize the benefits of HIF-activated pathways.

The majority of studies in 3D stem cell cultures are carried out in atmospheric oxygenation or under a single "hypoxic" oxygen level (often 1% or 5% O_2) and examine only a single culture size. We suspected that differences in culture size and external oxygen concentration (even within the hypoxic range) would significantly impact culture oxygenation and in turn affect cellular function. To test this, we prepared ADSC spheroids in a range of sizes and cultured them in three different oxygen concentrations. Centrifugal pelleting resulted in rapid formation of cohesive and spherical cultures while providing a high degree of control over spheroid size. Additionally, a wide range of sizes

could be produced (including spheroids both larger and smaller than those reported in this study). Culture size was highly reproducible and only dependent on the number of cells in the initial suspension.

HIF activity was monitored within the spheroids over 5 days. As the master regulator of transcriptional responses to low oxygen conditions, HIF activation may be the most meaningful indicator of cellular hypoxia [**48** Maxwell 1993]. Tracking HIF activity rather than oxygen concentration/distribution, as in other techniques [**316** Revsbech 1983],[**317** Krihak 1996],[**318** Acosta 2007], provides evidence of a behavioral response. This is useful, as the oxygen concentration required to trigger a behavioral effect can vary between cells or even within the same cell under different microenvironmental conditions [**126** Chi 2006],[**319** Gibbs 2012]. With our HIF marker, image capture settings could be adjusted to match observed signal with quantified HIF-1 levels. Furthermore, it allowed for non-invasive identification and localization of hypoxia in cells within the 3D cultures and could follow HIF activity in the same sample over time without requiring its sacrifice. Hydrogel encapsulation facilitated consistency in repeated imaging of the same sample. While the hydrogel capsule can alter oxygen diffusion to some degree, the nature of qualitative trends observed between spheroids of different sizes were not affected. We saw that reduced oxygenation resulted in increased transcriptional activity of HIF-1 in spheroids and that increasing spheroid size amplified this effect. Quicker onset and increased intensity of fluorescent signaling was observed as culture size increased and external oxygen concentration decreased.

These results are in line with other studies: HIF-1 was shown to be exponentially stabilized in monolayer cultures as oxygen concentration decreased from 6 to 0.5% [**105** Jiang 1996b], and higher protein levels of HIF-1α were observed in ischemic mouse limb buds implanted with spheroid cultures rather than dispersed HUVECs [**311** Bhang 2012b]. Similarly, small ADSC clusters (100-200μm) were shown to contain higher protein levels of HIF-1α than monolayer ADSCs in both 20% and 1% O_2 [**303** Bhang 2011]. Our studies provided evidence on transcriptional activity of HIF-1 and examined a range of larger spheroid sizes (350 - 800 μm) that better represent the size of cultures commonly prepared in osteochondral tissue engineering.

Because of the potential for a capsule to impact diffusion, spheroids for VEGF secretion studies were not encapsulated. Our results indicated that VEGF release is impacted by both external oxygenation and spheroid size, with VEGF profiles differing as these two parameters were altered. In 1% and 2% O_2, 10k spheroids appeared to provide optimal secretion. Compared to cultures incubated in 20% O_2, 60k, 20k, 10k, and 5k spheroids and monolayers incubated in hypoxic conditions O_2 showed an approximate 1.5, 3.5, 5.5, 2.5, and 2.5-fold increase in VEGF production per cell, respectively. However, in our HIF tracking studies, 20k and 60k spheroids displayed greater HIF activity than 10k spheroids. We suspect that this is due to the severity of hypoxia occurring within these spheroids, especially in the spheroid core. Severe hypoxia is known to result in a rapid and dramatic reduction in protein turnover, inhibiting protein translation and transduction [**28** Hochachka 1996],[**320** Pettersen 1986],[**321** Koumenis 2002]. Additionally, sudden, severe hypoxia can trigger apoptotic

pathways or even result in cellular necrosis [**322** Greijer 2004],[**323** Kiang 2006],[**324** Burton 2009]. Results from our nuclear dye exclusion assay indicated few non-viable cells, even in 60k spheroids cultured at 1% O_2. However, histological examination revealed significant acellularity and evidence of necrosis in these spheroids. This interior cell death indicates severe central hypoxia and offers an explanation for the lower than anticipated VEGF secretion from 60k and 20k spheroids.

Taken together, our data suggests that the profile of VEGF release from a 3D ADSC spheroid is the result of a balance between two opposing effects of hypoxia: 1) Decreased oxygen tension resulting from cellular oxygen utilization and diffusional limitations stabilizes HIF-1 and induces upregulation of VEGF. 2) Excessive hypoxic tension, such as increasingly occurs in the interior of spheroids as size is increased, can lead to global protein down-regulation and cell death. ADSCs have demonstrated pro-angiogenic potential and may represent a preferential source for cell-based delivery in tissue engineering and regenerative medicine. Furthermore, the benefits of 3D culture are recognized. Considering culture geometry and expected environmental oxygen concentration allow for optimization of angiogenic function of 3D ADSC cultures and will be essential to balancing the beneficial and detrimental effects of hypoxia to achieve their successful utilization in tissue engineering and regenerative medicine.

Acknowledgements

The authors would like to thank Dr. Melissa Moss and the Instrument Resource Facility and the University of South Carolina School of Medicine for the generous use of equipment and assistance with histology. The authors would also like to acknowledge

support for this work provided by a grant from the National Institutes of Health (RO3AR062816).

Chapter 5

Conclusion

Although oxygen tension is a potent signaling stimulus in cells, it often remains unconsidered in experiments carried out under standard culture conditions. However, to drive restorative function of transplant tissues *in vivo*, proper *in vitro* application of physiological cues that contribute to regulating cell behavior will be needed. In particular, physiological oxygen concentrations are well below the atmospheric concentration, in a range that is often viewed as hypoxic in relation to standard culture practices. Within this range, HIFs govern cellular responses to local reductions in oxygen concentration. These responses can result in down-regulation of typical cell functions and programmed cell death, or alternatively, stimulation of adaptive behaviors involved in beneficial processes such as growth, differentiation, and repair. However, surprisingly few cell transplantation and tissue engineering efforts consider the role of HIF activity in tissue function, even though the intended therapeutic site is a physiological environment within the body. Due to its ability to regulate cell behavior, cell therapies may benefit from a view that treats oxygen as similar to other paracrine factors: a biomolecule that must be presented to cells at the proper concentration in order to illicit the intended response. However, because specific responses to a particular oxygen concentration can be cell-type and context dependent,

HIF activity may represent a more reliable indicator of microenvironmental oxygen conditions that affect cell behavior. In the present work, a fluorescent reporter system was used to identify HIF activity in cells and demonstrate how an understanding of HIF activity can be used to instruct decisions that affect the therapeutic potential of different cell transplantation strategies.

HIF activity was characterized in encapsulated, 3D β-cell clusters and in 3D ADSC spheroids. Transplantation of encapsulated β-cells is a regenerative medicine therapy aimed at restoring normoglycemia in patients with T1DM through secretion of insulin from the transplanted tissue which is protected from immune destruction by the encapsulating material. To maintain important cell-to-cell contacts which contribute to β-cell survival and secretory function, β-cells are often transplanted as native, 3D islets or as reaggregated islet-like clusters. Lack of vascularization, low oxygenation at the implant site, and oxygen gradients resulting from the 3D nature of the tissues and the protective capsule have all been suggested to contribute to hypoxia-induced loss of function in such therapies. ADSCs have been applied in regenerative medicine therapies to help restore ischemic tissue injuries. ADSCs have potent angiogenic properties that are upregulated under hypoxic conditions. 3D, spheroid culture of ADSCs may modulate their hypoxic status and contribute to their survival through cell-cell interaction. Inclusion of ADSC spheroids in *in vitro* engineered tissues or *in vivo* regenerating tissues may contribute to the formation of a pro-angiogenic niche within the tissue which could help drive rapid vascularization and assist tissue integration and survival. Both of these therapies offer the promise of improved outcomes in patient. Each also demonstrates a

role for hypoxia in the success of the therapy. In β-cell encapsulation and transplantation, cellular hypoxia should be avoided in order to prevent HIF-regulated loss of insulin secretion, while when using ADSCs to drive angiogenesis, promotion of hypoxia can contribute to upregulation of HIF-regulated, pro-angiogenic behaviors. The ability to identify HIF activity within cells in each of these systems can guide culturing and engineering decisions in order to optimize their therapeutic potential.

The use of a fluorescent reporter system to identify HIF activity in β-cells or ADSCs has not been reported previously. The present studies indicate that the reporter is a viable and useful tool for determining the hypoxic status of cells used in regenerative therapies. β-cells and ADSCs cultured in 1% and 2% O_2, conditions under which HIF should be stable, exhibited fluorescent signaling indicating HIF transcriptional activity. Cells cultured as monolayers in 20% O_2, conditions under which HIF should not be stable, did not exhibit fluorescence. Compared with other methods commonly used to identify HIF, such as Western blotting and immunostaining, the reporter technique was favorable because it allowed for repeated observation of HIF activity over time. Additionally, the fluorescent signal could be observed through PEGDM matrices, meaning that encapsulated cells did not need to be removed from the capsule in order for HIF activity to be examined.

HIF activity, indicated by the reporter, correlated well to differences in behavior between signaling and non-signaling tissues. HIF activity in β-cell clusters corresponded to much lower GSIS than in clusters that did not display HIF activity. Recently-aggregated β-cell clusters that displayed fluorescent signaling also failed to achieve a

cohesive, islet-like morphology over time, while non-signaling clusters gradually became smooth and round, much like native islets. Surprisingly, HIF activity did not appear to correspond to a substantial drop in viability in β-cell clusters over 2 weeks. In ADSC spheroids, increased HIF activity corresponded to an increase in VEGF secretion, although spheroid size also appeared to indirectly effect VEGF secretion by affecting regional cell survival. Intense fluorescent signaling corresponded to the appearance of pre-apoptotic or necrotic morphologies in large spheroids.

Using the HIF reporter system in 3D tissue cultures also provided information about how tissue size affects the formation of oxygen gradients within the tissue, and allowed for regional identification of heterogeneous HIF activity. β-cell clusters incubated in 20% O_2 that were smaller than 250-300μm did not display fluorescent signaling. However, larger clusters displayed HIF activity in their central region in 20% O_2, which increased in size as cluster size increased to maintain a signal-free peripheral region of consistent thickness. Likewise, onset of fluorescent signaling in ADSC spheroids occurred in central regions.

Finally, results from the present studies offer instructive suggestions about the design decisions for β-cell and ADSC transplantation therapies. In β-cells, large clusters displayed central regional HIF activity. Thus, it may be beneficial to utilize clusters that are smaller than 250μm in order to avoid hypoxia-induced loss of function. Additionally, 1% O_2 culture induced strong HIF activity and reduced GSIS which was not remediated by an increase in oxygen concentration within the hypoxic range to 2% O_2. Therefore strategies to ensure implant-site oxygenation of >2% could be beneficial to the success

of β-cell therapies. Finally, incubation in low oxygen conditions did not allow for normal morphological arrangement of recently-aggregated β-cell clusters. This suggests that reaggregation and hypoxic preconditioning techniques should not be employed simultaneously in β-cells. In ADSC, external oxygen concentration and culture size were both shown to contribute to pervasiveness of HIF activity in spheroids. Increasing spheroid size and decreasing external oxygenation could both be used to augment HIF activity. Moderate elevation of HIF activity was shown to correlate to an increase in VEGF secretion per cell, however, very high levels of HIF activity correlated to increased cell death which reduced secretion efficiency. This suggests that for a desired application, optimal cell function can be driven by careful selection of culture parameters to effect hypoxic status. In the study, 400μm spheroids were shown to produce VEGF most efficiently. This is the first report to show that tissue size can be used to optimize cell-based delivery of angiogenic factors from ADSCs. Overall, then, the studies reported in this work point to the important ways in which oxygen tension can affect cell behavior in cell transplantation therapies and highlights the usefulness of the fluorescent HIF reporter system. Conclusions from these studies, and others which may utilize HIF tracking, should be instructive in guiding the use of appropriate physiological stimuli in tissue engineering and regenerative therapies to drive optimal restorative function.

References

1) Duursma E.K., Boisson M.P.R.M. Global oceanic and atmospheric oxygen stability considered in relation to the carbon cycle and to different time scales. Oceanologica Acta 1994, 17(2);117-141.

2) Castresana J., Saraste M. Evolution of energetic metabolism – the respiration-early hypothesis. Trends Biochem Sci 1995, 20(11);443-448.

3) Dismukes G.C., Klimov V.V., Baranov S.V., Kozlov Yu.N., DasGupta J., Tyryshkin A. The origin of atmospheric oxygen on Earth: The innovation of oxygenic photosynthesis. Proc Natl Acad Sci USA 2001, 98(5);2170-2175.

4) Kump L.R. The rise of atmospheric oxygen. Nature 2008, 451(7176);277-278.

5) Stamati K., Mudera V, Cheema U. Evolution of oxygen utilization in multicellular organisms and implications for cell signaling in tissue. J of Tissue Eng 2011, 2(1);1-12.

6) Whitney E., Rolfes S. Understanding Nutrition, 10th ed, 2005;6. Thomson-Wadsworth.

7) Solaini G., Baracca A., Lenaz G., Sgarbi G. Hypoxia and mitochondrial oxidative metabolism. Biochim Biophys Acta 2010, 1797(6-7);1171-1177.

8) Brunori M., Antontni G., Malatesta F., Sarti P., Wilson M.T. Cytochrome-c oxidase. Eur J Biochem 1987, 169;1-8.

9) Bergamini C.M., Gambetti S., Dondi A., Cervellati C. Oxygen, reactive oxygen species and tissue damage. Curr Pharm Des 2004, 10(14);1611-1626.

10) Raymond J., Sergrè D. The effect of oxygen on biochemical networks and the evolution of complex life. Science 2006, 311(5768);1764-1767.

11) Summons R.E., Bradley A.S., Jahnke L.L., Waldbauer J.R. Steroids, triterpenoids and molecular oxygen. Philos Trans R Soc Lond B Biol Sci 2006, 361(1470);951-968.

12) Jiang Y.Y., Kong D.X., Qin T., Zhang H.Y. How does oxygen rise drive evolution? Clues from oxygen-depedent biosynthesis of nuclear receptor ligands. Biochem Bioph Res Co 2010, 391(2);1158-1160.

13) Thannickal V.J. Oxygen in the evolution of complex life and the price we pay. Am J Resp Cell Mol 2009, 40(5);507-510.

14) Andreyev A.Y., Kushnareva Y.E., Starkov A.A. Mitochondrial metabolism of reactive oxygen species. Biochemistry (Mosc) 2005, 70(2);200-214.

15) Gibson J.S., Milner P.I., White R., Fairfax T.P., Wilkins R.J. Oxygen and reactive oxygen species in articular cartilage: modulators of ionic homeostasis. Pflugers Arch 2008, 455(4);563-573.

16) Chance B., Williams B.R. Respiratory enzymes in oxidative phosphorylation. J Biol Chem 1955, 217(1);383-451.

17) Priestley J. Observations on different kinds of air. Phiolosophical Transactions 1772, 62;147.

18) Lavoisier, A. Traite´ Ele´mentaire de Chimie. Pre´sente´ dans un Ordre Nouveau et d'apre´s De´couvertes Modernes. Paris: Cuchet, 1789.

19) Hochscheid S., Bentivegna F., Hays G.C. First records of dive durations for a hibernating sea turtle. Biol Lett 2005, 1(1);82-86.

20) Watkins W.A., Daher M.A., DiMarzio N.A. Sperm whale dives tracked by radio tag telemetry. Marine Mammal Sci 2002, 18(1);55-68.

21) Irving L. Respiration in diving mammals. Physiol Rev 1939, 19(1);112-134.

22) Leach R.M., Treacher D.F. Oxygen transport – 2. Tissue hypoxia. BMJ 1998, 317(7169);1370-1373.

23) Carreau A., El Hafny-Rahbi B., Matejuk A., Grillon C., Kieda C. Why is the partial oxygen pressure of human tissue a crucial parameter? Small molecules and hypoxia. J Cell Mol Med 2011, 15(6);1239-1253.

24) Fermor B., Christensen S.E., Youn I., Cernanec J.M., Davies C.M., Weinberg J.B. Oxygen, nitric oxide, and articular cartilage. Eur Cell Mater 2007, 13;5-65.

25) Ivanovic Z. Hypoxia or in situ normoxia: The stem cell paradigm. J Cell Physiol 2009, 219(2);271-275.

26) Simon M.C., Keith B. The role of oxygen availability in embryonic development and stem cell function. Nat Rev Cell Biol 2008, 9(4);285-296.

27) Semenza G.L. Hypoxia-inducible factors in physiology and medicine. Cell 2012a, 148(3);399-408.

28) Hochachka P.W., Buck L.T., Doll C.J., Land S.C. Unifying theory of hypoxia tolerance: Molecular/metabolic defense and rescue mechanisms for surviving oxygen lack. Proc Natl Acad Sci USA 1996, 93;9493-9498.

29) Shimizu S., Eguchi Y., Kamiike W., Itoh Y., Hasegawa J., Yamabe K., Otsuki Y., Matsuda H., Tsujimoto Y. Induction of apoptosis as well as necrosis by hypoxia and predominant prevention of apoptosis by bcl-2 and bcl-x_L. Cancer Res 1996, 56(9);2161-2166.

30) Zhang H., Bosch-Marce M., Shimoda L.A., Tan Y.S., Baek J.H., Wesley J.B., Gonzalez F.J., Semenza G.L. Mitochondrial autophagy is an HIF-1-dependent adaptive metabolic response to hypoxia. J Biol Chem 2008, 283(16);10892-10903.

31) Azad M.B., Chen Y., Henson E.S., Cizeau J., McMillan-Ward E., Israels S.J., Gibson S.B. Hypoxia induces autophagic cell death in apoptosis-competent cells through a mechanism involving BNIP3. Autophagy 2008, 4(2);195-204.

32) Kumar V., Abbas A.K., Fausto N., Aster J.C., Perkins J.A. Robbins and Cotran pathologic basis of disease, 8th ed. Saunders Elsevier 2010, Philidelphia, PA, USA.

33) Wilson D.F., Ericińska M., Drown C., Silver I.A. The oxygen dependence of cellular energy metabolism. Arch Biochem Biophys 1979, 195(2);485-493.

34) Erecińska M., Wilson D.F. Regulation of cellular energy metabolism. J Membr Biol 1982, 70(1);1-14.

35) Rumsey W.L., Schlosser C., Nuutinen E.M., Robiolio M., Wilson D.F. Cellular energetics and the oxygen dependence of respiration in cardian myocytes isolated form adult rat. J Biol Chem 1990, 265(26);15392-15402.

36) Schumaker P.T., Chandel N., Agusti A.G. Oxygen conformance of cellular respiration in hepatocytes. Am J Physiol 1993, 265(4);L395-L402.

37) Budinger G.R., Chandel N., Shao Z.H., Li C.Q., Melmed A., Becker L.B., Schumacker P.T. Cellular energy utilization and supply during hypoxia in embryonic cardiac myocytes. Am J Physiol 1996, 270(1);L44-L53.

38) Chandel N.S., Budinger G.R., Choe S.H., Schumacker P.T. Cellular respiration during hypoxia. Role of xytochrome oxidase as the oxygen sensor in hepatocytes. J Biol Chem 1997, 272(30);18808-18816.

39) Budinger G.R., Duranteau J., Chandel N.S., Schumacker P.T. Hibernation during hypoxia in cardiomyoctes. Role of mitochondria as the O_2 sensor. J Biol Chem 1998, 273(6);3320-3326.

40) Brown G.C., Hafner R.P., Brand M.D. A 'top-down' approach to the determination of control coefficients in metabolic control theory. Eur J Biochem 1990a, 188(2);321-325.

41) Brown G.C., Lakin-Thomas P.L., Brand M.D. Control of respiration and oxidative phosphorylation in isolated rat liver cells. Eur J Biochem 1990b, 192(2);355-362.

42) Eguchi Y., Shimizu S., Tsujimoto Y. Intracellular ATP levels determine cell death fate by apoptosis or necrosis. Cancer Res 1997, 57(10);1835-1840.

43) López-Barneo J., López-López J.R., Ureña J., González C. Chemotransduction in the carotid body: K^+ current modulated by pO_2 in type I chemoreceptor cells. Science 1988, 241(4865);580-582.

44) Bondurant M.C., Koury M.J. Anemia induces accumulation of erythropoietin mRNA in the kidney and liver. Molec Cell Biol 1986, 6(7);2731-2733.

45) Schuster S.J., Badiavas E.V., Costa-Giomi P., Weinmann R., Erslev A.J., Caro J. Stimulation of erythropoietin gene transcription during hypoxia and cobalt exposure. Blood 1989, 73(1);13-16.

46) Semenza G.L., Wang G.L. A nuclear factor induced by hypoxia via de novo protein synthesis binds to the human erythropoietin gene enhancer at a site required for transcriptional activation. Mol Cell Biol 1992, 12(12):5447-5454.

47) Semenza G.L., Nejfelt M.N., Chi S.M., Antonarakis S.E. Hypoxia-inducible nuclear factors bind to an enhancer element located 3' to the human erythropoietin gene. Proc Natl Acad Sci USA 1991, 88(13);5680-5684.

48) Maxwell P.H., Pugh C.W., Ratcliffe P.J. Inducible operation of the erythropoietin 3' enhancer in multiple cell lines: Evidence for a widespread oxygen-sensing mechanism. Proc Natl Acad Sci USA 1993, 90(6);2423-2427.

49) Wang G.L., Semenza G.L. General involvement of hypoxia-inducible factor 1 in transcriptional response to hypoxia. Proc Natl Acad Sci USA 1993a, 90(9);4304-4308.

50) Wiener C.M., Booth G., Semenza G.L. *In vivo* expression of mRNAs encoding hypoxia-inducible factor 1. Biochem Biophys Res Comm 1996, 225(2);485-488.

51) Rytkönen K.T., Williams T.A., Renshaw G.M., Primmer C.R., Nikinmaa M. Molecular evolution of the metazoan PHD-HIF oxygen-sensing system. Mol Biol Evol 2011, 28(6);1913-1926.

52) Wang G.L., Jiang B.H., Rue E.A., Semenza G.L. Hypoxia-inducible factor 1 is a basic-helix-loop-helix-PAS heterodimer regulated by cellular O_2 tension. Proc Natl Acad Sci USA 1995, 92(12);5510-5514.

53) Kewley R.J., Whitelaw M.L., Chapman-Smith A. The mammalian basic helix-loop-helix/PAS family of transcriptional regulators. Int J Biochem Cell Biol 2004, 36(2);189-204.

54) Semenza G.L., Jiang B.H., Leung S.W., Passantino R., Concordet J.P., Maire P., Giallongo A. Hypoxia response elements in the aldolase A, enolase 1, and lactate dehydrogenase A gene promoters contain essential binding sites for hypoxiainducible factor 1. J Biol Chem 1996, 271(51); 32529–37.

55) Taylor B.L., Zhulin I.B. PAS domains: internal sensors of oxygen, redox potential, and light. Microbiol Mol Biol Rev 1999, 63(2);479-506.

56) Murre C., McCaw P.S., Vaessin H., Caudy M., Jan L.Y., Jan Y.N., Cabrera C.V., Buskin J.N., Hauschka S.D., Lassar A.B., Weintraub H., Baltimore D. Interactions between heterologous helix-loop-helix proteins generate complexes that bind specifically to a common DNA sequence. Cell 1989, 58(3);537-544.

57) Reisz-Porszasz S., Probst M.R., Fukunaga B.N., Hankinson O. Identification of functional domains of the aryl hydrocarbon receptor nuclear translocator protein (ARNT). Mol Cell Biol 1994, 14(9);6075-86.

58) Ema M., Morita M., Ikawa S., Tanaka M., Matsuda Y., Gotoh O., Saijoh Y., Fujii H., Hamada H., Kikuchi Y., Fujii-Kuriyama Y. Two new members of the murine Sim gene family are transcriptional repressors and show different expression patterns during mouse embryogenesis. Mol Cell Biol 1996, 16(10);5865-5875.

59) Jiang B.H., Rue E., Wang G.L., Roe R., Semenza G.L. Dimerization, DNA binding, and transactivation properties of hypoxia-inducible factor 1. J Biol Chem 1996a, 271(30);17771-17778.

60) Kobayashi A., Numayama-Tsuruta K., Sogawa K., Fujii-Kuriyama Y. CBP/p300 functions as a possible transcriptional coactivator of Ah receptor nuclear translocator (Arnt). J Biochem 1997, 122(4);703-710.

61) Ferré-D'Amaré A.R., Prendergast G.C., Ziff E.B., Burley S.K. Recognition by Max of its cognate DNA through a dimeric b/HLH/Z domain. Nature 1993, 363(6424);38-45.

62) Pongratz I., Antonsson C., Whitelaw M.L., Poellinger L. Role of the PAS domain in regulation of dimerization and DNA binding specificity of the dioxin receptor. Molec Cell Biol 1998, 18(7);4079-4088.

63) Crews S.T. Control of cell lineage-specific development and transcription by bHLH-PAS proteins. Genes Dev 1998, 12(5);607-620.

64) Jiang B.H., Zheng J.Z., Leung S.W., Roe R., Semenza G.L. Transactivation and inhibitory domains of hypoxia-inducible factor 1 alpha. Modulation of transcriptional activity by oxygen tension. J Biol Chem 1997, 272(31);19253-19260.

65) Huang L.E., Schau M., Bunn H.F. Regulation of hypoxia inducible factor 1alpha is mediated by an O_2-dependent degradation domain via the ubiquitin-proteasome pathway. Proc Natl Acad Sci USA 1998, 95(14);7987-7992.

66) Ema M., Hirota K., Mimura J., Abe H., Yodoi J., Sogawa K., Poellinger L., Fujii-Kuriyama Y. Molecular mechanisms of transcription activation by HLF and HIF1alpha in response to hypoxia: their stabilization and redox signal-induced interaction with CBP/p300. EMBO J 1999, 18(7);1905-1914.

67) O'Rourke J.F., Tian Y.M., Ratcliffe P.J., Pugh C.W. Oxygen-regulated and transactivating domains in endothelial PAS protein 1: comparison with hypoxia-inducible factor -1 alpha. J Biol Chem 1999, 274(4);2060-2071.

68) Maynard M.A., Oi H., Chung J., Lee E.H., Kondo Y., Hara S., Conaway R.C., Conaway J.W., Ohh M. Multiple splice variants of the human HIF-3 alpha locus are targets of the con Hippel-Lindau E3 ubiquitin ligase complex. J Biol Chem 2003, 278(13);11032-11040.

69) Makino Y., Kanopka A., Wilson W.J., Tanaka H., Poellinger L. Inhibitory PAS domain protein (IPAS) is a hypoxia-inducible splicing variant of the hypoxia-inducible factor-3alpha locus. J Biol Chem 2002, 277(36);32405-32408.

70) Chilov D., Camenisch G., Kvietikova I., Ziegler U., Gassmann M., Wenger R.H. Induction and nuclear translocation of hypoxia-inducible factor-1 (HIF-1): heterodimerization with ARNT is not necessary for nuclear accumulation of HIF-1alpha. J Cell Sci 1999, 112(8);1203-1212.

71) Brière J.J., Favier J., Bénit P., El Chouzzi V., Lorenzato A., Rabier D., Di Renzo M.F., Gimenez-Rogueplo A.P., Rustin P. Mitochondrial succinate is instrumental for HIF1alpha nuclear translocation in SDHA-mutant fibroblasts under normoxic conditions. Hum Mol Genet 2005, 14(21);3263-3269.

72) Arany Z., Huang L.E., Eckner R., Bhattacharya S., Jiang C., Goldberg M.A., Bunn H.F., Livingston D.M. An essential role for p300/CBP in the cellular response to hypoxia. Proc Natl Acad Sci USA 1996, 93(23);12969-12973.

73) Brunelle J.K., Bell E.L., Quesada N.M., Vercauteren K., Tiranti V., Zeviani M., Scarpulla R.C., Chandel N.S. Oxygen sensing requires mitochondrial ROS but not oxidative phosphorylation. Cell Metab 2005, 1(6);409-414.

74) Epstein A.C.R., Gleadle J.M., McNeill L.A., Hewitson K.S., O'Rourke J., Mole D.R., Mukherji M., Metzen E., Wilson M.I., Dhanda A., Tian Y.M., Masson N., Hamilton D.L., Jaakkola P., Barstead R., Hodgkin J., Maxwell P.H., Pugh C.W., Schofield C.J., Ratcliffe P.J. *C. elegans* EGL-9 and mammalian homologs define a family of dioxygenases that regulate HIF by prolyl hydroxylation. Cell 2001, 107(1);43-54.

75) Bruick R.K., McKnight S.L. A conserved family of prolyl-4-hydroxylases that modify HIF. Science 2001, 294(5545);1337-1340.

76) Berra E., Benizri E., Ginouvès A., Volmat V., Roux D., Pouysségur J. HIF prolyl-hydroxylase 2 is the key oxygen sensor setting low steady-state levels of HIF-1α in normoxia. EMBO J 2003, 22(16):4082-4090.

77) Huang L.E., Arany Z., Livingston D.M., Bunn H.F. Activation of hypoxia-inducible transcription factor depends primarily upon redox-sensitive stabilization of its α subunit. J Biol Chem 1996, 271(50);32253-32259.

78) Ratcliffe P.J., O'Rourke J.F., Maxwell P.H., Pugh C.W. Oxygen sensing, hypoxia-inducible factor-1 and the regulation of mammalian gene expression. J Exp Biol 1998, 201(8);1153-1162.

79) Ivan M., Kondo K., Yang H., Kim W., Valiando J., Ohh M., Salic A., Asara J.M., Lane W.S., Kaelin W.G. Jr. HIFα targeted for VHL-mediated destruction by proline hydroxylation: Implications for O2 sensing. Science 2001, 292(5516);464-468.

80) Masson N., Willam C., Maxwell P.H., Pugh C.W., Ratcliffe P.J. Independent function of two destruction domains in hypoxia-inducible factor-α chains activated by prolyl hydroxylation. EMBO J 2001, 20(18);5197-5206.

81) Schofield C.J., Ratcliffe P.J. Oxygen sensing by HIF hydroxylases. Nat Rev Mol Cell Biol 2004, 5(5);343-354.

82) Baek J.H., Mahon P.C., Oh J., Kelly B., Krishnamachary B., Pearson M., Chan D.A., Giaccia A.J., Semenza G.L. OS-9 interacts with hypoxia-inducible factor 1alpha and prolyl hydroxylase to promote oxygen-dependent degradation of HIF-1alpha. Mol Cell 2005, 17(4);503-512.

83) Maxwell P.H., Wiesener M.S., Chang G.W., Clifford S.C., Vaux E.C., Cockman M.E., Wykoff C.C., Pugh C.W., Maher E.R., Ratcliffe P.J. The tumour suppressor protein VHL targets hypoxia-inducible factors for oxygen dependent proteolysis. Nature 1999, 399(6733);271-275.

84) Ohh M., Park C.W., Ivan M., Hoffman M.A., Kim T.Y., Huang E., Pavletich N., Chau V., Kaelin W.G. Ubiquitination of hypoxia-inducible factor requires direct binding to the β-domain of the von Hippel-Lindau protein. Nat Cell Biol 2000, 2(7);423-427.

85) Baek J.H., Liu Y.V., McDonald K.R., Wesley J.B., Hubbi M.E., Byun H., Semenza G.L. Spermidine/spermine-N1-acetyltransferase 2 is an essential component of the ubiquitin ligase complex that regulates hypoxia-inducible factor 1. J Biol Chem 2007, 282(32);23572-23580.

86) Kallio P.J., Okamoto K., O'Brien S., Carrero P., Makino Y., Tanaka H., Poellinger L. Signal transduction in hypoxic cells: inducible nuclear translocation and recruitment of the CBP/p300 coactivator by the hypoxia-inducible factor-1alpha. EMBO J 1998, 17(22);6573-6586.

87) Lando D., Peet D.J., Whelan D.A., Gorman J.J., Whitelaw M.L. Asparagine hydroxylation of the HIF transactivation domain: A hypoxia switch. Science 2002a, 295(5556);858-861.

88) Lando D., Peet D.J., Gorman J.J., Whelan D.A., Whitelaw M.L., Bruick R.K. FIH-1 is an asparaginyl hydroxylase enzyme that regulates the transcriptional activity of hypoxia-inducible factor. Genes Dev 2002b, 16(12);1466-1471.

89) Koivunen P., Hirsila M., Gunzler V., Kivirikko K.I., Myllyharju J. Catalytic properties of the asparaginyl hydroxylase (FIH) in the oxygen sensing pathway are distinct from those of its prolyl 4-hydroxylases. J Biol Chem 2004, 279(11);9899-9904.

90) Taguchi A., Yanagisawa K., Tanaka M., Cao K., Matsuyama Y., Goto H., Takahashi T. Identification of hypoxia-inducible factor-1 alpha as a novel target for miR-17-92 microRNA cluster. Cancer Res 2008, 68(14);5540–5545.

91) Bruning U., Cerone L., Neufeld Z., Fitzpatrick S.F., Cheong A., Scholz C.C., Simpson D.A., Leonard M.O., Tambuwala M.M., Cummins E.P., Taylor C.T. MicroRNA-155

promotes resolution of hypoxia-inducible factor 1alpha activity during prolonged hypoxia. Mol Cell Biol 2011, 31(19); 4087–4096.

92) Chamboredon S., Ciais D., Desroches-Castan A., Savi P., Bono F., Feige J.J., Cherradi N. Hypoxia-inducible factor-1alpha mRNA: a new target for destabilization by tristetraprolin in endothelial cells. Mol Biol Cell 2011, 22(18); 3366–3378.

93) Liu Y.V., Baek J.H., Zhang H., Diez R., Cole R.N., Semenza G.L. RACK1 competes with HSP90 for binding to HIF-1α and is required for O2-independent and HSP90 inhibitor-induced degradation of HIF-1α. Mol Cell 2007, 25(2);207–217.

94) Pan Y., Mansfield K.D., Bertozzi C.C., Rudenko V., Chan D.A., Giaccia A.J., Simon M.C. Multiple factors affecting cellular redox status and energy metabolism modulate hypoxia-inducible factor prolyl hydroxylase activity in vivo and in vitro. Mol Cell Biol 2007, 27(3);912–925.

95) Finley L.W., Carracedo A., Lee J., Souza A., Egia A., Zhang J., Teruya- Feldstein J., Moreira P.I., Cardoso S.M., Clish C.B., Pandolfi P.P., Haigis M.C. SIRT3 opposes reprogramming of cancer cell metabolism through HIF1a destabilization. Cancer Cell 2011, 19(3);416–428.

96) Kaelin Jr.W.G., Ratcliffe P.J. Oxygen sensing by metazoans: the central role of the HIF hydroxylase pathway. Mol Cell 2008, 30(4);393–402.

97) Luo W., Hu H., Chang R., Zhong J., Knabel M., O'Meally R., Cole R.N., Pandey A., Semenza G.L. Pyruvate kinase M@ is a PHD3-stimulated coactivator for hypoxia-inducible factor 1. Cell 2001, 145(5);732-744.

98) Semenza G.L. Targeting HIF-1 for cancer therapy. Nat Rev Cancer 2003, 3(10);721-732.

99) Land S.C., Tee A.R. Hypoxia-inducible factor 1α is regulated by the mammalian target of rapamycin (mTOR) via an mTOR signaling motif. J Biol Chem 2007, 282(28);20534-20543.

100) Tanimoto K., Tsuchihara K., Kanai A., Arauchi T., Esumi H., Suzuki Y., Sugano S. Genome-wide identification and annotation of HIF-1α binding sites in two cell lines using massively parallel sequencing. Hugo J 2010, 4(1-4);35-48.

101) Mimura I., Tanaka T., Wada Y., Kodoma T., Nangaku M. Pathophysiological response to hypoxia - from the molecular mechanisms of maladay to drug discovery: epigenetic regulation of the hypoxia response via hypoxia-inducible factor and histone modifying enzymes. J Pharmacol Sci 2011, 115(4);453-458.

102) Xu J., Wang B., Xu Y., Sun L., Tian W., Shukla D., Barod R., Grillari J., Grillari-Voglauer R., Maxwell P.H., Esteban M.A. Epigenetic regulation of HIF-1α/2α binding to a reverse hypoxia-response element. Oncogene 2012, 31(8);1065-1072.

103) Vanharanta S., Shu W., Brenet F., Hakimi A.A., Heguy A., Viale A., Reuter V.E., Hsieh J.J., Scandura J.M., Massagué J. Epigenetic expansion of VHL-HIF signal output drives mutliorgan metastasis in renal cancer. Nat Med 2013, 19(1);50-56.

104) Nguyen M.P., Lee S., Lee Y.M. Epigenetic regulation of hypoxia inducible factor in disease and therapeutics. Arch Pharm Res 2013 [in press].

105) Jiang B.H., Semenza G.L., Bauer C., Marti H.H. Hypoxia-inducible factor 1 levels vary exponentially over a physiologically relevant range of O_2 tension. Am J Physiol 1996b, 271(4);1172-1180.

106) Bracken C.P., Fedele A.O., Linke S., Balrak W., Lisy K., Whitelaw M.L., Peet D.J. Cell-specific regulation of hypoxia-inducible factor (HIF)-1α and HIF-2α stabilization and transactivation in a graded oxygen environment. Journal Biol Chem 2006, 281(32);22575-22585.

107) Jaakkola P., Mole D.R., Tian Y.M., Wilson M.I., Gielbert J., Gaskell S.J., von Kriegsheim A., Hebestreit H.F., Mukherju M., Schofield C.J. Targeting of HIF-alpha to the von Hippel-Lindau ubiquitylation complex by O2-regulated prolyl hydroxylation. Science 2001, 292(5516);468–472.

108) Jeong J.W., Bae M.K., Ahn M.Y., Kim S.H., Sohn T.K., Bae M.H., Yoo M.A., Song E.J., Lee K.J., Kim K.W. Regulation and destabilization of HIF-1alpha by ARD1-mediated acetylation. Cell 2002, 111(5);709–720.

109) Moroz E., Carlin S., Dyomina K., Burke S., Thaler H.T., Blasberg R., Serganova I. Real-time imaging of HIF-1alpha stabilization and degradation. PLoS One 2009, 4(4);e5077.

110) Hirsila M., Koivunen P., Günzler V., Kivirikko K.I., Myllyharju J. Characterization of the human prolyl 4-hydroxylases that modify the hypoxia-inducible factor. J Biol Chem 2003, 278(33);30772-30780.

111) Wang G.L. Semenza G.L. Characterization of hypoxia-inducible factor 1 and regulation of DNA binding activity by hypoxia. J Biol Chem 1993b, 268(29);21513-21518.

112) Jewell U.R., Kvietikova I., Scheid A., Bauer C., Wenger R.H., Gassmann M. Induction of HIF-1alpha in response to hypoxia is instantaneous. FASEB J 2001, 15(7);1312-1314.

113) Maltepe E., Schmidt J.V., Baunoch D., Bradfield C.A., Simon M.C. Abnormal angiogenesis and response to glucose and oxygen deprivation in mice lacking the protein ARNT. Nature 1997, 386(6623);403-407.

114) Iyer N.V., Kotch L.E., Agani F., Leung S.W., Laughner E., Wenger R.H., Gassmann M., Gearhart J.D., Lawler A.M., Yu A.Y., Semenza G.L. Cellular and developmental control of O2 homeostasis by hypoxia-inducible factor 1a. Genes Dev 1998, 12(2);149– 162.

115) Ryan H.E., Lo J., Johnson R.S. HIF-1a is required for solid tumor formation and embryonic vascularization. EMBO J 1998, 17(11);3005–3015.

116) Melillo G., Musso T., Sica A., Taylor L.S., Cox G.W., Varesio L. A hypoxia-responsive element mediates a novel pathway of activation of the inducible nitric oxide synthase promoter. J Exp Med 1995, 182(6);1683–1693.

117) Loboda A., Jozkowicz A., Dulak J. HIF-1 and HIF-2 transcription factors – similar but not identical. Mol Cells 2010, 29(5);435-442.

118) Semenza G.L. HIF-1: mediator of physiological and pathophysiological response to hypoxia. J Appl Physiol 2000, 88(4);1474-1480.

119) Ke Q., Costa M. Hypoxia-Inducible Factor-1 (HIF-1). Molec Pharmacol 2006, 70(6);1469-1480.

120) .Manola D.J., Rowan A., Lavoie T., Natarajan L., Kelly B.D., Ye S.Q., Garcia J.G., Semenza G.L. Transciptional regulation of vascular endothelial cell response to hypoxia by HIF-1. Blood 2005, 105(2);659-669.

121) Goda N., Ryan H.E., Khadivi B., McNulty W., Rickert R.C., Johnson R.S. Hypoxia-inducible factor 1α is essential for cell cycle arrest during hypoxia. Mol Cell Biol 2003, 23(1);359-369.

122) Mole D.R., Blancher C., Copley R.R., Pollard P.J., Gleadle J.M., Ragoussis J., Ratcliffe P.J. Genome-wide association of hypoxia-inducible factor (HIF)-1alpha and HIF-2alpha DNA binding with expression profiling of hypoxia-inducible transcripts. J Biol Chem 2009, 284(25);16767-16775.

123) Schödel J., Oikonomopoulos S., Ragoussis J., Pugh C.W., Ratcliffe P.J., Mole D.R. High-resolution genome-wide mapping of HIF-binding sites by ChIP-seq. Blood 2011, 117(23);e207-e217.

124) Ortiz-Barahona A., Villar D., Pescador N., Amigo J., del Peso L. Genome-wide identification of hypoxia-inducible factor binding sites and target genes by a

probabilistic model integrating transcription-profiling data and in silico binding site prediction. Nucleic Acids Res 2010, 38(7);2332-2345.

125) Stroka D.M., Burkhardt T., Desbaillets I., Wenger R.H., Neil D.A., Bauer C., Gassmann M., Candinas D. HIF-1 is expressed in normoxic tissue and displays an organ-specific regulation under systemic hypoxia. FASEB J 2001, 15(13);2445-2453.

126) Chi J.T., Wang Z., Nuyten D.S., Rodriguez E.H., Schaner M.E., Salim A., Wang Y., Kristensen G.B., Helland A., Børresen- Dale A.L., Giaccia A., Longaker M.T., Hastie T., Yang G.P., van de Vijver M.J., Brown P.O. Gene expression programs in response to hypoxia: cell type specificity and prognostic significance in human cancers. PLoS Med 2006, 3(3);e47.

127) Gardner L.B., Corn P.G. Hypoxic regulation of mRNA expression. Cell Cycle 2008, 7(13);1916–1924.

128) Brachen C.P., Fedele A.O., Linke S., Balrak W., Lisy K., Whitelaw M.L., Peet D.J. Cell-specific regulation of hypoxia-inducible factor (HIF)-1α and HIF-2α stabilization and transactivation in a graded oxygen environment. J Biological Chem 2006, 281(32);22575-22585.

129) Lendahl U., Lee K.L., Yang H., Poellinger L. Generating specificity and diversity in the transcriptional response to hypoxia. Nature Rev Genet 2009, 10(12);821-832.

130) Benita Y., Kikuchi H., Smith A.D., Zhang M.Q., Chung D.C., Xavier R.J. An integrative genomics approach identifies Hypoxia Inducible Factor-1 (HIF-1)-target genes that form the core response to hypoxia. Nucleic Acids Res 2009, 37(14);4587-4602.

131) Semenza G.L. Oxygen sensing, homeostasis, and disease. N Engl J Med 2011a, 365(6);537-547.

132) Kenneth N.S., Rocha S. Regulation of gene expression by hypoxia. Biochem J 2008, 414(1);19-29.

133) Hu C.J., Wang L.Y., Chodosh L.A., M B.K., Simon C. Differential roles of hypoxia-inducible factor 1α (HIF-1α) and HIF-2α in hypoxic gene regulation. Mol Cell Biol 2003, 23(24);9361-9374.

134) Raval R.R., Lau K.W., Tran M.G., Sowter H.M., Mandriota S.J., Li J.L., Pugh C.W., Maxwell P.H., Harris A.L., Ratcliffe P.J. Contrasting properties of hypoxia-inducible factor 1 (HIF-1) and HIF-2 in von Hippel-Lindau-associated renal cell carcinoma. Mol Cell Biol 2005, 25(13);5675-5686.

135) Covello K.L., Kehler J., Yu H., Gordan J.D., Arsham A.M., Hu C.J., Labosky P.A., Simon M.C., Keith B. HIF- 2alpha regulates Oct-4: effects of hypoxia on stem cell function, embryonic development, and tumor growth. Genes Dev 2006, 20(5);557-570.

136) Makino Y., Cao R., Svensson K., Bertilsson G., Asman M., Tanaka H., Cao Y., Berkenstam A., Poellinger L. Inhibitory PAS domain protein is a negative regulator of hypoxia-inducible gene expression. Nature 2001, 414(6863); 550–554.

137) Krohn K.A., Link J.M., Mason R.P. Molecular imaging of hypoxia. J Nucl Med 2008, Suppl 2;129S-148S.

138) Kim Y.R., Huang I.J., Lee S.R., Tejima E., Mandeville J.B., van Meer M.P., Dai G., Choi Y.W., Dijkhuizen R.M., Lo E.H., Rosen B.R. Measurements of BOLD/CBV ratio show altered fMRI hemodynamics during stroke recovery in rats. J Cereb Blood Flow Metab 2005, 25(7);820–829.

139) Leontiev O., Buxton R.B. Reproducibility of BOLD, perfusion, and CMRO2 measurements with calibrated-BOLD fMRI. Neuroimage 2007, 35(1);175–184.

140) Mason R.P., Shukla H.P., Antich P.P. In vivo oxygen tension and temperature: simultaneous determination using 19F NMR spectroscopy of perfluorocarbon. Magn Reson Med 1993, 29:296–302.

141) Zhao D., Jiang L., Mason R.P. Measuring changes in tumor oxygenation. Methods Enzymol 2004, 386;378–418.

142) Vaupel P., Schlenger K., Knoop C., Hockel M. Oxygenation of human tumors: evaluation of tissue oxygen distribution in breast cancers by computerized O2 tension measurements. Cancer Res 1991, 51(12);3316–3322.

143) Collingridge D.R., Piepmeier J.M., Rockwell S., Knisely J.P. Polargraphic measurements of oxygen tension in human glioma and surrounding peritumoural brain tissue. Radiother Oncol 1999, 53(2);127-131.

144) Kim J.G., Song Y., Zhao D., Constantinescu A., Mason R.P., Liu H. Interplay of tumor vascular oxygenation and tumor pO_2 observed using near-infrared spectroscopy, an oxygen needle electrode, and 19F MR pO_2 mapping. J Biomed Opt 2003, 8(1);53-62.

145) Mason R.P., Hunjan S., Constantinescu A., Song Y., Zhao D., Hahn E.W., Antich P.P., Peschke P. Tumor oximetry: comparison of 19F MR EPI and electrodes. Adv Exp Med Biol 2003, 530;19–27.

146) Jorge P.A., Mayeh M., Benrashid R., Caldas P., Santos J.L., Farahi F. Applications of quantum dots in optical fiber luminescent oxygen sensors. Appl Opt 2006, 45(16);3760-3767.

147) Adamsen T.C.H., Grierson J.R., Krohn K.A. A new synthesis of the labeling precursor for [18F]-fluoromisonidazole. J Labelled Comp Radiopharm 2005, 48;923–927.

148) Varia M.A., Calkins-Adams D.P., Rinker L.H., Kennedy A.S., Novotny D.B., Fowler W.C. Jr., Raleigh J.A. Pimonidazole: a novel hypoxia marker for complementary study of tumor hypoxia and cell proliferation in cervical carcinoma. Gynecol Oncol 1998, 71(2);270-277.

149) Olive P.L., Durand R.E., Raleigh J.A., Luo C., Aquin-Parsons C. Comparison between the comet assay and pimonidazole binding for measuring tumour hypoxia. Br J Cancer 2000, 83(11);1525-1531.

150) Nordsmark M., Loncaster J., Aquino-Parsons C., Chou S.C., Ladekarl M., Havsteen H., Lindegaard J.C., Davidson S.E., Varia M., West C., Hunter R., Overgaard J., Raleigh J.A. Measurements of hypoxia using pimonidazole and polarographic oxygen-sensitive electrodes in human cervix carcinomas. Radiother Oncol 2003, 67(1);35-44.

151) Gross J.D., Constantinidis I., Sambanis A. Modeling of encapsulated cell systems. J Theor Biol 2007, 244(3);500-510.

152) Cheema U., Brown R.A., Alp B., MacRobert A.J. Spatially defined oxygen gradients and vascular endothelial growth factor expression in an engineered 3D cell model. Cell Mol Life Sci 2008, 65(1);177-186.

153) Buchwald P. FEM-based oxygen consumption and cell viability models for avascular pancreatic islets. Theor Biol Med Model 2009, 6;5.

154) Shibata T., Giaccia A.J., Brown J.M. Development of a hypoxia-responsive vector for tumor-specific gene therapy. Gene Ther 2000, 7(6);493–498.

155) Payen E., Bettan M., Henri A., Tomkiewitcz E., Houque A., Kuzniak I., Zuber J., Scherman D., Beuzard Y. Oxygen tension and a pharmacological switch in the regulation of transgene expression for gene therapy. J Gene Med 2001, 3(5);498–504.

156) Koshikawa N., Takenaga K., Tagawa M., Sakiyama S. Therapeutic efficacy of the suicide gene driven by the promoter of vascular endothelial growth factor gene against hypoxic tumor cells. Cancer Res 2000, 60(11);2936–2941.

157) Harada H., Kizaka-Kondoh S., Hiraoka M. Optical imaging of tumor hypoxia and evaluation of efficacy of a hypoxia-targeting drug in living animals. Mol Imaging 2005, 4(3);82–193.

158) Vordermark D., Shibata T., Brown J.M. Green fluorescent protein is a suitable reporter of tumor hypoxia despite an oxygen requirement for chromophore formation. Neoplasia 2001, 3(6);527–534.

159) Serganova I., Doubrovin M., Vider J., Ponomarev V., Soghomonyan S., Beresten T., Ageyeva L., Serganov A., Cai S., Balatoni J., Blasberg R., Gelovani J. Molecular imaging of temporal dynamics and spatial heterogeneity of hypoxia-inducible factor-1 signal transduction activity in tumors in living mice. Cancer Res 2004, 64(17);6101–6108.

160) Laschke M.W., Harder Y., Amon M., Martin I., Farhadi J., Ring A., Torio-Padron N., Schramm R., Rücker M., Junker D., Häufel J.M., Carvalho C., Heberer M., Germann G., Vollmar B., Menger M.D. Angiogenesis in tissue engineering: breathing life into constructed tissue substitutes. Tissue Eng 2006, 12(8);2093-2104.

161) Langer R., Vacanti J.P. Tissue engineering. Science 1993, 260(5110);920-926.

162) Mason C., Dunnill P. A brief definition of regenerative medicine. Regen Med 2008, 3(1);1-5.

163) Kelly W.D., Lillehei R.C., Merkel F.K., Idezuki Y., Goetz F.C. Allotransplantation of the pancreas and duodenum along with the kidney in diabetic nephropathy. Surgery 1967, 61(6);827-837.

164) Lim F., Sun A.M. Microencapsulated islets as bioartificial endocrine pancreas. Science 1980, 210(4472);908-910.

165) Dufrane D., Goebbels R.M., Saliez A., Guiot Y., Gianello P. Six-month survival of microencapsulated pig islets and alginate biocompatibility in primates: Proof of concept. Transplantation 2006a, 81(9);1345-1353.

166) Abalovich A.G., Bacqué M.C., Grana D., Milei J. Pig pancreatic islet transplantation into spontaneously diabetic dogs. Transplant Proc 2009, 41(1);328-330.

167) Elliott R.B., Escobar L., Tan P.L.J., Muzina M., Zwain S., Buchanan C. Live encapsulated porcine islets from a type 1 diabetic patient 9.5 yr after xenotransplantation. Xenotransplantation 2007, 14(2);157-161.

168) Tuch B.E., Foster J.L., Keogh G.W., Vaithilingam V., Williams L.J., Philips R., Wu W. Safety and viability of microencapsulated human islets transplanted into diabetic humans. Diabetes Care 2009, 32(10);1887-1889.

169) Langlois G., Dusseault J., Bilodeau S., Tam S.K., Magassouba D., Hallé J.P. Direct effect of alginate purification on the survival of islets immobilized in alginate-based microcapsules. Acta Biomaterialia 2009, 5(9);3433-3440.

170) Liu X.Y., Nothias J.M., Scavone A., Garfinkel M., Millis J.M. Biocompatibility investigation of polyethylene glycol and alginate-poly-L-lysine for islet encapsulation. ASAIO J 2010, 56(3);241-245.

171) Bryant S.J., Anseth K.S. Hydrogel properties influence ECM production by chondrocytes photoencapsulated in poly(ethylene glycol) hydrogels. J Biomed Mater Res 2002, 59(1);63-72.

172) Rice M.A., Anseth K.S. Encapsulating chondrocytes in copolymer gels: Bimodal degradation kinetics influence cell phenotype ad extracellular matrix development. J Biomed Mater Res A 2004, 70(4);560-568.

173) Burdick J.A., Anseth K.S. Photoencapsulation of osteoblasts in injectable RGD-modified hydrogels for bone tissue engineering. Biomaterials 2002, 23(22);4315-4323.

174) Benton J.A., Fairbanks B.D., Anseth K.S. Characterization of valvular interstitial cell function in three dimensional matrix metalloproteinase degradable PEG hydrogels. Biomaterials 2009, 30(34);6593-6603.

175) Nuttelman C.R., Tripodi M.C., Anseth K.S. *In vitro* osteogenic differentiation of human mesenchymal stem cells photoencapsulated in PEG hydrogels. J Biomed Mater Res A 2004, 68(4);773-782.

176) Cruise G.M., Scharp D.S., Hubbell J.A. Characterization of permeability and network structure of interfacially photopolymerized poly(ethylene glycol) diacrylate hydrogels. Biomaterials 1998, 19(14);1287-1294.

177) Lin-Gibson S., Bencherif S., Cooper J.A., Wetzel S.J., Antonucci J.M., Vogel B.M., Horkay F., Washburn N.R. Synthesis and characterization of PEG dimethacrylates and their hydrogels. Biomacromolecules 2004, 5(4);1280-1287.

178) Weber L.M., Lopez C.G., Anseth K.S. Effects of PEG hydrogel crosslinking density on protein diffusion and encapsulated islet survival and function. J Biomed Mater Res A 2009, 90(3);720-729.

179) Weber L.M., He J., Bradley B., Haskins K., Anseth K.S. PEG-based hydrogels as an in vitro encapsulation platform for testing controlled β-cell microenvironments. Acta Biomater 2006, 2(1);1-8.

180) Bryant S.J., Nuttelman C.R., Anseth K.S. Cytocompatibility ofUV and visible light photoinitiating systems on cultured NIH/3T3 fibroblasts *in vitro*. J Biomater Sci Polym Ed 2000, 11(5);439-457.

181) De Vos P., De Haan B.J., Wolters G.H.J., Strubbe J.H., Van Schilfgaarde R. Improved biocompatibility but limited graft survival after purification of alginate for microencapsulation of pancreatic islets. Diabetologia 1997, 40(3);262-270.

182) Suzuki K., Bonner-Wier S., Trivedi N., Yoon K.H., Hollister-Lock J., Colton C.K., Weir G.C. Function and survival of macroencapsulated syngeneic islets transplanted into streptozocin-diabetic mice. Transplantation 1998, 66(1);21-28.

183) De Vos P., Van Straaten J.F.M., Nieuwenhuizen A.G., de Groot M., Ploeg R.J., De Haan B.J., Van Schilfgaarde R. Why do microencapsulated islet grafts fail in the absence of fibrotic overgrowth? Diabetes 1999, 48(7);1381-1388.

184) Dionne K.E., Colton C.K., Yarmush M.L. Effect of oxygen on isolated pancreatic tissue. ASAIO Trans 1989, 35(3);739-741.

185) Dionne K.E., Colton C.K., Yarmush M.L. Effect of oxygen on insulin secretion by isolated rat and canine islets of Langerhans. Diabetes 1993, 42(1);12-21.

186) de Groot M., Schuurs T.A., Keizer P.P.M., Fekken S., Leuvenink H.G.D., Van Schilfgaarde R. Response of encapsulated rat pancreatic islets to hypoxia. Cell Transplant 2003, 12(8);867-875.

187) Shapiro A.M.J, Lakey J.R.T., Ryan E.A., Korbutt G.S., Toth E., Warnock G., Kneteman N.M., Rajotte R.V. Islet transplantation in seven patients with type 1 diabetes mellitus using a glucocorticoid-free immunosuppressive regimen. New Engl J Med 2000, 343(4);230-238.

188) Shapiro J.A.M., Ricordi C., Hering B.J., Auchincloss H., Lindblad R., Robertson R.P., Secchi A., Brendel M.D., Berney T., Brennan D.C., Cagliero E., Alejandro R., Ryan E.A., DiMercurio B., Morel P., Polonsky K.S., Reems J., Bretzel R.G., Bertuzzi F., Froud T., Kandaswamy R., Sutherland D.E.R., Eisenbarth G., Segal M., Preiksaitis J., Korbutt G.S., Barton F.B., Viviano L., Seyfert-Margolis V., Bluestone J., Lakey J.R.T. International trial of the Edmonton Protocol for islet transplantation. New Engl J Med 2006, 355(13);1318-1330.

189) Schrezenmeir J., Kirchgessner J., Gerö L., Kunz L.A., Beyer J., Mueller-Klieser W. Effect of microencapsulation on oxygen distribution in islet organs. Transplantation 1994, 57(9);1308-1314.

190) Lehmann R., Zuellig R.A., Kugelmeier P., Baenninger P.B., Moritz W., Perren A., Clavien P.A., Weber M., Spinas G.A. Superiority of small islets in human islet transplantation. Diabetes 2007, 56(3);594-603.

191) Cavallari G., Zuellig R.A., Lehmann R., Weber M., Moritz W. Rat pancreatic islet size standardization by the "Hanging Drop" technique. Transplant Proc 2007, 39(6);2018-2020.

192) Sweet I.R., Khalil G., Wallen A.R., Steedman M., Schenkman K.A., Reems J.A., Kahn S.E., Callis J.B. Continuous measurement of oxygen consumption by pancreatic islets. Diabetes Technol Ther 2002, 4(5);661-672.

193) Wang W., Upshaw L., Strong D.M., Robertson R.P., Reems J.A. Increased oxygen consumption rates in response to high glucose detected by a novel oxygen biosensor system in non-human primate and human islets. J Endocrinol 2005, 185(3);445-455.

194) Dufrane D., van Steenberghe M., Goebbels R.M., Saliez A., Guiot Y., Gianello P. The influence of implantation site on the biocompatibility and survival of alginate encapsulated pig islets in rats. Biomaterials 2006b, 27(17);3201-3208.

195) Zehetner J, Danzer C., Collins S., Eckhardt K., Gerber P.A., Ballschmieter P., Galvanovskis J., Shimomura K., Ashcroft F.M., Thorens B., Rorsman P., Krek W. PVHL is a regulator of glucose metabolism and insulin secretion in pancreatic β cells. Genes Dev 2008, 22(22);3135-3146.

196) Cantley J., Selman C., Shukla D., Abramov A.Y., Forstreuter F., Esteban M.A., Claret M., Lingard S.J., Clements M., Harten S.K., Asare-Anane H., Batterham R.L., Herrera P.L., Persaud S.J., Duchen M.R., Maxwell P.H., Withers D.J. Depletion of the von Hippel-Lindau gene in pancreatic β cells impairs glucose homeostasis in mice. J Clin Invest 2009, 119(1);125-135.

197) Puri S., Cano D.A., Hebrok M. A role for von Hippel-Lindau protein in pancreatic β-cell function. Diabetes 2009, 58(2);433-441.

198) Griffith L.G., Naughton G. Tissue engineering — current challenges and expanding opportunities. Science 2002, 295(5557);1009–1014.

199) Ikada Y. Challenges in tissue engineering. J R Soc Interface 2006, 2(10);589–601.

200) Rouwkema J., Rivron N.C., van Blitterswijk C.A. Vascularization in tissue engineering. Trends Biotechnol 2008, 26(8);434-441.

201) Lovett M., Lee K., Edwards A., Kaplan D.L. Vascularization strategies for tissue engineering. Tissue Eng Part B Rev 2009, 15(3);353-370.

202) Santos M.I., Reis R.L. Vascularization in bone tissue engineering: physiology, current strategies, major hurdles and future challenges. Macromol Biosci 2010, 10(1);12-27.

203) Novosel E.C., Kleinhans C., Kluger P.J. Vascularization is the key challenge in tissue engineering. Adv Drug Deliv Rev 2011, 63(4-5);300-311.

204) Horch R.E., Kneser U., Polykandriotis E., Schmidt V.J., Sun J., Arkudas A. Tissue engineering and regenerative medicine—where do we stand? J Cell Mol Med 2012, 16(6);1157-1165.

205) Laschke M.W., Menger M.D. Vascularization in tissue engineering: angiogenesis versus inosculation. Eur Surg Res 2012, 48(2);85-92.

206) Folkman J., Hochberg M. Self-regulation of growth in three dimensions. J Exp Med 1973, 138(4);745-753.

207) Colton C.K. Implantable biohybrid artificial organs. Cell Transplant 1995, 4(4);415-436.

208) Carmeliet P., Jain R.K. Molecular mechanisms and clinical applications of angiogenesis. Nature 2001, 473(7347);298-307.

209) Carmeliet P. Mechanisms of angiogenesis and arteriogenesis. Nat Med 2000, 6(4);389-395.

210) Hirschi K.K., Skalak T.C., Peirce S.M., Little C.D. Vascular assembly in natural and engineered tissues. Ann N Y Acad Sci 2002, 961;223-242.

211) Zisch A.H., Lutolf M.P., Hubbell J.A. Biopolymeric delivery matrices for angiogenic growth factors. Cardiovasc Pathol 2003, 12(6);295-310.

212) Sokolsky-Papkov M., Agashi K., Olaye A., Shakesheff K., Domb A.J. Polymer carriers for drug delivery in tissue engineering. Adv Drug Deliv Rev 2007, 59(4-5);187-206.

213) Übersax L., Merkle H.P., Meinel L. Biopolymer-based growth factor delivery for tissue repair: from natural concepts to engineered systems. Tissue Eng Part B Rev 2009, 15(3);263-289.

214) Fu Y., Kao W.J. Drug release kinetics and transport mechanisms of non-degradable and degradable polymeric delivery systems. Expert Opin Drug Deliv 2010, 7(4);429-444.

215) Helm C.L., Fleury M.E., Zisch A.H., Boschetti F., Swartz M.A. Synergy between interstitial flow and VEGF directs capillary morphogenesis in vitro through a gradient amplification mechanism. Proc Natl Acad Sci USA 2005, 102(44);15779-15784.

216) Mizuno H. Adipose-derived stem cells for tissue repair and regeneration: ten years of research and a literature review. J Nippon Med Sch 2009, 76(2);56-66.

217) Kilroy G.E., Foster S.J., Wu X., Ruiz J., Sherwood S., Heifetz A., Ludlow J.W., Stricker D.M., Potiny S., Green P., Halvorsen Y.D., Cheatham B., Storms R.W., Gimble J.M. Cytokine profile of human adipose-derived stem cells: expression of angiogenic, hematopoietic, and pro-inflammatory factors. J Cell Physiol 2007, 212(3);702-709.

218) Hong S.J., Traktuev D.O., March K.L. Therapeutic potential of adipose-derived stem cells in vascular growth and tissue repair. Curr Opin Organ Transplant 2010, 15(1);86-91.

219) Rasmussen J.G., Frøbert O., Pilgaard L., Kastrup J., Simonsen U., Zachar V., Fink T. Prolonged hypoxic culture and trypsinization increase the pro-angiogenic potential of human adipose tissue-derived stem cells. Cytotherapy 2011, 13(3);318-328.

220) Planat-Benard V., Silvestre J.S., Cousin B., André M., Nibbelink M., Tamarat R., Clergue M., Manneville C., Saillan-Barreau C., Duriez M., Tedgui A., Levy B., Pénicaud L., Casteilla L. Plasticity of human adipose lineage cells toward endothelial cells: physiological and therapeutic perspectives. Circulation 2004, 109(5);656-663.

221) Miranville A., Heeschen C., Sengenès C., Curat C.A., Busse R., Bouloumié A. Improvement of postnatal neovascularization by human adipose tissue-derived stem cells. Circulation 2004, 110(3);349-355.

222) Cao Y., Sun Z., Liao L., Meng Y., Han Q., Zhao R.C. Human adipose tissue-derived stem cells differentiate into endothelial cells in vitro and improve postnatal neovascularization in vivo. Biochem Biophys Res Commun 2005, 332(2);370-379.

223) Colazzo F., Chester A.H., Taylor P.M., Yacoub M.H. Induction of mesenchymal to endothelial transformation of adipose-derived stem cells. J Heart Valve Dis 2010, 19(6);736-744.

224) Keerl S., Gehmert S., Gehmert S., Song Y.H., Alt E. PEGF and bFGF modulate tube formation in adipose tissue-derived stem cells. Ann Plast Surg 2010, 64(4);487-490.

225) Shi Z., Neoh K.G., Kang E.T., Poh C.K., Wang W. Enhanced endothelial differentiation of adipose-derived stem cells by substrate nanotography. J Tissue Eng Regen Med 2012, [in press].

226) Kim W.S., Park B.S., Sung J.H., Yang J.M., Park S.B., Kwak S.J., Park J.S. Wound healing effect of adipose-derived stem cells: a critical role of secretory factors on human dermal fibroblasts. J Dermatol Sci 2007, 48(1);15-24.

227) Lu F., Mizuno H., Uysal C.A., Cai X., Ogawa R., Hyakusoku H. Improved viability of random pattern skin flaps through the use of adipose-derived stem cells. Plast Reconstr Surg 2008, 121(1);50-58.

228) Kim W.S., Park B.S., Sung J.H. The wound-healing and antioxidant effects of adipose-derived stem cells. Expert Opin Biol Ther 2009, 9(7);879-887.

229) Nambu M., Kishimoto S., Nakamura S., Mizuno H., Yanagibayashi S., Yamamoto N., Azuma R., Nakamura S., Kiyosawa T., Ishihara M., Kanatani Y. Accelerated wound healing in healing-impared *db/db* mice by autologous adipose tissue-derived stromal cells combined with atelocollagen matrix. Ann Plast Surg 2009, 62(3);317-321.

230) Nakagami H., Maeda K., Morishita R., Iguchi S., Nishikawa T., Takami Y., Kikuchi Y., Saito Y., Tamai K., Ogihara T., Kaneda Y. Novel autologous cell therapy in ischemic limb disease through growth factor secretion by cultured adipose tissue-derived stromal cells. Arterioscler Thromb Vasc Biol 2005, 25(12);2542-2547.

231) Moon M.H., Kim S.Y., Kim Y.J., Kim S.J., Lee J.B., Bae Y.C., Sung S.M., Jung J.S. Human adipose tissue-derived mesenchymal stem cells improve postnatal neovascularization in a mouse model of hindlimb ischemia. Cell Physiol Biochem 2006, 17(5-6);279-290.

232) Kim Y., Kim H., Cho H., Bae Y., Suh K., Jung J. Direct comparison of human mesenchymal stem cells derived from adipose tissues and bone marrow in mediating neovascularization in response to vascular ischemia. Cell Physiol Biochem 2007, 20(6);867-876.

233) Miyahara Y., Nagaya N., Kataoka M., Yanagawa B., Tanaka K., Hao H., Ishino K., Ishida H., Shimizu T., Kangawa K., Sano S., Okano T., Kitamura S., Mori H. Monolayered mesenchymal stem cells repair scarred myocardium after myocardial infarction. Nat Med 2006, 12(4);459-465.

234) Valina C., Pinkernell K., Song Y.H., Bai X., Sadat S., Campeau R.J., Le Jemtel T.H., Alt E. Intracoronary administration of autologous adipose tissue-derived stem cells improves left ventricular function, perfusion, and remodelling after acute myocardial infarction. Eur Heart J 2007, 28(21);2667-2677.

235) Cai L., Johnstone B.H., Cook T.G., Tan J., Fishbein M.C., Chen P.S., March K.L. IFATS collection: Human adipose tissue-derived stem cells induce angiogenesis and nerve sprouting following myocardial infarction, in conjunction with potent preservation of cardiac function. Stem Cells 2009, 27(1);230-237.

236) Schenke-Layland K., Strem B.M., Jordan M.C., Deemedio M.T., Hedrick M.H., Roos K.P., Fraser J.K., Maclellan W.R. Adipose tissue-derived cells improve cardiac function following myocardial infarction. J Surg Res 2009, 153(2);217-223.

237) Wang L., Deng J., Tian W., Xiang B., Yang T., Li G., Wang J., Gruwel M., Kashour T., Rendell J., Glogowski M., Tomanek B., Freed D., Deslauriers R., Arora R.C., Tian G. Adipose-derived stem cells are an effective cell candidate for treatment of heart failure: an MR imaging study of rat hearts. Am J Physiol Heart Circ Physiol 2009, 297(3);H1020-H1031.

238) Takahashi T., Kalka C., Masuda H., Chen D., Silver M., Kearney M., Magner M., Isner J.M., Asahara T. Ischemia- and cytokine-induced mobilization of bone marrow-derived endothelial progenitor cells for neovascularization. Nat Med 1999, 5(4);434-438.

239) Crosby J.R., Kaminski W.E., Schatteman G., Martin P.J., Raines E.W., Seifert R.A., Bowen-Pope D.F. Endothelial cells of hematopoietic origin make a significant contribution to adult blood vessel formation. Circ Res 2000, 87(9);728-730.

240) Ceradini D.J., Gurtner G.C. Homing to hypoxia: HIF-1 as a mediator of progenitor cell recruitment to injured tissue. Trends Cardiovasc Med 2005, 15(2);57-63.

241) Nakao N., Nakayama T., Yahata T., Muguruma Y., Saito S., Miyata Y., Yamamoto K., Naoe T. Adipose tissue-derived mesenchymal stem cells facilitate hematopoiesis in vitro and in vivo: advantages over bone marrow-derived mesenchymal stem cells. Am J Pathol 2010, 177(2);547-554.

242) Askari A.T., Unzek S., Popovic Z.B., Goldman C.K., Forudi F., Kiedrowski M., Rovner A., Ellis S.G., Thomas J.D., DiCorleto P.E., Topol E.J., Penn M.S. Effect of stromal-cell-derived factor 1 on stem-cell homing and tissue regeneration in ischaemic cardiomyopathy. Lancet 2003, 362(9385);697-703.

243) Ceradini D.J., Kulkarni A.R., Callaghan M.J., Tepper O.M., Bastidas N., Kleinman M.E., Capla J.M., Galiano R.D., Levine J.P., Gurtner G.C. Progenitor cell trafficking is regulated by hypoxic gradients through HIF-1 induction of SDF-1. Nat Med. 2004, 10(8);858-864.

244) Traktuev D.O., Merfeld-Clauss S., Li J., Kolonin M., Arap W., Pasqualini R., Johnstone B.H., March K.L. A population of multipotent CD34- positive adipose stromal cells share pericyte and mesenchymal surface markers, reside in a periendothelial location, and stabilize endothelial networks. Circ Res 2008, 102(1);77–85.

245) Traktuev D.O., Prater D.N., Merfeld-Clauss S., Sanieevaiah A.R., Saadatzadeh M.R., Murphy M., Johnstone B.H., Ingram D.A., March K.L. Robust functional vascular network formation in vivo by cooperation of adipose progenitor and endothelial cells. Circ Res 2009, 104(12);1410–1420.

246) Gimble J.M., Katz A.J., Bunnell B.A. Adipose-derived stem cells for regenerative medicine. Circ Res 2007, 100(9);149-1260.

247) Matsumoto A., Matsumoto S., Sowers A.L., Koscielniak J.W., Trigg N.J., Kuppusamy P., Mitchell J.B., Subramanian S., Krishna M.C., Matsumoto K. Absolute oxygen tension (pO_2) in murine fatty and muscle tissue as determined by EPR. Magn Reson Med 2005, 54(6);1530-1535.

248) Pasarica M., Sereda O.R., Redman L.M., Alberado D.C., Hymel D.T., Roan L.E., Rood J.C., Burk DH, Smith SR. Reduced adipose tissue oxygenation in human obesity: evidence for rarefaction, macrophage chemotaxis, and enflammation without an angiogenic response. Diabetes 2009, 58(3);718-715.

249) Mohyeldin A., Garzón-Muvdi T., Quiñones-Hinojosa A. Oxygen in stem cell biology: a critical component of the stem cell niche. Cell Stem Cell 2010, 7(2);150-161.

250) Rehman J., Traktuev D., Li J., Merfeld-Clauss S., Temm-Grove C.J., Bovenkerk J.E., Pell C.L., Johnstone B.H., Considine R.V., March K.L. Secretion of angiogenic and antiapoptotic factors by human adipose stromal cells. Circulation 2004, 109(10);1292-1298.

251) Rosová I., Dao M., Capoccia B., Link D., Nolta J.A. Hypoxic preconditioning results in increased motility and improved therapeutic potential of human mesenchymal stem cells. Stem Cells 2008, 26(8);2173-2182.

252) Lee E.Y., Xia Y., Kim W.S., Kim M.H., Kim T.H., Kim K.J., Park B.S., Sung J.H. Hypoxia-enhanced wound-healing function of adipose-derived stem cells: increase in stem cell proliferation and up-regulation of VEGF and bFGF. Wound Repair Regen 2009, 17(4);540-547.

253) Liu L., Gao J., Yuan Y., Chang Q., Liao Y., Lu F. Hypoxia preconditioned human adipose derived mesenchymal stem cells enhance angiogenic potential via secretion of increased VEGF and bFGF. Cell Biol Int 2013, (in press).

254) Levy A.P., Levy N.S., Wegner S., Goldberg M.A. Transcriptional regulation of the rat vascular endothelial growth factor gene by hypoxia. J Biol Chem 1995, 270(22);13333-13340.

255) Liu Y., Cox S.R., Morita T., Kourembanas S. Hypoxia regulates vascular endothelial growth factor gene expression in endothelial cells. Identification of a 5' enhancer. Circ Res 1995, 77(3);638-643.

256) Forsythe J.A., Jiang B.H., Iyer N.V., Agani F., Leung S.W., Koos R.D., Semenza G.L. Activation of vascular endothelial growth factor gene transcription by hypoxia-inducible factor 1. Mol Cell Biol 1996, 16(9);4604-4613.

257) Tang Y.L., Zhu W., Cheng M., Chen L., Zhang J., Sun T., Kishore R., Phillips M.I., Losordo D.W., Qin G. Hypoxic preconditioning enhances the benefit of cardiac progenitor cell therapy for treatment of myocardial infarction by inducing CXCR4 expression. Circ Res 2009, 104(10);1209–1216.

258) Yue Y., Zhang P., Liu D., Yang J.F., Nie C., Yang D. Hypoxia preconditioning enhances the viability of ADSCs to increase the survival rate of ischemic skin flaps in rats. Aesthetic Plast Surg 2013, 37(1);159-170.

259) Chacko S.M., Ahmed S., Selvendiran K., Kuppusamy M.L., Khan M., Kuppusamy P. Hypoxic preconditioning induces the expression of prosurvival and proangiogenic markers in mesenchymal stem cells. Am J Physiol Cell Physiol 2010, 299(6), C1562–C1570.

260) Abdollahi H., Harris L.J., Zhang P., McIlhenny S., Srinivas V., Tulenko T., Dimuzio P.J., Dimuzio P.J. The role of hypoxia in stem cell differentiation and therapeutics. J Surg Res 2010, 165(1);112-117.

261) Zachar V, Duroux M, Emmersen J, Rasmussen JG, Pennisi CP, Yang S, Fink T. Hypoxia and adipose-derived stem cell-based tissue regeneration and engineering. Expert Opin Biol Ther 2011, 11(6);775-786.

262) Geiger F., Lorenz H., Xu W., Szalay K., Kasten P., Claes L., Augat P., Richter W. VEGF producing bone marrow stromal cells (BMSC) enhance vascularization and resorption of a natural coral bone substitute. Bone 2007, 41(4);516-522.

263) Baraniak P.R., McDevitt T.C. Stem cell paracrine actions and tissue regeneration. Regen Med 2010, 5(1);121-143.

264) Shweiki, D., Neeman, M., Itin, A., Keshet, E. Induction of vascular endothelial growth factor expression by hypoxia and by glucose deficiency in multicell spheroids: implications for tumor angiogenesis. Proc Natl Acad Sci USA 1995, 92(3);768-772.

265) Bates R.C., Edwards N.S., Yates, J.D. Spheroids and cell survival. Crit Rev Oncol Hematol 2000, 36(2-3);61-74.

266) Gaedtke L., Thoenes L., Culmsee C., Mayer B., Wagner E. Proteomic analysis reveals differences in protein expression in spheroid versus monolayer cultures of lowpassage colon carcinoma cells. J Proteome Res 2007, 6(11);4111-4118.

267) Bhang S.H., Lee S., Shin J.Y., Lee T.J., Kim B.S. Transplantation of cord blood mesenchymal stem cells as spheroids enhances vascularization. Tissue Eng Part A 2012a, 18(19-20);2138-47.

268) Saleh F.A., Genever P.G. Turning round: multipotent stromal cells, a three-dimensional revolution? Cytotherapy 2011, 13(8);903-912.

269) Baraniak P.R., McDevitt T.C. Scaffold-free culture of mesenchymal stem cell spheroids in suspension preserves mutlilineage potential. Cell Tissue Res 2012, 347(3);701-11.

270) Skiles M.L., Fancy R., Topiwala P., Sahai S., Blanchette J.O. Correlating hypoxia with insulin secretion using a fluorescent hypoxia detection system. J Biomed Mater Res B Appl Biomater 2011a, 97(1);148-55.

271) Semenza G.L. HIF-1 and mechanisms of hypoxia sensing. Curr Opin Cell Biol 2001, 13(2);167-171.

272) Matta S.G., Wobken J.D., Williams F.G., Bauer G.E. Pancreatic islet cell reaggregation systems: efficiency of cell reassociation and endocrine cell topography of rat islet-like aggregates. Pancreas 1994, 9(4);439-449.

273) Carlsson P.O., Liss P., Andersson A., Jansson L. Measurements of oxygen tension in native and transplanted rat pancreatic islets. Diabetes 1998, 47(7);1027-1032.

274) Dulong J.L., Legallais C. A theoretical study of oxygen transfer including cell necrosis for the design of a bioartificial pancreas. Biotechnol Bioeng 2007, 96(5);990-998.

275) Moritz W., Meier F., Stroka D., Giuliani M., Kugelmeier P., Nett PhC., Lehmann R., Candinas D., Gassmann M., Weber M. Apoptosis in hypoxic human pancreatic islets correlates with HIF-1α expression. FASEB J 2002, 16(7);745-747.

276) Ma T., Grayson W.L., Frölich M., Vunjak-Novakovic G. Hypoxia and stem cell-based engineering of mesenchymal tissues. Biotechnol Prog 2009, 25(1);32-42.

277) He J., Genetos D.C., Yellowley C.E., Leach J.K. Oxygen tension differentially influences osteogenic differentiation of human adipose stem cells in 2D and 3D cultures. J Cell Biochem 2010, 110(1);87-96.

278) Skiles M.L., Wilder N.B., Sahai S., Blanchette J.O. Identifying HIF activity in three-dimensional cultures of islet-like clusters. Int J Artif Organs 2013, 36(3);175-183.

279) Davalli A.M., Ogawa Y., Ricordi C., Scharp D.W., Bonner-Weir S., Weir G.C. A selective decrease in the beta cell mass of human islets transplanted into diabetic nude mice. Transplantation 1995, 59(6);817-820.

280) Carlsson P.O., Palm F., Andersson A., Liss P. Markedly decreased oxygen tension in transplanted rat pancreatic islets irrespective of the implantation site. Diabetes 2001, 50(3);489-495.

281) Miao G., Ostrowski R.P., Mace J., Hough J., Hopper A., Peverini R., Chinnock R., Zhang J., Hathout E. Dynamic production of hypoxia-inducible factor-1α in early transplanted islets. Am J Transplant 2006, 6(11);2636-2643.

282) .259. Cornolti R., Figliuzzi M., Remuzzi A. Effect of micro- and macroencapsulation on oxygen consumption by pancreatic islets. Cell Transplant 2009, 18(2);195-201.

283) Semenza G.L. Hypoxia-inducible factor 1: regulator of mitochondrial metabolism and mediator of ischemic preconditioning. Biochim Biophys Acta 2011b, 1813(7);1263-1268.

284) Lo J.F., Wang Y., Blake A., Yu G., Harvat T.A., Jeon H., Oberholzer J., Eddington D.T. Islet preconditioning via multimodal microfluidic modulation of intermittent hypoxia. Anal Chem 2012, 84(4);1987-1993.

285) Schuit F.C., Huypens P., Heimberg H., Pipeleers D.G. Glucose sensing in pancreatic β-cells a model for the study of other glucose-related cells in gut, pancreas, and hypothalamus. Diabetes 2001, 50(1);1-11.

286) Cassavaugh J., Lounsbury K.M. Hypoxia-mediated biological control. J Cell Biochem 2011, 112(3);735-744.

287) Yu A.Y., Frid M.G., Shimoda L.A., Wiener C.M., Stenmark K., Semenza G.L. Temporal, spatial, and oxygen-related expression of hypoxia-inducible factor-1 in the lung. Am J Physiol 1998, 275(4 pt 1);L818-L826.

288) Springett R., Swartz H.M. Measurements of oxygen *in vivo*: overview and perspectives on methods to measure oxygen within cells and tissues. Antioxid Redox Sign 2007, 9(8);1295-1301.

289) Grist S.M., Chrostowski L., Cheung K.C. Optical oxygen sensors for applications in microfluidic cell culture. Sensors 2010, 10(10);9286-9316.

290) Luther M.J., Davies E., Muller D., Harrison M., Bone A.J., Persaud S.J., Jones P.M. Cell-to-cell contact influences proliferative marker expression and apoptosis in MIN6 cells grown in islet-like structures. Am J Endocrinol Metab 2005, 288(3);E502-E509.

291) Hauge-Evans A.C., Squires P.E., Persaud S.J., Jones P.M. Pancreatic β-cell-β-cell interactions are required for integrated responses to nutrient stimuli. Diabetes 1999, 48(7);1402-1408.

292) Lin C.C., Anseth K. Cell-cell communication mimicry with poly(ethylene glycol) hydrogels for enhancing β-cell function. Proc Natl Acad Sci USA 2011, 108(16);6380-6385.

293) Luther M.J., Hauge-Evans A., Souza K.L.A., Jörns A., Lenzen S., Persaud S.J., Jones P.M. MIN6 β-cell-β-cell interactions influence insulin secretory responses to nutrients and non-nutrients. Biochem Biophys Res Commun 2006, 343(1);99-104.

294) Schietke R., Warnecke C., Wacker I., Schödel J., Mole D.R., Campean V., Amann K., Goppelt-Struebe M., Behrens J., Eckardt K.U., Wiesener M.S. The lysyl oxidases LOX and LOXL2 are necessary and sufficient to repress E-cadherin in hypoxia. J Biologic Chem 2010, 285(9);6658-6669.

295) Evans A.J., Russel R.C., Roche O., Burry T.N., Fish J.E., Chow V.W., Kim W.Y., Saravanan A., Maynard M.A., Gervais M.L., Sufan R.I., Roberts A.M., Wilson L.A., Betten M., Vandewalle C., Berx G., Marsden P.A., Irwin M.S., The B.T., Jewett

M.A. Ohh M. VHL promotes E2 box-dependent E-cadherin transcription by HIF-mediated regulation of SIP1 and Snail. Molec Cell Biol 2007, 27(1);157-169.

296) Lee D.Y., Park S.J., Nam J.H., Byun Y. Optimal aggregation of dissociated islet cells for functional islet-like cluster. J Biomater Sci Polym Ed 2008, 19(4);441-452

297) Levenberg S., Rouwkema J., Macdonald M., Garfein E.S., Kohane D.S., Darland D.C., Marini R., Van Blitterswijk C.A., Mulligan R.C., D'Amore P.A., Langer R. Engineering vascularized skeletal muscle tissue. Nat Biotechnol 2005, 23(7);879-884.

298) Kunz-Schughart L.A., Schroeder J.A., Wondrak M., van Rey F., Lehle K., Hofstaedter F., Wheatley D.N. Potential of fibroblasts to regulate the formation of three-dimensional vessel-like structures from endothelial cells *in vitro*. Am J Physiol Cell Physiol 2006, 290(5);C1385-1398.

299) Blasi A., Martino C., Balducci L., Saldarelli M., Soleti A., Navone S.E., Canzi L., Cristini S., Invernici G., Parati E.A., Alessandri G. Dermal fibroblasts display similar phenotypic and differentiation capacity to fat-derived mesenchymal stem cells, but differ in anti-inflammatory and angiogenic potential. Vasc Cell 2011, 3(1);5.

300) Halfon S., Abramov N., Grinblat B., Ginis I. Markers distinguishing mesenchymal stem cells from fibroblasts are downregulated with passaging. Stem Cells Dev 2011, 20(1);53-66.

301) Nie C., Yang D., Xu J., Si Z., Jin X., Zhang J. Locally administered adipose-derived stem cells accelerate wound healing through differentiation and vasculogenesis. Cell Transplant 2011, 20(2);205-216.

302) Kang Y., Park C., Kim D., Seong C.M., Kwon K., Choi C. Unsorted human adipose tissue-derived stem cells promote angiogenesis and myogenesis in murine ischemic hindlimb model. Microvasc Res 2010, 80(3);310-316.

303) Bhang S.H., Cho S.W., La W.G., Lee T.J., Yang H.S., Sun A.Y., Baek S.H., Rhie J.W., Kim B.S. Angiogenesis in ischemic tissue produced by spheroid grafting of human adipose-derived stromal cells. Biomaterials 2011, 32(11);2734-2747.

304) Shweiki D., Itin A., Soffer D., Keshet E. Vascular endothelial growth factor induced by hypoxia may mediate hypoxia-induced angiogenesis. Nature 1992, 359(6398);843-845.

305) Germain S., Monnot C., Muller L., Eichmann A. Hypoxia-driven angiogenesis: role of tip cells and extracellular matrix scaffolding. Curr Opin Hematol 2010, 17(3);245-251.

306) Maxwell P.H., Ratcliffe P. Oxygen sensors and angiogenesis. Semin Cell Dev Biol 2002, 13(1);29-37.

307) Fong G.H. Regulation of angiogenesis by oxygen sensing mechanisms. J Mol Med 2009, 87(6);549-560.

308) Rey S., Semenza G.L. Hypoxia-inducible factor-1-dependent mechanisms of vascularization and vascular remodelling. Cardiovasc Res 2010, 86(2);236-242.

309) Brahimi-Horn C., Berra E., Pouysségur J. Hypoxia: the tumor's gateway to progression along the angiogenic pathway. Trends Cell Biol 2001, 11(11);S32-S36.

310) Semenza G.L. Hypoxia-inducible factors: mediators of cancer progression and targets for cancer therapy. Trends Pharmacol Sci 2012b, 33(4);207-214.

311) Bhang S.H., Lee S., Lee T.J., La W.G., Yang H.S., Cho S.W., Kim B.S. Three-dimensional cell grafting enhances the angiogenic efficacy of human umbilical vein endothelial cells. Tissue Eng Part A 2012b, 18(3-4);310-319.

312) Zelzer E., Mamluk R., Ferrara N., Johnson R.S., Schipani E., Olsen B.R. VEGFA is necessary for chondrocyte survival during bone development. Development 2004, 131(9);2161-2171.

313) Araldi E., Schipani E. Hypoxia, HIFs and bone development. Bone 2010, 47(2);190-196.

314) Skiles M.L., Sahai S., Blanchette J.O. Tracking hypoxic signaling within encapsulated cell aggregates. J Vis Exp 2011b, 16(58);3521.

315) Sahai S., McFarland R., Skiles M.L., Sullivan D., Williams A., Blanchette J.O. Tracking hypoxic signaling in encapsulated stem cells. Tissue Eng Part C Methods 2012, 18(7);557-565.

316) Revsbech N.P., Ward D.M. Oxygen microelectrode that is insensitive to medium chemical composition: use in an acid microbial mat dominated by cyanidium caldarium. Appl Environ Microbiol 1983, 45(3);755-759.

317) Krihak M.K., Shahriari M.R. Highly sensitive, all solid state fiber optic sensor based on the sol-gel coating technique. Electron Lett 1996, 32(3);240-242.

318) Acosta M.A., Leki P.Y., Kostov Y.V., Leach J.B. Fluorescent microparticles for sensing cell microenvironment oxygen levels within 3D scaffolds. Biomaterials 2007, 30(17);3068-3074.

319) Gibbs B.F., Yasinska I.M., Pchejetski D., Wyszynski R.W., Sumbayev V.V. Differential control of hypoxia-inducible factor 1 activity during pro-inflammatory reactions of human haematopoietic cells of myeloid lineage. Int J Biochem Cell Biol 2012, 44(11);1739-1749.

320) Pettersen E.O., Juul N.O., Rønning O.W. Regulation of protein metabolism of human cells during and after acute hypoxia. Caner Res 1986, 46(9);4346-4351.

321) Koumenis C., Naczki C., Koritzinsky M., Rastani S., Diehl A., Sonenberg N., Koromilas A., Wouters B.G. Regulation of protein synthesis by hypoxia via activation of the endoplasmic reticulum kinase PERK and phospohorylation of the translation initiation factor eIFα. Mol Cell Biol 2002, 22(21);7405-7416.

322) Greijer A.E., van der Wall E. The role of hypoxia inducible factor 1 (HIF-1) in hypoxia induced apoptosis. J Clin Pathol 2004, 57(10);1009-1014.

323) Kiang J.G., Tsen K.T. Biology of hypoxia. Chin J Physiol 2006, 49(5);223-233.

324) Burton T.R., Gibson S.B. The role of bcl-2 family member BNIP3 in cell death and disease: NIPing at the heels of death. Cell Death Differ 2009, 16(4);515-523.

JOHN WILEY AND SONS LICENSE TERMS AND CONDITIONS

Apr 17, 2013

This is a License Agreement between Matthew L Skiles ("You") and John Wiley and Sons ("John Wiley and Sons") provided by Copyright Clearance Center ("CCC"). The license consists of your order details, the terms and conditions provided by John Wiley and Sons, and the payment terms and conditions.

All payments must be made in full to CCC. For payment instructions, please see information listed at the bottom of this form.

License Number	3131480979680
License date	Apr 17, 2013
Licensed content publisher	John Wiley and Sons
Licensed content publication	Journal of Biomedical Materials Research
Licensed content title	Correlating hypoxia with insulin secretion using a fluorescent hypoxia detection system
Licensed copyright line	Copyright © 2011 Wiley Periodicals, Inc.
Licensed content author	Matthew L. Skiles,Romone Fancy,Pritesh Topiwala,Suchit Sahai,James O. Blanchette
Licensed content date	Feb 2, 2011
Start page	148
End page	155
Type of use	Dissertation/Thesis
Requestor type	Author of this Wiley article
Format	Print and electronic
Portion	Full article
Will you be translating?	No
Total	0.00 USD
Terms and Conditions	

and the right to reproduce the Materials pursuant to Section 2 herein during the continuance of this Agreement. You agree that you own no right, title or interest in or to the Materials or any of the intellectual property rights therein. You shall have no rights hereunder other than the license as provided for above in Section 2. No right, license or interest to any trademark, trade name, service mark or other branding ("Marks") of WILEY or its licensors is granted hereunder, and you agree that you shall not assert any such right, license or interest with respect thereto.

5. NEITHER WILEY NOR ITS LICENSORS MAKES ANY WARRANTY OR REPRESENTATION OF ANY KIND TO YOU OR ANY THIRD PARTY, EXPRESS, IMPLIED OR STATUTORY, WITH RESPECT TO THE MATERIALS OR THE ACCURACY OF ANY INFORMATION CONTAINED IN THE MATERIALS, INCLUDING, WITHOUT LIMITATION, ANY IMPLIED WARRANTY OF MERCHANTABILITY, ACCURACY, SATISFACTORY QUALITY, FITNESS FOR A PARTICULAR PURPOSE, USABILITY, INTEGRATION OR NON-INFRINGEMENT AND ALL SUCH WARRANTIES ARE HEREBY EXCLUDED BY WILEY AND ITS LICENSORS AND WAIVED BY YOU.

6. WILEY shall have the right to terminate this Agreement immediately upon breach of this Agreement by you.

7. You shall indemnify, defend and hold harmless WILEY, its Licensors and their respective directors, officers, agents and employees, from and against any actual or threatened claims, demands, causes of action or proceedings arising from any breach of this Agreement by you.

8. IN NO EVENT SHALL WILEY OR ITS LICENSORS BE LIABLE TO YOU OR ANY OTHER PARTY OR ANY OTHER PERSON OR ENTITY FOR ANY SPECIAL, CONSEQUENTIAL, INCIDENTAL, INDIRECT, EXEMPLARY OR PUNITIVE DAMAGES, HOWEVER CAUSED, ARISING OUT OF OR IN CONNECTION WITH THE DOWNLOADING, PROVISIONING, VIEWING OR USE OF THE MATERIALS REGARDLESS OF THE FORM OF ACTION, WHETHER FOR BREACH OF CONTRACT, BREACH OF WARRANTY, TORT, NEGLIGENCE, INFRINGEMENT OR OTHERWISE (INCLUDING, WITHOUT LIMITATION, DAMAGES BASED ON LOSS OF PROFITS, DATA, FILES, USE, BUSINESS OPPORTUNITY OR CLAIMS OF THIRD PARTIES), AND WHETHER OR NOT THE PARTY HAS BEEN ADVISED OF THE POSSIBILITY OF SUCH DAMAGES. THIS LIMITATION SHALL APPLY NOTWITHSTANDING ANY FAILURE OF ESSENTIAL PURPOSE OF ANY LIMITED REMEDY PROVIDED HEREIN.

9. Should any provision of this Agreement be held by a court of competent jurisdiction to be illegal, invalid, or unenforceable, that provision shall be deemed amended to achieve as nearly as possible the same economic effect as the original provision, and the legality, validity and enforceability of the remaining provisions of this Agreement shall not be affected or impaired thereby.

10. The failure of either party to enforce any term or condition of this Agreement shall not constitute a waiver of either party's right to enforce each and every term and condition of this Agreement. No breach under this agreement shall be deemed waived or excused by either party unless such waiver or consent is in writing signed by the party granting such waiver or consent. The waiver by or consent of a party to a breach of any provision of this Agreement shall not operate or be construed as a waiver of or consent to any other or subsequent breach by such other party.

11. This Agreement may not be assigned (including by operation of law or otherwise) by you without WILEY's prior written consent.

12. Any fee required for this permission shall be non-refundable after thirty (30) days from receipt

13. These terms and conditions together with CCC's Billing and Payment terms and conditions (which are incorporated herein) form the entire agreement between you and WILEY concerning this licensing transaction and (in the absence of fraud) supersedes all prior agreements and representations of the parties, oral or written. This Agreement may not be amended except in writing signed by both parties. This Agreement shall be binding upon and inure to the benefit of the parties' successors, legal representatives, and authorized assigns.

14. In the event of any conflict between your obligations established by these terms and conditions and those established by CCC's Billing and Payment terms and conditions, these terms and conditions shall prevail.

15. WILEY expressly reserves all rights not specifically granted in the combination of (i) the license details provided by you and accepted in the course of this licensing transaction, (ii) these terms and conditions and (iii) CCC's Billing and Payment terms and conditions.

16. This Agreement will be void if the Type of Use, Format, Circulation, or Requestor Type was misrepresented during the licensing process.

17. This Agreement shall be governed by and construed in accordance with the laws of the State of New York, USA, without regards to such state's conflict of law rules. Any legal action, suit or proceeding arising out of or relating to these Terms and Conditions or the breach thereof shall be instituted in a court of competent jurisdiction in New York County in the State of New York in the United States of America and each party hereby consents and submits to the personal jurisdiction of such court, waives any objection to venue in such court and consents to service of process by registered or certified mail, return receipt requested, at the last known address of such party.

Wiley Open Access Terms and Conditions

- Any translations, for which a prior translation agreement with Wiley has not been agreed, must prominently display the statement: "This is an unofficial translation of an article that appeared in a Wiley publication. The publisher has not endorsed this translation."

Conditions applicable to non-commercial licenses (CC BY-NC and CC BY-NC-ND)

For non-commercial and non-promotional purposes individual non-commercial users may access, download, copy, display and redistribute to colleagues Wiley Open Access articles. In addition, articles adopting the CC BY-NC may be adapted, translated, and text- and data-mined subject to the conditions above.

Use by commercial "for-profit" organizations

Use of non-commercial Wiley Open Access articles for commercial, promotional, or marketing purposes requires further explicit permission from Wiley and will be subject to a fee. Commercial purposes include:

- Copying or downloading of articles, or linking to such articles for further redistribution, sale or licensing;
- Copying, downloading or posting by a site or service that incorporates advertising with such content;
- The inclusion or incorporation of article content in other works or services (other than normal quotations with an appropriate citation) that is then available for sale or licensing, for a fee (for example, a compilation produced for marketing purposes, inclusion in a sales pack)
- Use of article content (other than normal quotations with appropriate citation) by for-profit organizations for promotional purposes
- Linking to article content in e-mails redistributed for promotional, marketing or educational purposes;
- Use for the purposes of monetary reward by means of sale, resale, license, loan, transfer or other form of commercial exploitation such as marketing products
- Print reprints of Wiley Open Access articles can be purchased from: corporatesales@wiley.com

  The modification or adaptation for any purpose of an article referencing the CC BY-NC-ND License requires consent which can be requested from RightsLink@wiley.com .

Other Terms and Conditions:

BY CLICKING ON THE "I AGREE..." BOX, YOU ACKNOWLEDGE THAT YOU HAVE READ AND FULLY UNDERSTAND EACH OF THE SECTIONS OF AND PROVISIONS SET FORTH IN THIS AGREEMENT AND THAT YOU ARE IN AGREEMENT WITH AND ARE WILLING TO ACCEPT ALL OF YOUR OBLIGATIONS AS SET FORTH IN THIS AGREEMENT.

v1.8

Dear Dr Skiles,
According to the copyright regulations applied by IJAO, authors retain the following rights:

Retained rights

Provided the source is fully quoted at all times, Authors are hereby granted the right to:
a) reproduce the manuscript in whole or in part in any printed book or thesis of which they are the author(s).
b) They and any academic institution where they work at the time may reproduce the Manuscript in a reasonable number of copies for the
purpose of course teaching. This does not apply if a commercial charge is made for the training course.
c) To post a copy of the Manuscript as accepted for publication after peer review (in Word or Text format) on the Authors' website provided that
they also link to the article to the Journal's web site.
d) To reuse figures or tables created by them and contained in the Manuscript in other works created by them.

You may therefore proceed with your dissertation.
With kind regards,
Lucia Steele

Lucia Steele
Permissions
Wichtig Editore Srl | Via Friuli 72 | 20135 Milan (Italy)
Office +39 025455122 ext. 24
Mobile +39 3939129472
lucia.steele@wichtig.it | *Skype: luciasteele62*